From the Institute

for Cardiovascular Prevention

of the Ludwig-Maximilians-Universität Munich

Director: Univ.-Prof. Dr. med. Christian Weber

NET-attraction: The role of neutrophil extracellular traps in monocyte adhesion and its impact on atherosclerosis during endotoxemia.

DISSERTATION

Zum Erwerb des Doctor of Philosophy (Ph.D.)

an der Medizinischen Fakultät der

Ludwig-Maximilians-Universität München

submitted by

Ariane Helfrich

Munich

2020

From the Institute

for Cardiovascular Prevention

of the Ludwig-Maximilians-Universität Munich

Director: Univ.-Prof. Dr. med. Christian Weber

NET-attraction: The role of neutrophil extracellular traps in monocyte adhesion and its impact on atherosclerosis during endotoxemia.

DISSERTATION

Zum Erwerb des Doctor of Philosophy (Ph.D.)

an der Medizinischen Fakultät der

Ludwig-Maximilians-Universität München

submitted by

Ariane Helfrich

from

Frankfurt/Oder, Germany

Munich

2020

Supervisor:	Prof. Dr. Dr. med. Oliver Söhnlein
Second evaluator:	Prof. Dr. Barbara Schraml-Schotta
Dean:	Prof. Dr. med. dent. Reinhard Hickel
Date of oral defense:	09.06.2020

Abstract

Atherosclerosis, as a primary pathophysiologic condition of cardiovascular disease, is chronic inflammation. Acute infection is a well-established risk factor causing the destabilization of pre-existing atherosclerotic lesions, leading to a dramatic increase probability to suffer from myocardial infarction or stroke. However, the nature of the underlying processes remains unclear. Of note, epidemiologic studies show that endotoxemia results in heightened lesion development as well as the acceleration of atheroprogression. Endotoxins are potent activators of circulating immune cells including neutrophils, which foster vascular inflammation through expelled chromatin, called neutrophils extracellular traps (NETs) (Figure 1).

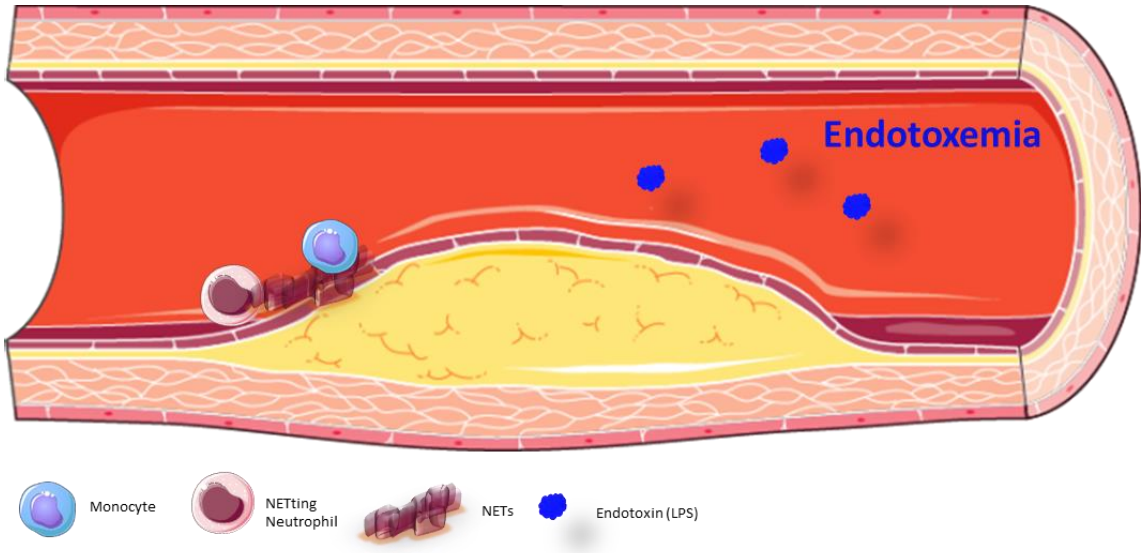

Figure 1: Graphical abstract- NETs as a monocyte adhesion scaffold.

Bacteria and their products as lipopolysaccharide (LPS) activate leukocytes including neutrophils. Upon activation, neutrophils are able to release extracellular traps (NETs), which have been shown to play a crucial role during atherogenesis. We hypothesize that neutrophil extracellular traps facilitate monocyte adhesion, resulting in accelerated atherosclerotic lesion formation under endotoxemia conditions. Main figure components from https://smart.servier.com/.

Here we hypothesized a NET-induced acceleration of atherosclerosis during infection. We observed increased leukocyte recruitment in a NET-dependent manner in hypercholesteremic and endotoxemia *Apoe*$^{-/-}$ mice, which led to highly increased lesion formation. This effect was abolished when the NET-formation was inhibited by the pharmacological compound BB Cl-amidine. Specifically, we discovered a NET-resident histone H2A driven leukocyte adhesion, which was based on charge interaction. These findings provide a new pathophysiological link between NET-borne H2A and monocyte adhesion at the site of developing atherosclerotic lesions. Targeting NET-formation has been already shown to be a promising strategy to limit atherosclerotic lesion formation. However, it's overall inhibition may also lead to insufficient host defense. Therefore, the here newly described histone H2A-dependent myeloid cell recruitment to the atherosclerotic site helps to develop a more specific myeloid cell adhesion inhibition to therapeutically limit atherosclerosis during infection.

Table of Contents

List of Illustrations

List of Tables

List of Abbreviations

A	
ABTS	2,2’-azino-bis(3-ethylbenzothiazoline-6-sulfonic acid
AFM	Atomic force microscopy
Apoe	Apoliporotein E
ApoB100	Apolipoprotein 100
B	
BB Cl-A	BB Cl-amidine
BSA	Bovine serum albumin
BW	Bodyweight
C	
CAD	Cardiovascular disease
CAP37	Cationic antimicrobial protein of 37 kD
CD	Cluster of differentiation
CCL	CC chemokine ligand
CHIP	Cyclical histone 2A interference peptide
D	
DAMP	Danger-associated molecular pattern
DNA	Deoxyribonucleic acid
E	
EDTA	Ethylenediaminetetraacetic
EU/ml	Endotoxin units/ ml
e.g.	Exempli gratia

F	
FCS	Fetal calf serum
H	
h	Hour
HBSS	Hank's balanced salt solution
H&E	Hematoxylin and eosin staining
HFD	High fat diet
HNP	Human neutrophil peptide
I	
ICAM1	Intercellular adhesion molecule
IL	Interleukin
IVM	Intravital microscopy
K	
kD	Kilo dalton
kg	Kilogram
L	
LBP	LPS binding protein
LDL	Low-density lipoprotein
LFA1	Lymphocyte function-associated antigen 1
LPS	Lipopolysaccharide
M	
MAC1	Macrophage antigen 1
min	Minute
MMP	Metalloproteinase

mM	Millimolar
ml	Millilitre
mOsm	Milliosmolar
MPO	Myeloperoxidase
mV	Millivolt
N	
NADPH oxidase	Nicotinamide adenine dinucleotide phosphate oxidase
NE	Neutrophil elastase
NETs	Neutrophil extracellular traps
ng	Nanogram
nM	Nanomolar
O	
oxLDL	Oxidized low-density lipoprotein
P	
PAD4	Peptidylarginine deiminase 4
PAMPs	Pathogen associated molecular pattern
PBS	Phosphate buffered saline
PCR	Polymerase chain reaction
PFA	Paraformaldehyde
PMA	Phorbol myristate acetate
pN	Piconewton
PRRs	Pattern recognition receptors
PSGL1	P-selectin glycoprotein ligand 1

R	
rcf	Relative centrifugal force
ROS	Reactive oxygen species
rpm	Revolution per minute
S	
SEM	Standard error of the mean
SLE	Systemic lupus erythematosus
T	
TNF-α	Tumor necrosis factor α
TLR	Toll-like receptor
TWEEN-20	Polyoxyethylene (20) sorbitan monolaurate
V	
V	Volt
VCAM1	Vascular cell adhesion molecule 1
VLA4	Very late antigen 4
VWF	Von Willebrand factor
Additional Character	
°C	degree celsius
µg	microgram
µM	micromolar
µl	microlitre

1. Introduction

1.1. The immune system

The survival of all multicellular beings depends on its ability to detect infectious pathogens and to induce an appropriate immune response [1]. Traditionally, the immune system is divided into the innate and adaptive immune system [2]. Evolutionary, the innate immune recognition appears in all multicellular organisms and is older than the adaptive immune system [3]. B cells and T cells belong to the adaptive immune response, while the innate immune response is built by neutrophils, basophils, eosinophils, mast cells, monocytes, and macrophages as well as dendritic cells and natural killer cells [2, 4] (Figure 2).

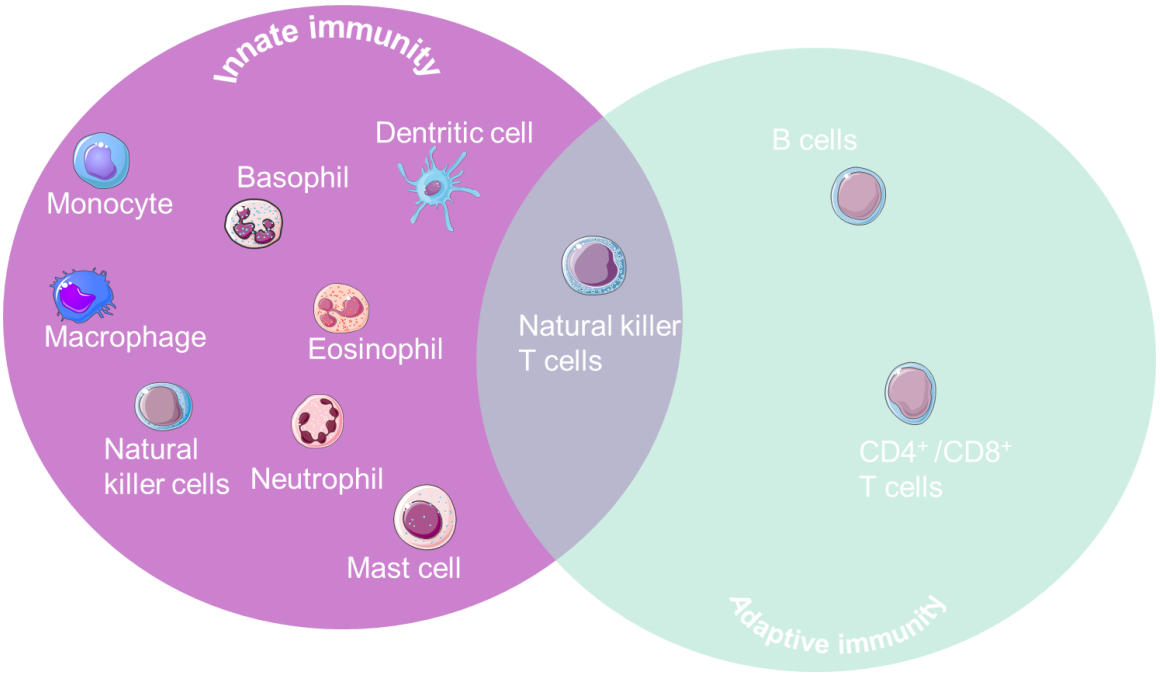

Figure 2: **Overview of the immune system.**

The innate immune system is divided into innate and adaptive immune responses. The innate immunity acts as the first line of defense, eliminating pathogens. It consists of neutrophils, basophils, eosinophils, monocytes, macrophages, mast cells, and natural killer cells. B cells and CD4/CD8 positive T cells belong to the adaptive immune response. The cytotoxic natural killer T cells are in the interface of the innate and adaptive immune response. Figure adapted from Dranoff, G. 2004 [4]. Main figure components from https://smart.servier.com/.

The innate immune cells are designed to defend the host organism against pathogens by detecting pathogen-associated molecular patterns (PAMPs), such as lipopolysaccharide (LPS), through pattern recognition receptors (PRRs) and eliminate the observed pathogens while maintaining self-tolerance [3, 5, 6]. PAMPs *e.g.* LPS, originate from gram-negative bacteria and activate immune cells [7]. Once the innate immune cells are activated, they clear pathogens from the organism by phagocytosis, or they lyse microbes through released antimicrobial peptides [8].

Further, activated innate immune cells secrete several types of molecules to the environment, such as cytokines. Cytokines are divided into pro- and anti-inflammatory cytokines [9]. Pro-inflammatory cytokines are able to recruit cells to the sites of infection via their chemotactic activity and activate endothelial cells to upregulate the adhesion molecules expression on their surface [10, 11]. The cytokine family includes chemokines, interleukins (IL) and tumor necrosis factor (TNF).

However, circulating immune cells adhere to the activated endothelium via the endothelial cell-expressed adhesion molecules and selectins and its leukocyte expressed respective ligands. The recruitment cascade of leukocytes includes cell rolling on the endothelium, cell adhesion, and transmigration into the inflamed tissue [11].

The first line of defense is built by the most abundant circulating leukocyte in human organism, the neutrophils. They account for 50-70% of the circulating leukocytes. Neutrophils are scavenging phagocytes that clear pathogens from the environment [12]. They are recruited to the site of infection or injury to trigger the inflammatory response [13]. In sterile inflammation, where no bacterial particles are present, the recruitment of neutrophils is mediated by *e.g.* danger-associated pattern molecules (DAMPs) released from damaged tissue or cells [14]. Neutrophils migrate to the site of inflammation to neutralize the pro-inflammatory particles and promote the recruitment of monocytes, which potentiate the pro-inflammatory

environment [15, 16]. When particles as DAMPs are cleared, neutrophils undergo apoptosis and are ingested by macrophages. The clearance of apoptotic cells promotes resolution of inflammation [17]. If this mechanism is imbalanced, chronic inflammation can occur and cause different types of diseases such as atherosclerosis [18].

1.2. Neutrophils

Neutrophils belong to the innate immune system, constitute the first line of defense, and account for up to 70% of the human circulating leukocytes under steady-state conditions. During hematemesis up to 2 $x10^{11}$ neutrophils are produced daily, originating from hematopoietic stem cells [19]. They are characterized by a multilobulated nucleus and equipped with a variety of cytoplasmic granules, which are formed during neutrophil maturation in the bone marrow, a process called granulopoiesis [13, 20]. Recent studies have shown that circulating neutrophil numbers are fluctuating under steady-state conditions, following circadian rhythmicity [21-23].

Neutrophils play an essential role during infection and injury. To control infections, neutrophils can eliminate pathogens in multiple ways either intracellular or extracellular. They engulf pathogens by phagocytosis into phagosomes and eliminate them by nicotinamide adenine dinucleotide phosphate (NADPH) oxygenase produced reactive oxygen species (ROS) and antimicrobial granules proteins which are translocated into the lysosome [24-27]. The granules, which store the granule proteins, are formed during different stages of maturation with varying produced proteins and are composed of diverse proteins [28]. In mature neutrophils are three different kinds of granules incorporated: the azurophilic granules (primary), specific (secondary) granules, and gelatinase (tertiary) granules. Additionally, secretory vesicles can be found in mature neutrophils (Figure 3). These granules store antimicrobial proteins which are important for pathogen clearance. The azurophilic granules contain myeloperoxidase and antimicrobial proteins, such as

cathepsin G. The later formed granules can be divided into specific (secondary) and gelatinase (tertiary) granules. Specific granules are filled with cytotoxic proteins as cathelicidin LL-37. Whereas, gelatinase granules are packed with matrix degradation enzymes gelatinase and lysozyme, which are important during neutrophil extravasation and diapedesis to reach the site of inflammation. Additionally, mature neutrophils show ficolin-1 granules and secretory vesicles that are rich in CD11b/CD18 promoting firm adhesion and endothelial transmigration. The granular proteins are released from activated neutrophils during a process called degranulation [28-30]

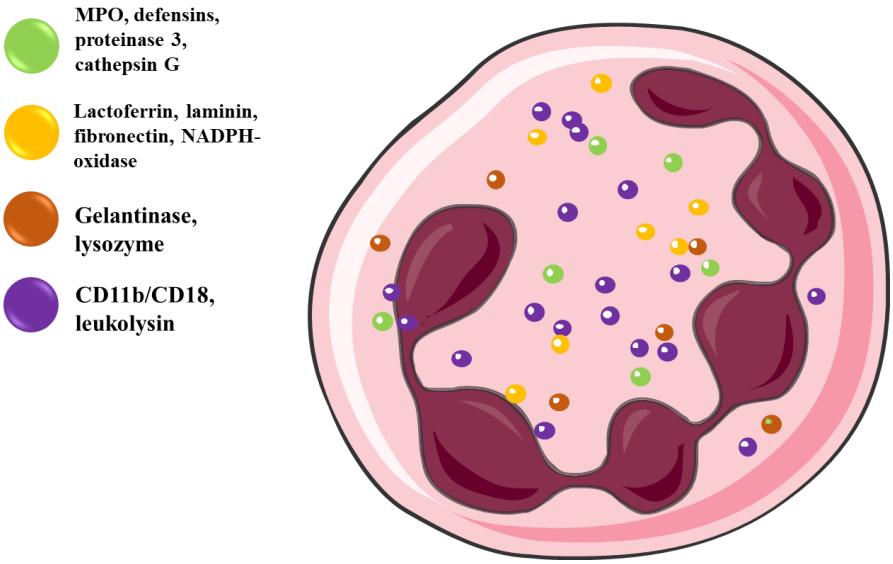

Figure 3: **Neutrophil granules proteins.**

Neutrophils bear characteristic granules with related proteins. The azurophilic granules (primary, green) contains myeloperoxidase, proteinase 3, and cathepsin G. Specific granules (secondary, yellow) are filled with lactoferrin, laminin, fibronectin, and NADPH-oxidase. Whereas, gelatinase granules (tertiary, brown) are packed with matrix degradation enzymes gelatinase and lysozyme, which are important during neutrophil extravasation and diapedesis. Additionally, mature neutrophils show secretory vesicle (purple) which are rich in CD11b/CD18 promoting firm adhesion and endothelial transmigration. Main figure components from https://smart.servier.com/.

As mentioned before, neutrophils are phagocytes and can efficiently kill pathogens in the phagosomes, where the antimicrobial granule proteins and ROS orchestrate an antimicrobial environment. Furthermore, neutrophils can also degranulate their granules proteins into the environment. Antimicrobial proteins like

LL-37 bind pathogen surface and are able to lyse bacteria [31]. Alternatively, neutrophils can eliminate or entrap microorganisms extracellular by releasing neutrophil extracellular traps (NETs) (Figure 4) [32, 33].

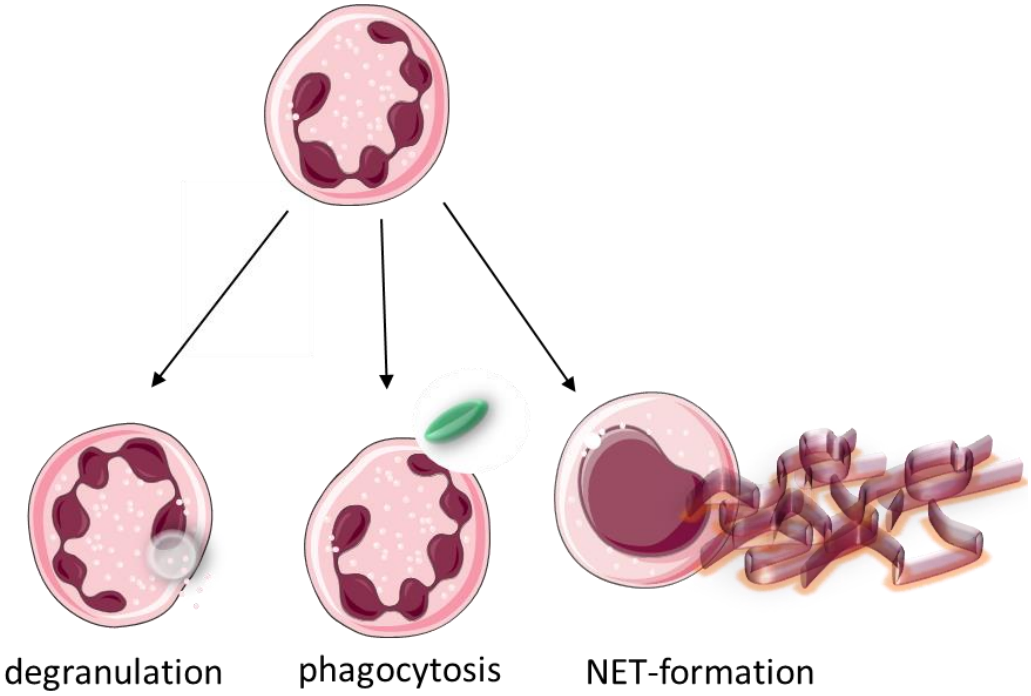

Figure 4: Neutrophil defense mechanisms.

Neutrophils exhibit different defense mechanisms. To protect the host neutrophils can release preformed granule proteins during degranulation or phagocyte invaders. Additionally, neutrophils are able to release extracellular traps to prevent pathogens from spreading. These NETs are decorated with granule proteins which have a microbicidal effect. Figure adapted from Kolaczkowska, E. 2013 [13]. Main figure components from https://smart.servier.com/.

However, released neutrophil-derived granule proteins can also attract monocyte to the sites of infection or injury. LL-37 and cathepsin G, for instance, are chemotactic for monocytes and α defensin in complex with chemokines has been shown to support monocyte adhesion [16, 34-36].

1.3. NETs

Neutrophils, as an essential part of the innate immune response, show phagocytic and antimicrobial activity upon infection to protect the host from damage and to ensure host survival [12]. In order to eliminate pathogens, neutrophils release preformed granule proteins to the environment, a process called degranulation, or phagocyte pathogens [27]. In 2004, Brinkmann *et al.* postulated a new defense strategy [32]. They observed the release of neutrophil chromatin to the environment upon neutrophil activation by microbes [37]. These chromatin structures are called neutrophil extracellular traps (NETs). They are released to limited pathogen spreading [33, 38]. NETs are decorated with granule proteins [39]. The granule proteins have a microbicidal activity to limit pathogen spreading [30] (Table 1).

Table 1: neutrophil extracellular trap associated proteins.

Summary of the main neutrophils-derived proteins, which decorate expelled neutrophil extracellular traps. Besides antimicrobial peptides or enzymes, also cell membrane-fragments from neutrophil membrane break up can be detected in NETs. Table adapted to Urban, C. 2009 [39].

compartment	protein
histones	H1, H2A, H2B, H3, H4
primary granules	Neutrophil elastase, cathepsin G, myeloperoxidase, defensins, cationic antimicrobial protein CAP37
secondary granules	lactoferrin, lysozyme, NADPH oxidase, cathelicidins
tertiary granules	cathepsin, metalloprotease, gelatinase
cytosol	proteinase 3, LL-37, S100 calcium-binding protein A8, -A9, -A12
cytoskeleton	actin, myosin-9

Neutrophils form NETs upon activation by pathogens like viruses, fungi, bacteria, and its products LPS and fMLP. Besides pathogens also host-derived autoantibodies, platelets, and cholesterol crystals have been shown to cause NET-formation (Figure 5) [32, 37, 40-45]. NETosis is regulated by the microbes' size [37]. Large microbes cause NETosis more likely than small pathogens, which can easily phagocyte into phagosomes [46]. Extracellular trap formation is also not restricted to neutrophils, mast cells and eosinophils have been described to form extracellular traps as well [47-49].

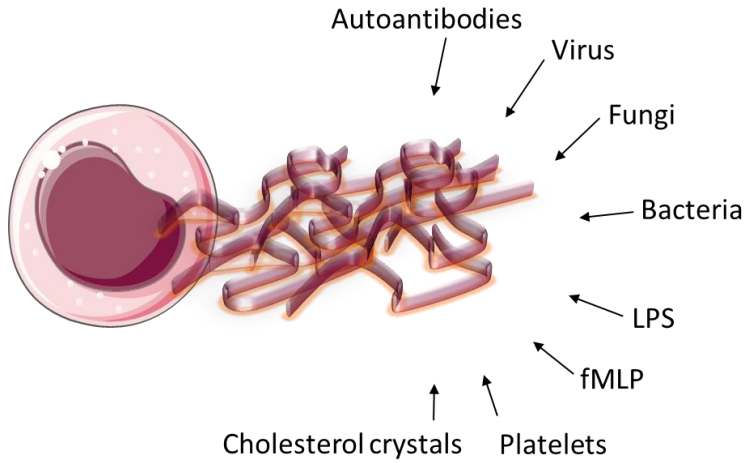

Figure 5: Trigger to release neutrophil extracellular traps.

Recently different NET-inducers have been described as visualized in the scheme. Apart from pathogens as viruses, fungi, or bacteria an also parts of pathogens can induce NET-formation. Besides pathogens, also host-derived components are sufficient NET-inducer like platelets or formed autoantibodies. Main figure components from https://smart.servier.com/.

Recent work has shown, that the neutrophil extracellular trap formation pathway is dependent on its stimulus [50]. The first investigations, focusing on NETs, stimulated neutrophils with phorbol myristate acetate (PMA) [32]. This NET-formation was later called NETosis due to cell death after NET-release [32, 33, 51]. However, this NET-formation mechanism was challenged by observations showing extracellular traps originating rather from mitochondrial deoxyribonucleic acid (DNA) than from genomic DNA, which was defined as vital NET-formation [52]. During vital NET-formation mitochondria are lysed to release the mitochondrial DNA. NETs formed from mitochondrial DNA are supposed to be vital since the neutrophils cell

membrane is not lysed and it has been observed that neutrophils are still able to phagocyte after they performed NET-release [53].

Besides differences in vital or suicidal NET-formation, also different NET-formation cascades have been described: the NADPH oxidase-dependent and NADPH oxidase-independent pathway. Antibodies, pathogens, and its products released from *e.g. Escherichia coli* or PMA induce the NADPH oxidase-dependent NET-formation [54, 55]. Upon stimulation, the cell cycle proteins cyclin-dependent kinase 4 and 6 are activated and NADPH oxidase forms reactive oxygen species (ROS), which in turn causes the degranulation of azurophilic granules into the cytoplasm, thereby leading to neutrophil elastase (NE) translocation into the nucleus [56, 57]. This protease degrades linker histones H1, causing chromatin relaxation. Due to DNA decondensation and nucleus swelling, the nuclei membrane disrupts, and chromatin is mixed with cytoplasm associated proteins [58]. In addition, NE also cleaves gasdermin D into its active form, leading to pore formation into granule membrane and cell membrane [59, 60]. Finally, the cell membrane breaks down and the chromatin-protein mixture is released into the environment as neutrophil extracellular traps (Figure 6). Released NETs are web-like DNA fibers composed of genomic DNA and are associated with 24 proteins: 11 cytoplasmatic proteins, 2 glycolytic enzymes, 5 cytoskeletal proteins, 3 S100 proteins, and the histones H2A, H3, and H4, which are the most abundant proteins in NETs [39].

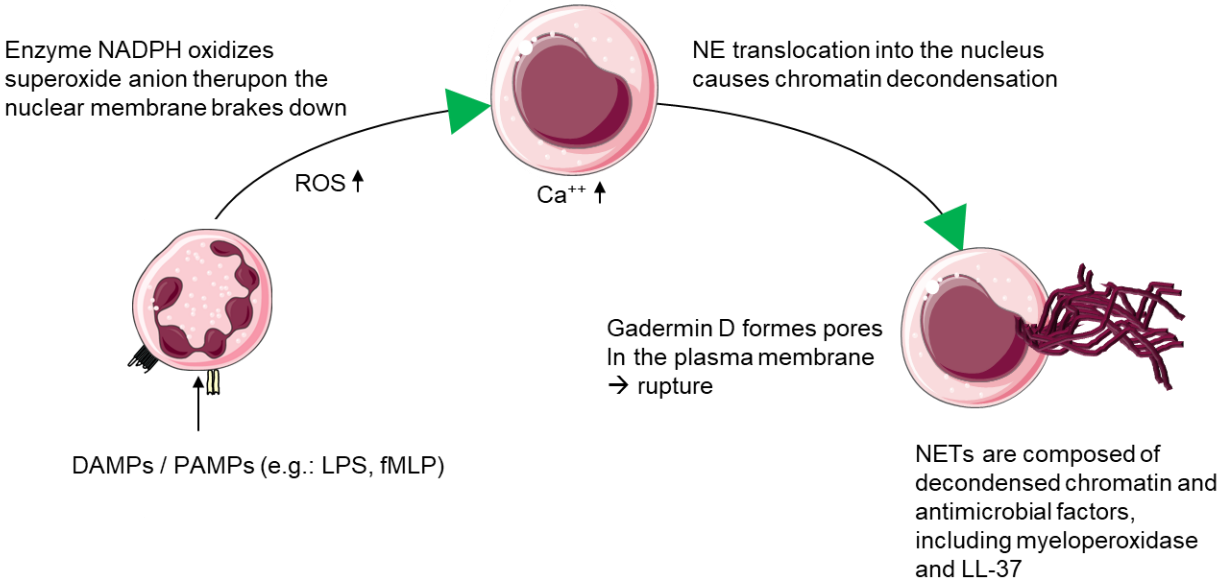

Figure 6: NADPH oxidase-dependent Neutrophil extracellular trap release.

One well-described pathway of NET-formation is illustrated, but the detailed cascade is still under discussion. Nevertheless, DAMPs or PAMPs activated neutrophils leading to granules protein release into the cytoplasm. One of the released proteins is myeloperoxidase, which catalyzes the reactive oxygen species (ROS) production causing oxidative stress. Further, NE originating from neutrophil granule is translocated into the nucleus. NE cleaves the histone. This process leads to a nucleus swelling, the breaks of the nuclei membrane lead to chromatin mixing with the cytoplasm. Finally, the cell membrane breaks down resulting in chromatin granule protein mixture exposure to the environment, recognized as neutrophil extracellular traps. Main figure components from https://smart.servier.com/.

NADPH oxidase-independent NET-formation can be caused by Streptomyocin-derived calcium ionophore A23187 [61]. This pathway is independent of ROS and neutrophil elastase. However, the histone H3 citrullination through peptidylarginine deiminase 4 (PAD4) is characteristic of the NADPH oxidase-independent pathway [62, 63]. PAD4 converts histone arginine to citrulline, resulting in a loss of positive charge on arginine residues and leading to chromatin decondensation [62]. Nevertheless, the complete mechanism of the NADPH oxidase independent pathway is not fully understood.

Neutrophil extracellular traps are formed upon infections to entrap bacteria [32]. Recent studies have shown that many pathogens evolved different strategies to escape NETs. *Streptococcus pyogenes* and *Streptococcus pneumoniae* synthesize DNase and digest NET-backbone structure DNA to escape NETs [64]. Others neutralize the pore-forming effect of LL-37 by protein M1 [65]. Furthermore, the defined surface charge, with varying d-alanyl residues expression of pathogens surface can prevent NET-entrapment. Pathogens lacking d-alanyl are entrapped due to charge interaction and can be killed by NETs [66]. Besides pathogens, also cholesterol crystals and autoantibodies were described to cause NET-formation and play a critical role in autoimmunity and chronic inflammation [43, 67-69].

Since extracellular DNA and the reactive granule proteins can cause inflammation, a well-balanced process between NET-release and clearance is vital. In order to regulate this process, NETs are cleared by DNAse I and DNAse I L3 in mice. Therefore the absence of these enzymes can lead to lethal NET-caused thrombosis [69, 70].

1.4. Monocytes

Monocytes belong to the innate immune system and are of myeloid origin. They develop in the bone marrow from the common myeloid progenitor, where also neutrophils originate from [25, 71]. Mature monocytes are released from the bone marrow to the circulation. The spleen is apart from lung and skin a peripheral extramedullary reservoir for monocytes [72, 73]. Monocytes account for 10 % of human circulating leukocytes [74]. They are phagocytic cells and play a critical role in infection and homeostasis. The monocyte subset in mice can be divided into inflammatory and anti-inflammatory monocytes, whereas in humans patrolling monocytes were discovered additionally [75-77]. Patrolling monocytes scan the vasculature and support the resolution of inflammation. In contrast, inflammatory monocytes express high levels of cytokines, *e.g.* tumor necrosis factor α and interleukin -1 (IL-1) to fuel inflammation and can differentiate into dendritic cells or

macrophages at the sites of infection, clearing pathogens from the organism [75]. Nevertheless, excessive monocyte activation causes tissue damage and trigger chronic inflammation [78-80].

1.5. Leukocyte recruitment

Leukocyte recruitment from bone marrow or spleen during infection or sterile inflammation requires the ability to sense signals, adhere, and finally transmigrate into the tissue. Tissue-resident cells, such as macrophages and dendritic cells, detect PAMPs from pathogens or DAMPs released from damaged cells and secrete in turn pro-inflammatory stimuli such as cytokines that activate endothelial cells to upregulate adhesion molecule expression and initiate leukocyte adhesion. The leukocyte adhesion on endothelial cells processes in a cascade-like manner [81].

First of all, leukocytes are captured from circulation on the endothelium. The cells slow down and finally arrest. Following leukocyte arrest on the endothelium, the cell adhesion is strengthened, and adherent leukocytes can transmigrate through the endothelium to reach the sites of inflammation. During every step of leukocyte recruitment, specific molecules play a critical role [11]. Capturing leukocytes on endothelial cells is dependent on P-selectin glycoprotein ligand 1 (PSGL1) and very late antigen 4 (VLA4), which are also involved in rolling and the interaction of the cell adhesion molecules intercellular adhesion molecule 1 (ICAM1) and vascular cell-adhesion molecule 1 (VCAM1) [82, 83]. Furthermore, inflamed endothelial cells express E- and P-selectin, which interact with leukocyte expressed PSGL1 [84]. The interaction of selectins with their ligands enables them to adhere to endothelial cells. Additionally, integrins such as VLA4 and lymphocyte function-associated antigen 1 (LFA1) or macrophage antigen 1 (MAC1) mediates leukocyte rolling through their adhesion molecule VCAM1 or ICAM1 [85]. During inflammation, endothelial cells are activated in order to upregulate adhesion molecule expression and release chemokines [86]. Chemokines are chemoattractants triggering the

arrest of rolling leukocytes through g- protein coupled receptor interaction. Adherent leukocyte crawl on the endothelium to find a site to transmigrate into the tissue either transcellular or paracellular (Figure 7) [11].

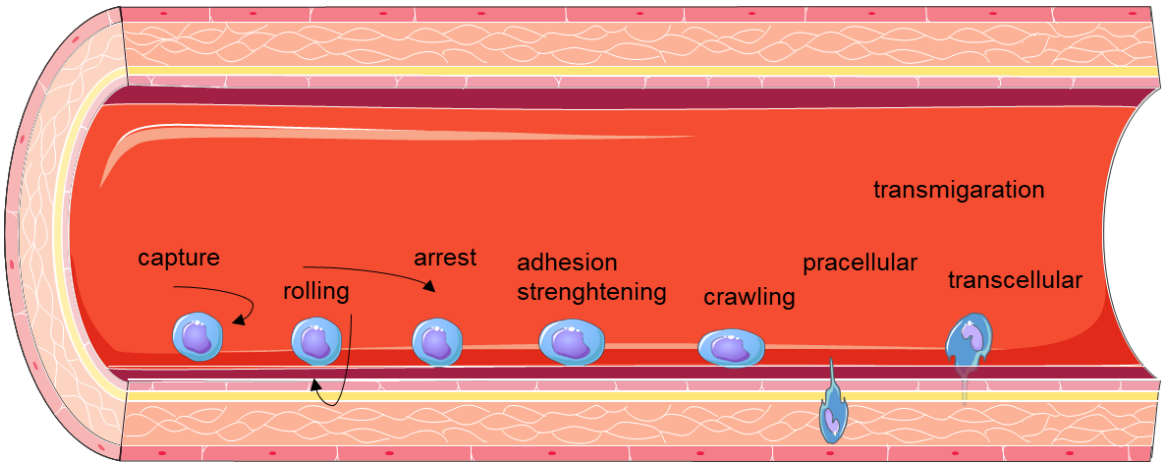

Figure 7: Leukocyte recruitment

Leukocyte recruitment cascade includes capturing of circulating cells, cell rolling on endothelium, leukocyte arrest and adhesion strengthening followed by crawling and finally transmigration. Figure adapted from Ley, K. 2007 [11]. Main figure components from https://smart.servier.com/.

1.6. Neutrophil pioneer monocytes to inflammatory sides

Neutrophils as the most abundant leukocytes in human peripheral blood are the first cells recruited to the site of infection and inflammation [12]. The first wave of polymorphonuclear leukocytes is followed by a second wave of monocytes recruitment by released soluble factors with attracting properties (Figure 8) [87]. This phenomenon can be explained by different kinds of adhesion molecules that facilitate leukocyte adhesion. Adhesion of neutrophils is most likely dependent on preformed or rapidly enzymatic cleaved molecules, which are easily externalized by neutrophils [35]. However, the classical adhesion pathway of monocytes requires a sequence of molecular interactions between monocytes and the endothelium. Selectins expressed on activated endothelium enables monocytes to roll on

endothelial cells and slow down [11]. Next, monocytes are exposed to chemokines presented on the endothelial surface, activating monocytes to firmly adhere. Finally, monocytes are activated for transendothelial migration and extravasation.

In addition to the classical adhesion pathway of monocytes, activated neutrophils can release preformed granule proteins on the endothelium to launch monocyte recruitment [16, 28, 29, 88, 89]. In line with this, it was shown that the lysate of neutrophils can cause monocyte chemotaxis [90]. In contrast, neutrophils from patients deficient in granule proteins did not cause monocyte chemotaxis. These findings indicate that granule proteins are crucial in monocyte recruitment, providing a second reason for monocytes being the second wave of recruited leukocytes to the site of injury or inflammation upon neutrophil recruitment [88].

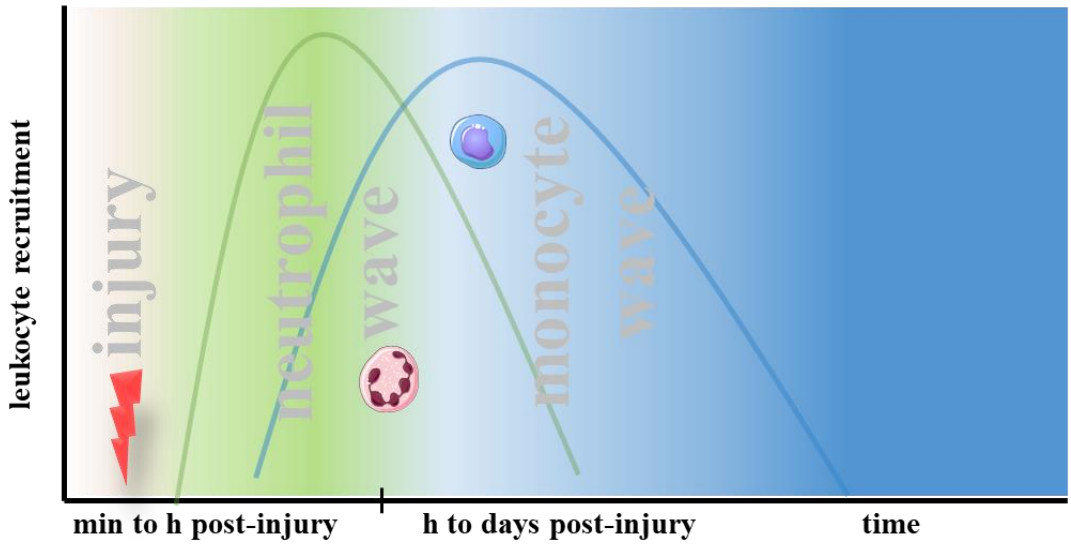

Figure 8: Leukocyte recruitment wave.

This graphical scheme shows the neutrophil and monocyte recruitment timing after injury. Classically, neutrophils are viewed as the first line of defense and are the first cells recruited to the site of inflammation or injury within minutes. This first wave is followed by a second wave of recruited monocytes. Main figure components from https://smart.servier.com/.

Neutrophils have various mechanisms for inducing monocyte recruitment. Upon binding to adhesion molecules expressed on endothelial cells, neutrophils release the content of secretory vesicles, which contain besides membrane receptors, proteinase-3, and the cationic antimicrobial protein of 37 kilo Dalton (kD)

(CAP37), among others [16]. These two proteins are able to activate endothelial cells to increase VCAM1 and ICAM1 expression on their surface, leading to enhanced monocyte and neutrophil adhesion. Additionally, integrins expressed on monocytes facilitate monocyte binding to both, proteinase-3 and CAP37. In this respect, it was also shown that neutrophil released LL-37, cathepsin G as well as the chemokine CCL2 can cause monocyte recruitment [16, 34, 91]. Interestingly, neutrophils can establish a partnership with other cells to induce monocyte recruitment. Thus, neutrophil released α defensins (HNP 1) form heterodimers with platelet-secreted CCL5 to promote monocyte adhesion [92]. In addition, myeloperoxidase released from primary granules causes monocyte adherence to endothelial cells as well. The granule proteins are highly cationic proteins, which bind to the anionic charge endothelial cell membrane [93]. The charge of the cell membrane is determined by glycoproteins and glycolipids expressed on the cell surface, called glycocalyx [94]. Noteworthy, leukocytes also show negatively charged surface glycocalyx, which causes adhesion to cationic granule protein MPO via charge interaction, a mechanism independent on adhesion molecules [93].

1.7. Neutrophils and monocytes in disease

Neutrophils and monocyte's interaction during innate immune response enables the host to efficiently defend against pathogens. Both cell types arise from the same precursor cells, therefore, it has been assumed that they potentially show common features [25, 71]. In fact, neutrophils and monocytes are both phagocytes, that can release effector molecules, such as cytokines, upon activation. Traditionally, neutrophils are described to be the first recruited cells to sites of infection, followed by a second wave of monocytes [87]. Neutrophils and monocytes together orchestrate an enhanced immune response. They regulate other immune cells and each other by releasing determined cytokines. Neutrophil clearance from the site of infection induces an important signal to resolve inflammation and limit leukocyte recruitment [95]. However, if this efficient pathogen elimination mechanism is not well balanced, the neutrophil-monocyte interplay can lead to tissue damage leading

to chronic inflammation. Chronic inflammation occurs if the immune system clears insufficient the initiating immune response signals, as PAMPs and DAMPs, or if the resolution of inflammatory response malfunctions [96].

One prominent chronic inflammatory disease is atherosclerosis. Atherosclerosis is characterized by the chronic inflammation of large and medium-sized arteries leading to peripheral vasculature disease [97]. Elevated low-density lipoprotein levels and hypercholesterolemia are one of the major risk factors for atherosclerosis. It has been shown that hypercholesterolemia increases neutrophil levels in circulation, which is known as neutrophilia. In fact, neutrophilia is a potent initiator of plaque development. If the amount of circulating neutrophils is decreased, reduced numbers of monocyte can be detected within the lesion, leading to moderated plaque development [98, 99].

1.8. Atherosclerosis

Atherosclerosis, a complex and progressive lipid-driven disorder of the arterial vessel wall, is known as a chronic inflammation, where disease progression is a consequence of the failed resolution of inflammation. It is the primary pathophysiology of cardiovascular disease (CAD) whose clinical outcome has life-threatening consequences. The most common risk factors for atherosclerosis are hyperlipidemia, hypertension, or smoking. Even though the treatment of well-established risk factors, CADs are still the leading cause of mortality [100].

Usually, the arterial vessel wall is composed of the intima, the media, and the outer layer called the adventitia. The intima, the inner layer closest to the bloodstream, is formed by a single endothelial cell layer as well as connective tissue consisting of collagen, elastin, and proteoglycans. As mentioned before (1.5), in steady-state, the endothelial cells are not capable to bind leukocytes. Upon

activation, caused by infection or injury, the expression of the adhesion molecules E-selectin, P-selectin, or ICAM-1 and VACAM-1 is upregulated and enables leukocyte adhesion [101]. Further, activated endothelial cells secrete chemokines to recruit leukocytes. The shift of physiologic endothelium function to a pro-inflammatory state is characteristic of endothelial dysfunction. Endothelial dysfunction, including the permeability of the endothelium for plasma components, such as low-density lipoprotein (LDL), is a response to risk factors causing atherosclerosis [102]. Atherosclerotic lesion formation occurs in the intima, where translocated modified LDL is engulfed by macrophages causing foam cell formation and results in an initial step for fatty streak formation. Over time, fatty streaks develop into advanced atherosclerotic lesions. Inflammatory cells accumulate in the lesion, thereby promoting inflammation. The growing lipid core is covered by fibrous connective tissue forming the fibrous cap of the atherosclerotic lesion [103]. However, the pro-inflammatory environment leads to increased cell death within the lesion, resulting in necrotic core formation and fibrous cap thinning (Figure 9). If the plaque ruptures, the highly pro-thrombotic and pro-coagulant atherosclerotic lesion content is exposed to the bloodstream leading to thrombus formation and vessel occlusion. Dependent on the site, this event can lead to myocardial infarction or stroke [104].

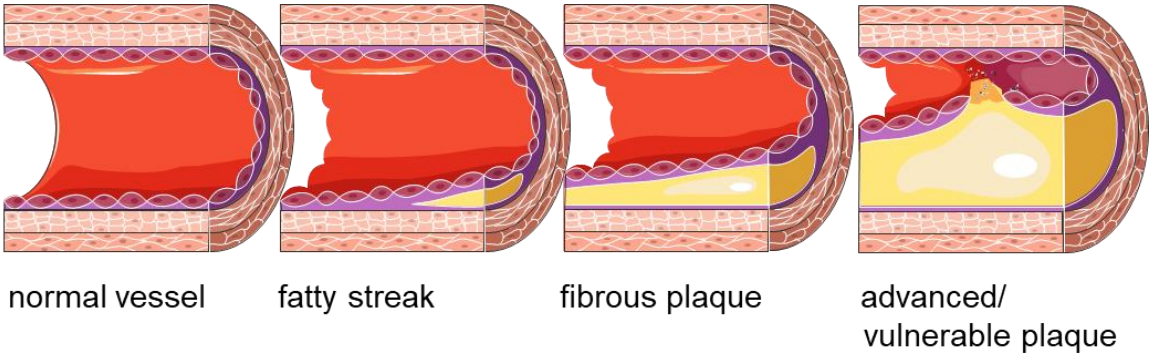

Figure 9: Atherosclerosis development: different stages.

The different stages of atherosclerosis development from normal healthy vessels to advanced plaque are shown. Atherosclerosis develops over decades where an initial fatty streak grows into a fibrous plaque up to vulnerable plaque. Main figure components from https://smart.servier.com/.

Atherosclerotic lesion formation occurs on large and medium-size arterial vessels at branch points, bifurcation, or curvature where the laminar flow is

disrupted. Endothelial cells at branch or curvature site show, in comparison to tubular regions, a polygonal shape. These areas, such as common carotid and left coronary arteries, have flow alterations and are typically sensitive to macromolecules deposition such as LDL [105]. Circulating LDL is transported by apolipoprotein B100 (ApoB100) and can accumulate within the intima by binding to proteoglycans of endothelial cells [106]. Finally, diffused LDL is oxidatively modified (oxLDL) by reactive oxygen species or enzymes originating from neutrophils or macrophages and is, therefore, a potent trigger of inflammation [107]. Additionally, oxLDL-causes endothelial cells activation resulting in a release of chemokines and cytokines. This causes leukocytes recruitment and the upregulation of adhesion molecules expression on the endothelium thereby facilitating leukocyte adhesion and transmigration into the intima [108, 109]. Transmigrated monocytes differentiate into macrophages which phagocytose oxLDL. At first glance, macrophages phagocyting oxLDL might clear the environment from pro-inflammatory agents, thereby limiting the inflammatory stimulus. However, lipid-laden macrophages become foam cells that secret pro-inflammatory factors and promote cell recruitment [110]. This early stadium of fatty streak development is reversible. Progressive atherosclerosis is later characterized by intimal thickening with typical extracellular lipid accumulation. Plaque progression is triggered by foam cell necrosis forming early fibro atheroma. The lipid-rich necrotic core is enclosed by smooth muscle cells forming the fibrous cap, which stabilize the lesion by secreting elastin and collagen [104]. Lesional macrophages secrete chemokines, including CCL2, to increase leukocyte recruitment into the plaque [98, 111]. Furthermore, the release of pro-inflammatory factors, such as interferon- γ and tumor-necrosis factor leads to a complex atherosclerotic lesion, where smooth muscle cell migration and proliferation contributes to stable lesion formation [112, 113]. However, macrophages promote plaque destabilization by releasing metalloproteinases (MMP), that in turn digest extracellular matrix proteins. This process leads to thinning of the fibrous cap resulting in plaque rapture (Figure 10) [114, 115].

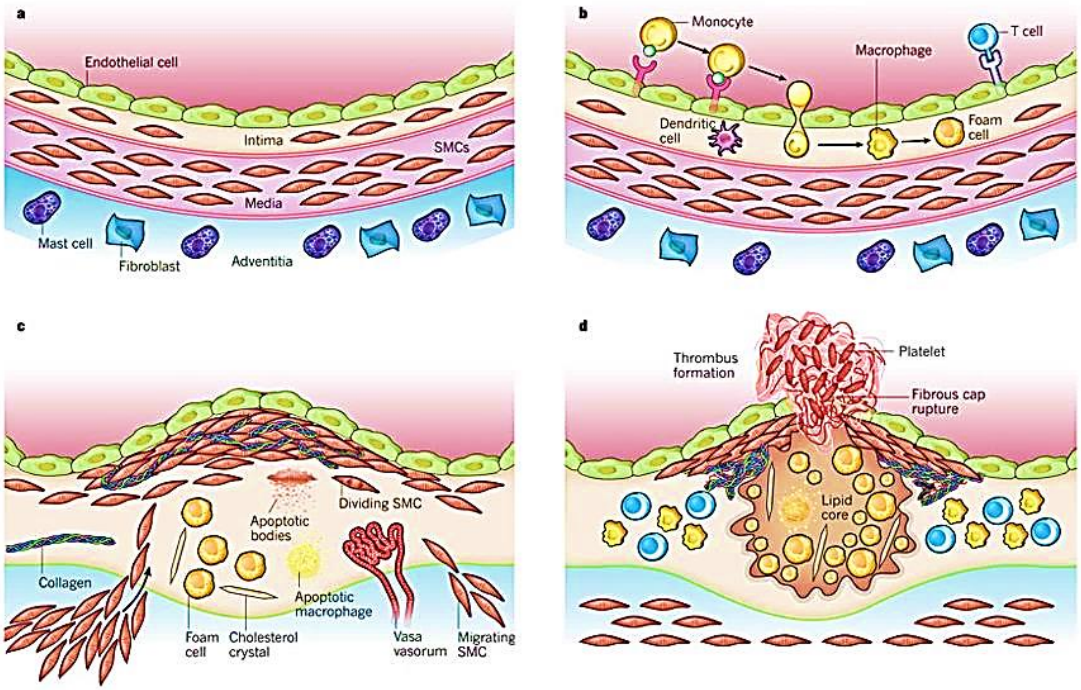

Figure 10: Development of atherosclerosis.

The physiological artery consists of three layers including intima, media, and adventitia (a). Atherosclerotic lesion development is initialized by activated endothelium expressing adhesion molecules which leads to enhanced leukocyte adhesion and migration. Monocyte-derived macrophages become foam cells upon oxidized lipid uptake (b). Atheroprogression is characterized by smooth muscle cell (SMC) migration from the media as well as SMC proliferation (c). In advanced atherosclerotic lesion, cell death of foam cells or SMC leads to necrotic or lipid core formation due to lipid release from dying cells (d). Figure from Libby, P. 2011 [103].

In addition to monocytes and monocytes-derived macrophages, neutrophils are supposed to play a critical role in atherosclerosis as well [95]. Peripheral neutrophil numbers increase under hypercholesterolemia conditions and are associated with an increased lesion size [98]. Neutrophil homeostasis is well regulated by the chemokine receptors CXCR2 and CXCR4 and their agonists CXCL1 and CXCL12 [116]. During hypercholesterolemia conditions neutrophil mobilizing chemokines, CXCL1, and CXCL8 are highly secreted by activated endothelial cells, causing an increased amount of circulating neutrophils [117, 118]. ICAM-1 upregulation on endothelial cells causes neutrophil adhesion, resulting in neutrophil-derived proteinase-3 and azurocidin release, which in turn triggers increased leukocyte adhesion, eventually leading to intima thickening [118, 119]. As

mentioned before, during neutrophil extravasation, neutrophils release granular proteins, which promote monocyte recruitment [120]. Additionally, neutrophil derived MPO modifies LDL oxidatively within the lesion, leading to increased lipid accumulation within the intima and foam cell formation. Therefore, neutrophils play a pivotal role during atheroprogression and plaque vulnerability. Neutrophils tend to accumulate close to the fibrous cap where released MMPs digest extracellular matrix [121-123]. Furthermore, activated neutrophils are able to release neutrophil extracellular traps, presenting certain granule proteins as well as NET-associated histones [39]. The presence of histones in atherosclerotic lesion has recently been shown to increase overall lesion vulnerability, characterized by lesion size and necrotic core area, while its neutralization improved lesion stability [124].

1.9. NETs in disease

Neutrophils as the first line of defense are able to form extracellular traps to bind pathogens by electrostatic forces, preventing their spread. However, an unbalanced NET production and clearance can be deleterious [125, 126]. During infections, these expelled traps persist for serval days [37]. Mechanisms to clear NETs are less well studied yet. It has been described that plasma DNAse degrades NETs and also macrophages can clear NETs from the environment [69, 127, 128]. Therefore, an equilibrium between NET production and clearance is essential, and any unbalance can cause diseases [54, 129]. Erythrocytes and platelets are easily trapped in NETs and initiated coagulation, leading to deep vein thrombosis [130]. Similarly, inappropriate cleared NETs can cause tissue damage according to their highly toxic components [131, 132]. As an example histones are the most abundant proteins associated with NETs and are highly toxic to endothelial cells [39, 133]. Further, it was shown that neutrophil extracellular traps can cause hepatic tissue damage during sepsis due to histone exposure to the environment. This effect was prevented in neutrophil elastase or PAD4-deficient mice which showed limited NET-formation [131].

Moreover, persistent neutrophil extracellular traps are potential causes of chronic inflammation, such as cystic fibrosis or atherosclerosis, or autoimmune diseases like arthritis or systemic lupus erythematosus (SLE) [43, 67, 132, 134, 135]. Chronic inflammation results from failed pro-inflammatory stimulus clearance as well as the initiation of the pro-resolving phase followed by tissue repair [136]. As mentioned, NETs contribute to chronic inflammation by stimulating other immune cells for cytokine release, which is a potent trigger of inflammation. In patients with cystic fibrosis, macrophages fail to clear NETs leading to massive inflammation [137]. Interestingly, patients who inhaled DNAse to degrade NETs had decreased NET-levels in the mucus and even an increased lung function was shown in mice [134].

Besides inappropriate NET-clearance, also uncontrolled NET-formation can cause diseases. So-called low-density neutrophils, found in an autoimmune disease like SLE are likely to form NETs spontaneously [138, 139]. SLE patients show autoantibodies against extracellular DNA, histones, and neutrophil antigens, which are all detectable in NETs. Autoantibodies have been reported to induce NET-formation leading to a vicious cycle of disease. SLE patients also show a decrease in DNAse I activity, which is produced and secreted by the pancreas, leading to a lack of NET-clearance [69]. Interestingly, NET-associated proteins can persist on the endothelium after DNA digestion. The von Willebrand factor (VWF) has been suggested to be a potent NET-protein binder by blocking VWF, which limited tissue damage [131]. The cytotoxic effect of NET-associated proteins has also been described in atherosclerosis, where endothelial dysfunction and smooth muscle cell lysis by NET-associated proteins resulted in vulnerable plaques [67, 124]. Consequently, genetic depletion of PAD4 in mice leads to reduced atherosclerotic lesion size or even reduces plaque vulnerability [124, 140]. Studies focusing on atherosclerosis, diabetes, or cancer highlight the impact of NETs in disease progression. Taken together, these studies show that not only the unbalanced NET-formation or -clearance fosters chronic inflammation, but also constant sterile inflammatory trigger, such as recurrent cigarette smoke inhalation, high fat and high cholesterol diet promotes chronic inflammation and thus pose a challenge [55, 141-143].

1.10. Endotoxemia

Endotoxins are small bacteria-derived molecules known as lipopolysaccharides (LPS) which are present in the outer membrane of gram-negative bacteria or cyanobacteria. They belong to the pyrogens, inducing inflammation. Bacteria extrude large amounts of LPS upon cell death, growth, and cell division. Approximately two million LPS molecules can be found in a single *Escherichia coli* cell membrane [144, 145]. LPS is a complex molecule consisting of a core polysaccharide chain, a hydrophilic O-specific polysaccharide chain, and the toxic lipophilic lipid component (lipid A) which can bind to the macrophage scavenger receptor or CD11b/CD18 [146]. Additionally, circulating LPS binds to the LPS binding protein (LBP). The 60 kDa LBP is a soluble acute-phase protein that interacts with monocytes and macrophages associated glycoprotein CD14 signaling through the TLR-4 MD-2 complex (Figure 11). This in turn activates pro-inflammatory cytokines production triggering inflammation [147]. Epidemiological studies show that circulating LPS (endotoxemia), can occur in apparently healthy subjects as well [148]. Circulating endotoxins might originate from gut microbiota, smoking, chronic infections, or recurrent infections. The link of circulating infectious agents to early atherosclerosis was already drawn in the late 1970s [149-151].

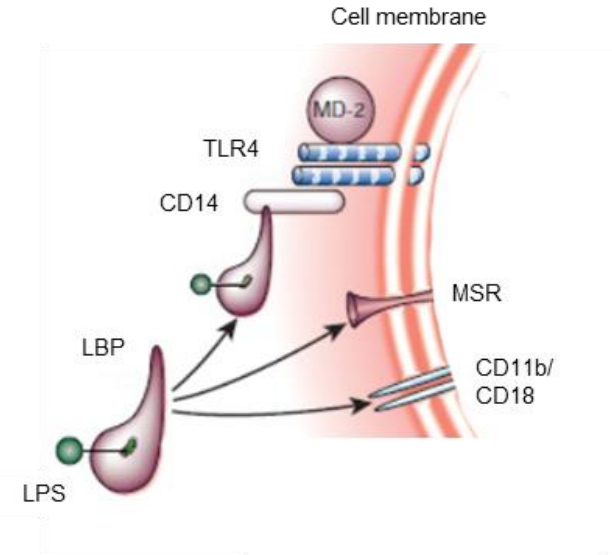

Figure 11: LPS interacting receptors.

Lipopolysaccharide binds LPS binding protein (LBP). This complex can interact with CD14 causing a signaling pathway through Toll-like receptor 4. Alternatively, macrophage scavenger receptor (MSR) or CD11b/CD18 expressed on the cell membrane sense LPS. Adapted from Cohen, J. 2002 [152].

1.11. Endotoxemia accelerates atherosclerosis

A growing body of evidence indicates infections as an additional potent risk factor causing atherosclerosis. This link has been drawn according to the seasonal incidences to suffer from myocardial infarction, which is higher during cold seasons when infections more frequently occur [153]. Retrospective studies analyze primary care data-settings revealing an increased risk to suffer from cardiovascular disease within the first days following an acute respiratory infection [154, 155]. Pathogens infecting the non-vasculature site can release pathogen-associated particles in the circulation, like PAMPs such as LPS, causing a systemic inflammatory response. Studies focusing on lung infection with gram-negative bacteria *Chlamydia pneumoniae* showed an increased atherosclerotic lesion size up to 70% compared to non-infected mice [156-159]. LPS causes pro-inflammatory response as upregulation of adhesion molecules on endothelial cells and increased cytokine production also by lesion associated macrophages, increasing leukocyte

recruitment [160, 161]. Further, it has been shown that polarized monocytes cause a dramatic increase in atheroprogression during endotoxemia [162]. Besides leukocytes and endothelial cells also platelets are activated by LPS which can lead to platelet-neutrophil crosstalk by forming CCL5 and HNP-1 heterodimers, which foster monocyte adhesion. Moreover, CCL5 can potentially cause neutrophil extracellular trap formation and fuel inflammation [92, 163]. In addition to CCL5, also activated platelets have been shown to induce NET-formation under endotoxemia conditions [164]. Neutrophil extracellular traps are able to cause endothelial dysfunction, which enhances leukocyte adhesion and accelerates atherosclerosis. This effect can be limited by pharmacological blocking of PAD4 with Cl-amidine which inhibits NET-formation [135]. Furthermore, if NETs are released within the atherosclerotic lesion, the NET-associated proteinases and histones affect plaque stability [67, 124, 141, 165].

1.12. Therapeutical approaches

Atherosclerosis develops over decades and starts with fatty streak development when LDL enters the arterial intima and accumulates over time [166]. The first changes occur at branch points and lead to increased endothelial cell adhesion molecules expression initiating leukocyte adhesion, fuel inflammation. Chronic inflammation is a key characteristic of atherosclerosis and its limitation seems to be a promising therapeutical strategy. Hypercholesterolemia has been described to cause neutrophilia to accelerate early atherosclerosis [98]. Treatment of hypercholesterolemia including statin therapy as shown in the JUPITER study has shown that the lowering of LDL levels leads to reduced risk to suffer from CVD [167, 168]. Nevertheless, recent studies suggest that lipid-lowering therapy can promote diabetes mellitus incidence [169, 170].

High lipid levels are associated with increased circulating neutrophils, which is strongly associated with accelerated atherosclerosis. Therefore, inhibition of

leukocyte adhesion is a potent strategy to limit inflammation and atheroprogression [98, 171, 172]. However, leukocyte adhesion at the site of infection is a crucial step to reach pathogens and eliminate them. Inhibition of leukocyte adhesion could lead to insufficient immune response during infection [173]. Interestingly, acute respiratory infections were shown to increases the risk to suffer from CVD [154, 155]. During infection, neutrophils are able to form neutrophil extracellular traps, which in turn cause endothelial dysfunction leading to atherosclerotic lesion growth [32, 135]. Additionally, NET-formation within the lesion has been shown to cause plaque vulnerability [124]. However, antibiotic treatment during infection seems not to prevent cardiovascular events but vaccination is shown to potentially lower the risk [174, 175]. Interestingly, mice studies genetically blocking NET-formation result in smaller lesion size [135]. These studies point to the important role of NETs during atherosclerosis and stress out the importance to understand the underlying mechanism to develop specific treatment strategies.

1.13. Research Rational

Atherosclerosis is a chronic inflammatory disease. Over the decades, atherosclerotic lesion develops in the large arteries and is composed of accumulated leukocytes and lipids. The literature ascribes macrophages as a major part of lesion development. However, there is a growing body of evidence pointing on neutrophils to play an important role during atherosclerosis development. Neutrophils generate reactive oxygen species, release granules proteins, cytokines, and neutrophil extracellular traps (NETs) and therefore fuel inflammation. NETs are complex DNA-structure composed of antimicrobial peptides, which are released upon infection or host-derived stimuli. NETs are described to entrap bacteria, preventing their spread in the host organism. Noteworthy, previous *in vivo* studies show reduced lesion formation if NET-release is blocked. NETs are able to cause endothelial dysfunction and therefore may trigger monocyte attraction. They are formed during infection to entrap bacteria and there is evidence that infection increases the risk to suffer from myocardial infarction. However, these studies lack

to show the relation of NETs and accelerated atherosclerosis during infection. Therefore, the present study aims to understand the pathophysiological mechanism of NETs in atheroprogression in the context of endotoxemia. The result of this study will contribute to a better understanding of NET-mediated atherosclerosis development and may serve to elucidate a therapeutic strategy to limit atherosclerosis.

2. Methodology

2.1. Methodology

To run the different *in vitro* and *in vivo* assays the following buffers and solutions were used unless otherwise stated in the text.

Table 2: Buffer and solutions

Buffers and solutions which were used in experiment settings unless otherwise stated differently. Solutions were prepared as described in the recipe.

Buffer/solution	recipe
Adhesion buffer	RPMI without phenol red supplemented with 1.3 mM calcium chloride, 10 mM HEPES and 1 mM magnesium chloride, pH 7.4
Antibody staining buffer for flow cytometry	20 ml 1x PBS, 4 ml 10 BSA, 400 µl mouse serum, 400 µl rabbit serum, 400 µl human serum
Antigen retrieval solution	70 ml aqua dest. with 20 mM citric acid, 83 mM sodium citrate supplemented with 0.5% Tween20
Blocking solution	6 ml PBS with 1% BSA and 3 drops horse serum
Digestion medium	RPMI with phenol red and 1% fetal calf serum, pH 7.4
MACS buffer	1x PBS with 0.5% BSA and 3 mM EDTA
Red blood cell lysis buffer	150 mM ammonium chloride, 10 mM potassium bicarbonate, 0.1 mM EDTA diNa, pH 7.4

2.2. Cell isolation

Human leukocytes were isolated as described below and cultured in adhesion buffer. Blood was drawn from healthy volunteers into 9 ml K3E EDTA S-Monovette® (Sarstedt) tubes using a 21G Safety Multifly® needle (Sarstedt).

2.2.1. Isolation of human neutrophils

Fresh drawn venous blood (5 ml) was layered on 5 ml Polymorphprep™ (37°C, Axis-Shield) in a 15 ml sterile centrifuge tube (Sarstedt). A density gradient was created by centrifuging the Polymorphprepr: Blood during 30 min at 500 g (acceleration: 9, deceleration: 0, Heraeus Megafuge 16, Thermo Fisher).

After centrifugation, the Polymorphprep™ gradient shows three cell layers; an upper ring of mononuclear cells, the second ring of polymorphonuclear cells, and a third sedimented erythrocyte (Figure 12). The Polymorphprep™ contains a polysaccharide that causes aggregation of erythrocytes, leading to sedimentation of these cells [176].

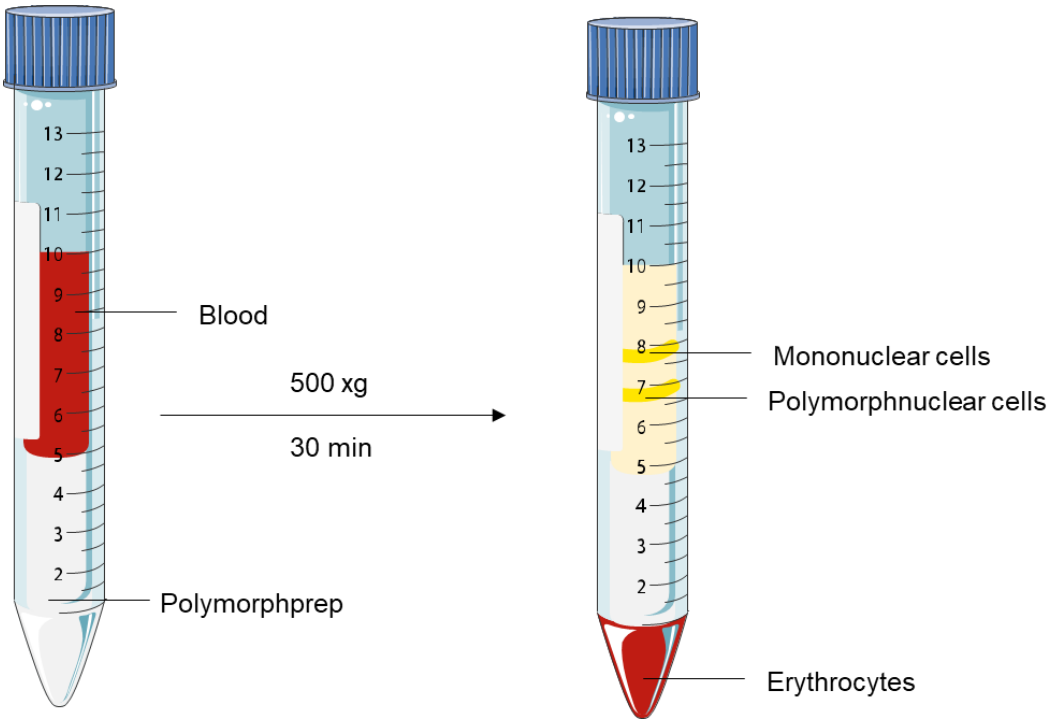

Figure 12: Schematic diagram of polymorphonuclear cell isolation.

Purification of polymorphonuclear cells using Polymorphprep™. Freshly drawn blood is layered on top of Polymorphprep™ 1:1 and centrifuged at 500 xg for 30 min. After centrifugation erythrocytes are sedimented. Above the erythrocytes are polymorphonuclear cells located followed by mononuclear cells and plasma.

The second ring contains polymorphnucelar cells, was collected into a 50 ml centrifuge tube (Sarstedt) and filled up with room temperature (RT) 1x PBS (Gibco), and washed once at 300 g for 5 min. The supernatant was removed, and the remaining erythrocytes were lysed with 3 ml of lysis buffer for 3 min at RT. Before repeating the centrifugation step, lysis was stopped by filling up the 50 ml centrifuge tube with 1x PBS. The washed cell pellet was resuspended in adhesion buffer and kept on ice for 30 min. The cell purity was verified by flow cytometry as described later and account for between 82.4 and 97.9% (Figure 13).

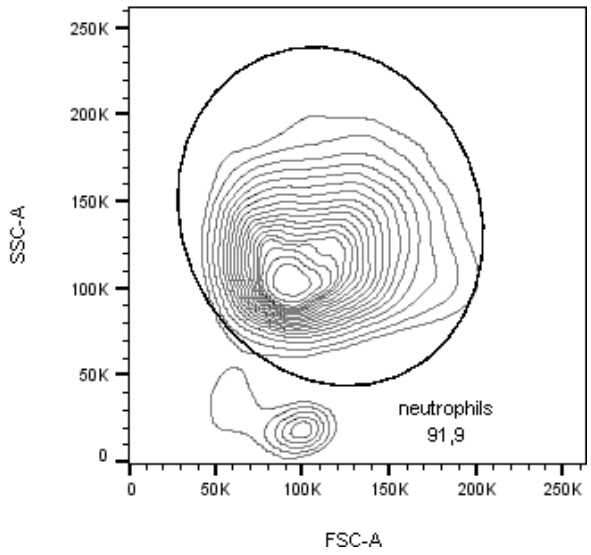

Figure 13: Flow cytometry of isolated neutrophils.

Neutrophils were isolated using Polymorphprep™ gradient centrifugation. Neutrophil purity accounts for 82.4 and 97.9%.

2.2.2. Isolation of human monocytes

Polymorphprep™ gradient isolation (see 2.2.1.) of leukocytes was also used to collect mononuclear cells followed by the isolation with the monocyte isolation kit II (MACS Miltenyi Biotec). The mononuclear cell ring was collected from the Polymorphprep™ gradient and washed three times with 1x PBS (Gibco) supplemented with 0.5 mM EDTA (Karl Roth), centrifugation for 5 min at 300 g. In the next step, the cell pellet was resuspended in MACS buffer, and isolated according to the user manual. Briefly, monocytes were negatively selected by adding a biotin-antibody mix to label all leukocytes except for monocytes and incubated on ice for 10 min. After incubation anti-biotin magnetic beads were added to the cells and incubated on ice for another 15 min. Cells were then washed with MACS buffer and centrifuged at 300 g for 5 min. The cell pellet was resuspended in MACS buffer and applied to a LS column (MACS Milenyi) attached to a magnet. The flow-through, containing monocytes were collected in a 50 ml tube (Sarstedt). The

purity was verified by flow cytometry counterstaining the cells with CD14-FITC antibodies.

2.3. NET- formation

Neutrophils were isolated via Polymorphprep™ gradient (see 2.2.1.) and adjusted to a final cell concentration of $4x10^6$/ml by counting the cell number in a Neubauer counting chamber (Carl Roth) and diluted in adhesion buffer to the intended cell concentration. 200.000 cells/well were seeded in 96-well flat-bottom plate (Falcon Corning) and left to settle down for 15 min at 37°C and 5% CO_2. The non-adherent cells were washed off with 100 µl 1x PBS (Gibco). Afterward, 50 µl of 25 µM calcium ionophore A23187 (Sigma Aldrich) diluted in adhesion buffer was added to neutrophils and incubated for 1 h at 37°C and 5% CO_2 to stimulate the cells for NET-release.

2.4. *In vitro* assays

To assess monocyte adhesion to NETs, adhesion assays under static and flow conditions were performed.

2.4.1. Static adhesion assay

Adhesion of monocytes to NETs was studied under static conditions. Isolated monocytes (see 2.2.2.) were stained with 3 µM of CellTrace™ calcein violet AM (Thermo Fisher Scientific) according to the instruction manual for 30 min at 37°C and 5% CO_2. Monocytes were then washed and 50.000 cells/well were seeded to washed wells containing either neutrophils or netting neutrophils (see 2.3.) for 15

min at 37°C and 5% CO_2 (Figure 14). Non-adherent monocytes were washed off three times using 100 µl 1x PBS (Gibco). Adherent monocytes were measured in a microplate reader (Tecan infinite™ 200 pro) with extinction 400 nm and emission 452 nm as a bottom read with multiple reads 3x3 and gain 50. Neutrophil extracellular traps were visualized by counterstaining extracellular DNA with SYTOX™ Green Nucleic Acid Stain (5 µM, Invitrogen) in a Leica microscope Dmi8 microscope.

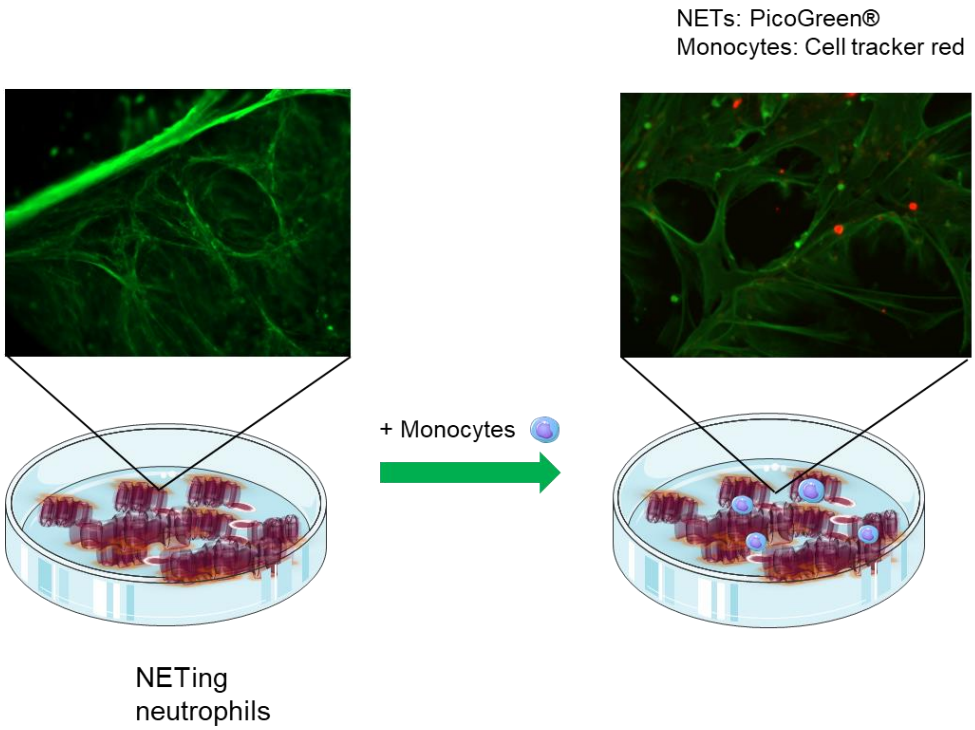

Figure 14: Scheme of static adhesion assay.

200.000 neutrophils/well were seeded into a 96-well plate and settled down for 15 min at 37°C and 5% CO_2. The non-adherent cells were washed off with 100 µl 1x PBS. Afterward, 50 µl of 25 µM calcium ionophore A23187 diluted in adhesion buffer was added to neutrophils and incubated for 1 h at 37°C and 5% CO_2 for NET -formation. Wells were washed and CellTrace™ calcein violet AM stained monocytes (50000 cells) were added on top of the NETs for 15 min and washed off again. The adherent monocytes were analyzed by fluorescent intensity measurements.

2.4.2. Flow adhesion assay

Adhesion of monocytes to NETs under flow condition was studied by using a 6 channel µ-slide VI 0.4 ibiTreat (Ibidi). Isolated neutrophils ($1x10^5$) (see 2.2.1.) were left to adhere in the flow chamber channel either with or without 25 µM calcium ionophore A23187 for 60 min (Figure 15). The channel was washed under applied flow (0.5 dynes/ cm^2) using a pump (PHD ULTRA syringe pump, Harvard Apparatus) for 3 min with 1x PBS. Afterward, the remaining buffer was removed from the reservoir 1 and 100 µl monocytes (see 2.2.2.) were added to the system. The flow was applied (0.5 dynes/ cm^2) for another 3 min, followed by a washing step with 1x PBS. Cells were fixed with 4% paraformaldehyde (PFA) for 5 min and 3 fields of interest were acquired with a Leica microscope Dmi8 to quantify adhesive monocytes using free available software ImageJ (National Institutes of Health). Neutrophil extracellular traps were visualized by counterstaining extracellular DNA with SYTOX™ Green Nucleic Acid Stain (5 µM, Invitrogen).

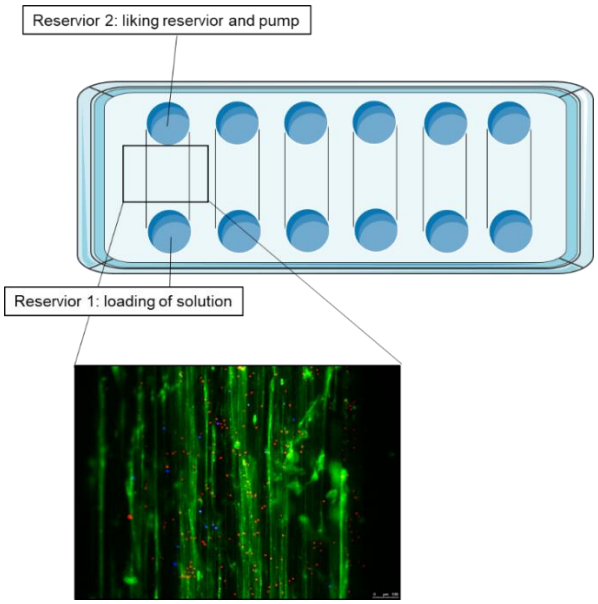

Figure 15: Scheme of flow adhesion assay.

Isolated neutrophils ($1x10^5$) applied through reservoir 1 with a 2 ml syringe and left for adhesion for 15 min. Afterward 25 µM calcium ionophore A23187 was added under flow and cells were incubated for 30 min to cause NET-formation (green). The channel was washed under applied flow (0.5 dynes/ cm^2) by a pump (PHD ULTRA syringe pump, Harvard Apparatus) for 3 min with 1x PBS. The remaining buffer was removed from the reservoir 1 and 100 µl monocytes (red) were added to the system. Flow was applied (0.5 dyne/ cm^2) for 3 min. Reservoir 1 was emptied and refilled with 1x PBS (Gibco) to wash off the non-adherent cells. Three pictures per channel were taken and analyzed by using ImageJ (National Institutes of Health).

2.4.3. NET digestion

The impact of neutrophil extracellular traps in monocyte adhesion was studied by removing the main compartment of NETs, DNA, in the static and flow adhesion assays. The DNA-backbone structure was digested with 10U of DNAseI (Sigma-Aldrich) for 30 min at 37°C and 5% CO_2. Before monocytes were applied to the system, the wells or channels were washed with 1x PBS (Gibco) to remove remaining DNA structures and DNAseI. The continuation of the assays was conducted as described in 2.4.1. or 2.4.2..

2.4.4. Blocking monocyte adhesion to NETs under static and flow conditions

Monocyte adhesion to NETs was studied under static (see 2.4.1.) and flow (see 2.4.2.) conditions. To figure out how monocytes adhere to NETs, the monocyte expressed adhesion molecules, g-protein coupled receptor, toll-like receptors or NET-associated proteins were blocked with either antagonists or antibodies for 30 min at 37°C and 5% CO_2 as followed (Table 3):

Table 3: Adhesion blocking reagents.

To study the molecules potentially involved in monocyte adhesion to NETs, the monocyte expressed adhesion molecules, their g-protein coupled receptors, and TLR were antagonized. Further, NET-associated proteins were blocked as mentioned in the table to determine its role.

Antagonist/ Antibody	Target	Concentration	Company
BX 471	CCR1	1 µM	Tocris
RS504393	CCR2	3 µM	Sigma Aldrich
SB 32437	CCR3	1 µM	Tocris
DAPTA	CCR5	0.1 µM	Tocris
SB 225002	CXCR2	1 µM	Tocris
AMD	CXCR4	1 µM	Sigma Aldrich
Cyclosporin H	FPR-1	10 µM	Tocris
WRW4	FPR-2	10 µM	Tocris
AR-C118925xx	P2Y2	10 µM	Tocris
A 740003	P2X7	0.1 µM	Tocris

BIO1211	VLA-4	10 µM	Tocris
CU CPT 22	TLR 1-2	100 µM	Tocris
C34	TLR 4	100 µM	Tocris
Hydroxychloroquine sulfate	TLR 9	100 µM	Tocris
Pertussis toxin	Pan g-protein coupled receptor	0,8 µg/ml	Sigma Aldrich
Rabbit polyclonal antibody	Histone H2A	10 µg/ml	Cell signal
Rabbit polyclonal antibody	Histone H3	10 µg/ml	Abcam
Rabbit polyclonal antibody	Histone citrulline H3	10 µg/ml	Abcam
Rabbit monoclonal antibody	Histone H4	10 µg/ml	Cell Signaling
Rabbit polyclonal antibody	Myeloperoxidase	10 µg/ml	Merck
Mouse monoclonal antibody	Proteinase 3	10 µg/ml	R&D Systems
Rabbit polyclonal antibody	Neutrophil elastase	10 µg/ml	Biorbyt
Rabbit polyclonal antibody	Cathepsin G	10 µg/ml	Biorbyt
Rabbit polyclonal antibody	LL-37	10 µg/ml	Santa Cruz Biotechnology

Mouse monoclonal antibody	Human neutrophil peptides 1-3	10 µg/ml	Hycult Biotech
LAM	Non-anticoagulant heparin	50 ug/ml	
BAPTA, AM	Calcium chelator	5 µM	Thermo Fisher Scientfic
CHIP	H2A binding peptide	200 µg/ml	

After incubation, cells or NETs were washed 3 times with 1x PBS (Gibco) and monocytes (50.000 cell/well) were added to each well containing neutrophils or NETs and set for adhesion as described in 4.2.1. or 4.2.2.

2.5. CHIP Peptide Design

Our collaboration partner used in silico computer analysis to find a protein structures which would bind with high specificity to the histone H2A as demonstrated by their previous work [124, 177, 178]. The derived histone H2A-peptide complexes were subsequently subjected to structural optimization and binding free energy calculations to predict the binding strength of peptides with histone H2A. The cyclic peptide CHIP (H-CEPLSEVEDYLDSSLKYNAKDTINYC-OH containing S-S bond between Cys at the N- and C-terminus), was selected for synthesis.

2.6. Biophysical assays

In nature, most particles carry a certain charge in aqueous solution. Also, cells, including monocytes, carry a certain cell membrane surface charge, which is a negative surface charge [179]. To test whether charge interaction plays a role in monocyte adhesion to NET-resident H2A, the monocyte membrane charge was modified with either 200 µM cholesterol sulfate (Sigma-Aldrich) and 1 µM sulfatase inhibitor STX (Sigma-Aldrich) or 200 µM oleylamine (Sigma-Aldrich). Cholesterol sulfate is a negatively charged compound and causes an increased negative cell membrane charge. Whereas oleylamine is a positively charged compound that causes a lowering of cell membrane surface charge [124]. Both compounds integrate into the phospholipid bilayer of the cell membrane with the lipophilic part.

2.6.1. Visualization of charge caused NET-adhesion.

Electrostatically NET -caused adhesion was studied under static conditions (see 2.4.1.). NETs were incubated with negatively charged silica beads (1 µm, 12.5 mg/ml, Kisker) for 15 min 37°C and 5% CO_2. Non-adherend beads were washed of 3x with 100 µl 1x PBS (Gibco). Extracellular traps were counterstained with DAPI (300nM) and negative charge silica fluoro beads were visualized with Leica microscope Dmi8.

2.6.2. Zeta-potential measurement

The zeta-potential is the electrical potential of a sample in suspension and it is measured in millivolts (mV). This method mathematically calculates the surface

charge by microelectrophoresis where the charged sample moves in a cuvette as a response to an electric field, based on the velocity detected by light scattering. The mathematical calculation is based on the Smoluchowski theory [180].

Leukocyte cell surface charge was measured by using a Malvern Zetasizer. The cuvette (DTS1070, Malvern Instruments) was filled with 600 µl 10 mM sodium chloride (Sigma Aldrich) and a mixture of 10 µl cell suspension (10^6 cells/ml) and 90 µl 300 mM sucrose (Sigma Aldrich). Measurements were performed as triplicates at 37°C. Each replicate with 50 runs and 150 V were applied. In between the replicate's measurement was paused for 2 min.

2.6.3. Atomic force microscopy

Atomic force microscopy (AFM) is a high-resolution method to study force interaction [181]. During force measurements, AFM records force spectroscopy curves showing force-interaction between the probe attached to the cantilever and the sample in a Petri dish. The small spring-like cantilever is flexible and in this kind of application tipless to avoid the destruction of the cell. A laser pointing to the end of the cantilever enables the system to notice the motion of the cantilever via a detector recording the deflection of the laser (Figure 16).

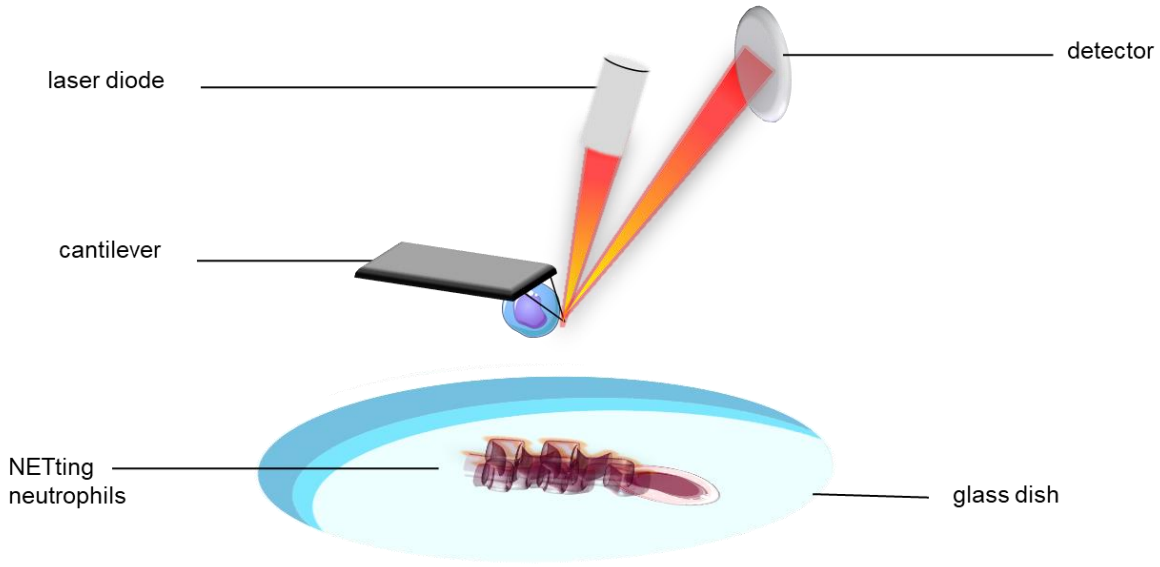

Figure 16: Scheme of atomic force microscopy.

Atomic force microscopy is a powerful tool to measure force interactions. The laser pointed on the cantilever deflects to the detector. This enables the system to detect the motion of the spring-like cantilever. The cell on the cantilever is probed on a sample in a dish to study force interactions.

An atomic force microscope (AFM, Nano Wizard II, JPK) was used to investigate the mechanical properties of single living monocytes with neutrophil extracellular trap under temperature-controlled conditions. To probe monocytes on neutrophil extracellular traps, neutrophils and monocytes were isolated as mentioned in 2.2.1. and 2.2.2. Neutrophils (50.000 cells) were seeded on fluoro dish (wpi, inc) with a glass bottom and left for adherence and NET-formation as described in 2.1. Monocytes were captured on cantilever (MLCT-010, Bruker) coated with 0,1 mg/ml concavalin A (Merck) for 30 min at RT. Before fishing monocytes, the dish and cantilever were washed 3x with Hank's balanced salt solution (Gibco) and cantilever was routinely calibrated on a clean area of the probing dish. Ten thousand monocytes were added to the dish and identified by using the Axiovert 200M microscope (Zeiss). The cantilever was manually guided above the monocyte and released to gently touch the monocyte. After the monocyte adheres to the cantilever (within 1 min), the cantilever with adherent monocyte was

lifted and monocyte viability was controlled by propodiumiodid (5 µl/sample, eBioscience) positive/negative staining (Figure 17).

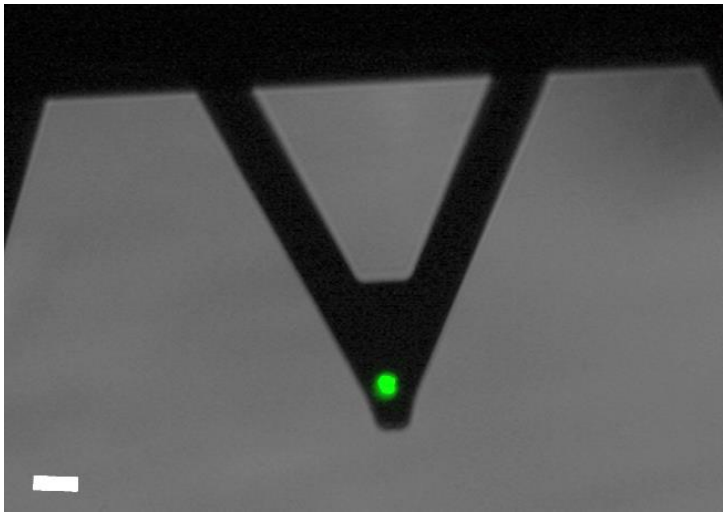

Figure 17: Cell attached to cantilever.

The concavalin A coated cantilever was used to fish a single monocyte. After fishing, the viability was proved by propodiumiodid positive or negative staining. The cell in the image was additionally stained witch calcein AM. Scale bar 20 µm.

AFM force spectroscopy was only performed with living cells. The single monocyte on cantilever tip was brought above a NET-structure and probed with an approach and retraction speed of 10 µm/s, the pulling range was set to 25 µm, the contact time was 0 sec and the maximal force applied to the monocyte was 200 pN. The monocytes were probed on an area of 10 µm resulting in ten acquired force curves. Before probing a next NET-structure, the monocyte was left lifted to recover for 10-15 min. The relevant data were analyzed by using JPK Data Processing software (Version spm-5.0.96) (Figure 18).

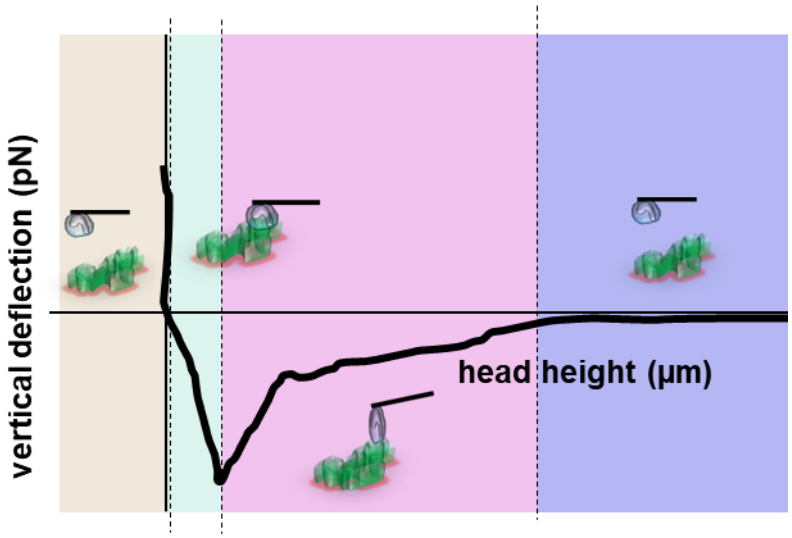

Figure 18: Scheme of atomic force microscopy and force curve.

A monocyte was fished with a cantilever (MLCT-010, Bruker) coated with concavalin A (0,1 mg/ml, Merck). The adherent monocyte was guided on top of the neutrophil extracellular trap and probed with a maximal force of 200 pN. The viability of monocytes was verified by propodiumiodid (5 µl/sample, eBioscience). The applied force curve can be divided into 4 parts. The approach of monocyte to NET-structure (orange), followed by the adhesion force between NETs and monocyte (green). The pink area reflects the detach force after monocyte adheres to NETs and the blue area shows the needed distance of monocyte to NET to separate them again (separation distance).

2.7. *In vitro* monocyte incubation with Histone H2A.

Monocytes isolated as described in 2.2.2. were either pre-incubated with 200 µM oleylamine or 200 µM ch-sulfate and 1 µM STX or left untreated. 10000 monocytes were left for adherence in a 24-well plate loaded with round coverslips at 37°C and 5% CO_2 for 15 min. Afterward, monocytes were incubated with 10 µg recombinant biotylinated-H2A (Biorbyt) for 15 min on ice. Cells were washed with cold 1x PBS and fixed with 4% PFA. Histone H2A was stained with streptavidin labeled with fluorescein isothiocyanate (FITC) and monocytes were visualized by phalloidine membrane staining (1/1000, Sigma-Aldrich) and incubated overnight at 4°C. Nuclei were counterstained with DAPI. Coverslips were transferred to a glass slide and mounted with prolonged antifade (Invitrogen). Samples were imaged with a Leica TCS SP8 microscope using a 63x oil objective. Raw images were deconvolved with Huygens Professional (v.16.10, Scientific Volume Imaging).

2.8. Animal experiments

In order to confirm the findings from in vitro experiments, *in vivo* experiments were conducted in mice.

2.8.1. Genotyping

Mice born in our animal facility were tail biopsied for genotyping. The biopsy was digested in lysis buffer with 0.2 mg/ml proteinase k (Qiagen, Hilden, Germany) overnight at 56°C. The next day, the QIAxtractor kit (Qiagen, Hilden, Germany) was used to isolate the DNA according to the manufacturer's instructions. For all genes, a PCR reagent mix was prepared, including 5x Green Gotaq Flexi buffer (final concentration 1x, Promega, Fichburg, USA), 1.5mM magnesium chloride (Sigma-Aldrich, St. Louis, USA), 0.2 mM dNTPs (Sigma-Aldrich, St. Louis, USA), 0.5 µM forward primer (Sigma-Aldrich, St. Louis, USA), 0.05 U/µl GoTaq DNA polymerase (Sigma-Aldrich, St. Louis, USA) and 200 ng genomic DNA. The PCR mix contained the primer pairs of either the wildtype or mutant allele. Each experiment included positive and negative (water) control. The PCR product was analyzed by gel electrophoresis (QIAxcel Advanced System, Qiagen, Hilden, Germany). As following, PCR reaction programs were used: For *Apoe* the common forward primer 5'GCC TAG CCG AGG GAG AGC CG 3', wildtype reverse primer 5'TGT GAC TTG GGA GCT CTG CAG C 3' and mutant reverse primer 5'GCC GCC CCG ACT GCA TCT 3'. The *Cx$_3$cr1* common forward primer 5'GGT TCC TAG TGG AGC TAG GG 3', wildtype reverse 5'TTC ACG TTC GGT CTG GTG GG 3' and mutant reverse primer 5'GAT CAC TCT CGG GAT GGA CG 3'. The cycler was programmed for 5 min 94°C, 30 sec 94°C, 30 sec 60°C, 72°C 30 sec (*Apoe*) or 60 sec (*Cx$_3$cr1*). The steps two to four were repeated for 35 cycles and continued for 5 min at 72°C followed by a 5 min cycle at 21°C.

2.8.2. *In vivo* experiment setting.

To study the impact of monocyte adhesion to NETs in the pathogenesis of atherosclerosis under endotoxemia, eight weeks old *Apoe*$^{-/-}$ and *Cx3cr1*$^{gfp/WT}$*Apoe*$^{-/-}$ mice were used and fed a high-fat diet (HFD) (21% fat and 0.15% cholesterol (ssniff, Soest, Germany)) for four weeks to induce hypercholesterolemia and the development of early atherosclerotic lesions. Further, to induce endotoxemia, mice were injected with 1 mg/kg lipopolysaccharide (LPS) (Escherichia coli, serotype 055:B5, Sigma Aldrich) in 1x PBS (Gibco) intraperitoneal (i.p.) four hours before the experiment. One group was additionally treated with BB Cl-amidine (BB Cl-A) (1mg/Kg BW, i.p., Cayman Chemical Company) to block NET-formation 12 h before and then with LPS. To investigate whether NET-resident H2A causes monocyte adhesion in vivo the animals receiving LPS were treated with antibody to H2A (20 µg/mouse, Biorbyt) or with a synthesized cyclic peptide-specific binding to H2A (5 mg/kg BW). All mice were housed at a 12-hour light/ 12-hour dark cycle (lights on at 7 am, lights off at 7 pm). The used strains were bred internal.

All animal experiments were approved by the local ethical committee for animal experimentation.

2.8.3. Intravital microscopy

Intravital microscopy was used to study live monocyte adhesion under endotoxemia conditions along the carotid artery in interaction with NETs. First of all, mice were anesthetized with midazolam (5,0 mg/kg), medetomidin (0,5 mg/kg) and fentanyl (0,05 mg/kg). After the loss of reflex, a jugular vein catheter (PE10, Becton Dickinson, Franklin Lakes, USA) was placed right-sided for antibody injection to detect Ly6G directly labelled with PE (1 µg, 1A8, Biolegend) and to apply DAPI (10 µg, Thermo Fisher Scientific) which stains extracellular DNA. Monocytes were

already detectable by green fluorescence protein expressed under the control of the Cx3cr1 receptor in the Cx3cr1$^{egfp/WT}$ Apoe$^{-/-}$ mice. The external carotid artery was imaged using an Olympus BX51 microscope equipped with a Hamamatsu 9100-02 EMCCD camera, and a 10x saline-immersion objective. The adhesion of labeled neutrophils and green fluorescent monocytes was imaged for 30 s. Afterward, one video per mouse was analyzed by counting the number of adherent myeloid cells.

2.9. Plasma lipid measurement

Plasma cholesterol and triglyceride were measured using the CHOD-PAP kit (Roche) and GOP-PAP kit (Roche), according to the manufacturer's instruction.

2.10. Histology

Hearts were fixed in 4% PFA for at least 24 hours and afterward transferred into 30% sucrose (Sigma-Aldrich) for 24 hours. Subsequently, hearts were frozen in tissue-tek O.C.T. compound (Sakura Finetek) and 4 µm sections were collected. The size of atherosclerotic lesions was assessed by hematoxylin and eosin staining. Therefore, specimens were placed into distillate water and transferred in into hematoxylin for 5 min. Excess staining was washed off with tap water for 5 min. Followed by eosin staining for 5 min and again excess staining was removed with tap water. Sections were dehydrated in an ascending ethanol series and finally into xylene. Afterward, specimens were mounted with Roti Histo kitt II (Roth) and stored at room temperature. To capture images a Leica DM4000 microscope with a 20x objective (Leica Microsystems) and a Leica DFC 365FX camera were used and images were analyzed with the free available software ImageJ (National Institutes of Health).

2.11. Immunohistochemistry

To quantify the neutrophil and Mac2 positive cells within the aortic roots, sections were stained with antibodies to Ly6G (1A8, BD Biosciences) and Mac2 (M3/38, biozol). Nuclei were counter-stained by DAPI (Thermo Fischer). A Leica DM4000 microscope with a 20x objective (Leica Microsystems) and a Leica DFC 365FX camera was used to capture images. Sections were primed with antigen retrieval buffer by microwaving the samples. Afterward, the samples were left to cool down and placed in 1x PBS. The tissue was marked with a liquid blocking PAP pen (Dako) and incubated with a blocking solution for 1 hour at room temperature. Afterward, specimens were incubated with the respective antibodies diluted in blocking solution overnight at 4°C. The next day the primary antibody was washed off using 1x PBS and 1x PBS-Tween. The corresponding secondary antibodies were diluted in blocking solution and incubated for 1 hour at room temperature. Nuclei were counterstained with DAPI. Sections were mounted in prolonged gold antifade (Invitrogen).

2.12. Endotoxin measurement

Endotoxin levels in plasma samples were measured with the Pierce Chromogenic Endotoxin Quant kit (Thermo Fisher Scientific) according to the user's instruction. Briefly, plasma samples were diluted 1/50 in endotoxin-free water and heat-inactivated for 15 min at 70°C. Afterward, an amebocyte lysate reagent was added to each sample and incubated for 30 min at 37°C. Finally, the pre-warmed chromogenic substrate was added to each sample, incubated for 6 min. The reaction was stopped by adding the provided stop solution to each sample. The endotoxin levels were quantified by measuring the optical density at 405 nm with Tecan infinite™ 200 pro. Samples were analyzed as duplicates and according to the standard curve plotted as endotoxin units per ml (EU/ml).

2.13. Cell-free DNA measurement

Cell-free DNA content in plasma samples was assessed with the Quant-iT PicoGreen dsDNA assay (Life Technologies). PicoGreen solution was diluted 1/200 in 1x TE buffer (supplied with the kit). Plasma samples were diluted 1/5 with 1x TE buffer and mixed 1:1 in a 96-well plate (Falcon corning) and incubated for 5 min at room temperature. Samples were quantified by fluorescence mean intensity at 480 nm emission with Tecan infinite™ 200 pro. According to the standard curve, cell-free DNA plasma concentration was plotted as µg/ml.

2.14. NETs-ELISA

The concentration of neutrophil extracellular traps in plasma samples was assessed by modified myeloperoxidase ELISA Kit (HK210-01, Hycult Biotech) and a cell death detection kit (Roche) as described elsewhere. In detail, plasma samples were added to the ready to use MPO-antibody coated wells and diluted 1/4 in the supplied dilution buffer, incubated for 60 min at room temperature. Wells were washed 4x with supplied washing buffer and subsequently incubated with anti-DNA antibody (diluted 1/40 according to the instruction). Samples were incubated for 90 min at RT and washed with a supplied washing buffer. Peroxidase 2,2'-azino-bis(3-ethylbenzothiazoline-6-sulfonic acid (ABTS) was added to the wells and incubated for 20 min in dark. Afterward, the color change was measured via the optical density at 405 nm with Tecan infinite™ 200 pro reader.

2.15. Flow cytometry

Flow cytometry is a measurement method which is applied in biological and medical analysis. It dissects different cell types by applied high flow and is laser-based.

According to the cell size, granularity or specific antibody staining cells can be specifically characterized. The forward scatter light gives information about size and side scatter light provides information about cell granularity. To determine specific cell-expressed molecules direct fluorescence-labelled antibodies were used.

2.15.1. Blood sample preparation for flow cytometry

Blood was drawn retrobulbar with a capillary and collected in EDTA tube (Sarstedt). 100 µl blood were lysed in 3 ml lysis buffer for 15 min at room temperature. Lysis was stopped with 3 ml of Hanks buffer. Samples were centrifuged for 5 min at 300 g. The cell pellet was directly resuspended in 50 µl staining solution with the corresponding antibodies (see 2.14.5).

2.15.2. Bone marrow sample preparation

The bone marrow of a mouse femur was flushed with 3 ml of Hanks. The sample was centrifuged (5 min, 300 g) and cell the pellet was resuspended in 1 ml lysis buffer to lyse the remaining erythrocytes for 1 min at RT. Lysis was stopped by adding 1ml of Hanks buffer. After centrifugation (5 min, 300 g) cell pellet was resuspended in 1 ml Hanks buffer and 100 µl of the sample was used for flow cytometry.

2.15.3. Spleen sample preparation

1/3 of mouse spleen (plump end) was minced through a 30 µm filter (CellTrics, Partec) which was washed with 3 ml Hanks buffer. The cell suspension was

centrifuged for 5 min at 300 g. To lyse the erythrocytes, the cell pellet was resuspended in 1 ml lysis buffer and after 1 min lysis (RT) was stopped by adding 1ml Hanks buffer. Sample was again centrifuged (5 min, 300xg) and cells were resuspended in 1 ml Hanks buffer. 50 µl of the cell suspension was used for flow cytometry.

2.15.4. Aorta sample preparation

To analyze the descending fat-free aorta, the aorta was minced in digestion medium (1,25 mg/ml liberase, Roche, 10% FCS in RPMI, gibco) and incubated for 1 h at 37°C (water bath). The aorta was pipetted up and down every 30 min up and down to support the digestion. After 1h of incubation 500 µl of Hanks buffer was added and the sample was filtered to obtain a single cell. The cell suspension was centrifuged for 5 min at 300 g. Cell pellet was resuspended in RPMI with 10% FCS for antigen retrieval and left 30 min at 37°C and 5% CO_2. After an additional centrifugation step (5 min, 300 g) the cell pellet was directly resuspended in antibody staining solution with respective antibodies (see 2.14.5).

2.15.5. Cell counts

Blood, bone marrow, and splenic single cells were conducted using combinations of antibodies specific for CD45 (A20, eBioscience), CD11b (M1/70, eBioscience), CD115 (AFS98, eBioscience). Before cell staining, red blood cell lysis was performed. Further, aorta was digested by liberase (1,25mg/ml, Roche) and single cells were labelled with antibodies to CD11b (M1/70 BioLegend), Ly6G (1A8, BioLegend), MHC II (M5/114.15.2, BD Bioscience), Gr1 (RB6-8C5, BioLegend), F4/80 (BM8, BioLegend), CD45 (A20, eBioscience). Cells were washed with Hanks buffer and directly analyzed by flow cytometry using a FACSCantoII (BD). Absolute

cell numbers were assessed by the use of CountBright™ absolute counting beads (Invitrogen). Data were analyzed with FlowJo Software (BD, 10.1 Flowjo LLC).

Table 4: Analysis strategy for myeloid cells determination in different organs.

To analyze the different cell types in the different organs the samples were stained with direct fluorescence antibodies to the specific proteins expressed on the cell surface. The different cells were determined by using the following strategies:

Cells	Blood/Bone marrow/Spleen	Aorta
Neutrophils	CD45+, CD11b+, Gr1high, CD115-	CD45+, CD11b+, MHCII-, F4/80-, Gr1high, Ly6G+
Classical monocytes	CD45+, CD11b+, Gr1high, CD115-	CD45+, CD11b+, MHCII-, F4/80-, Gr1high, Ly6G-
Non-classical monocytes	CD45+, CD11b+, Gr1low, CD115+	CD45+, CD11b+, MHCII-, F4/80- , Gr1low, Ly6G-
macrophages	-	CD45+, CD11b+, MHCII+, F4/80+

2.16. Statistics

All statistical analyses were performed using GraphPad Prism 8 software. Outliers were determined by Grubbs' test with $\alpha=0.05$. To test normal distribution, the D'Agostino-Pearson omnibus test for normality was used. If normality was passed, data were tested by a two-tailed unpaired t-test or one-way ANOVA with Dunnet's correction. The Mann-Whitney test or Kurskal-Wallis test with Dunn's correction was performed when data were not normally distributed. In all used tests a 95% confidence interval was utilized with $p<0.05$ was assumed as a significant difference. All data are represented as mean ±SEM.

3. Results

During infections, neutrophils are highly activated to clear pathogens by phagocytosis or degranulation of antimicrobial proteins to the environment [13]. An additional defense strategy has been described in 2004 [32]. It has been shown, that neutrophils are able to release their genomic DNA as filament fibers to the environment upon infection. Those fibers are called neutrophil extracellular traps (NETs) and are decorated with cationic antimicrobial proteins to kill bacteria [32, 39]. Besides, protecting the host from invading pathogens, NETs have been described to be involved in many diseases if they are extensively produced or not adequately cleared from the host tissue. Studies show evidence of tissue damage including endothelial dysfunction, an initial step of atherosclerosis if NETs persist for a long period [67]. The highly cationic NET-associated granule proteins have been shown to favor leukocyte adhesion either by specific receptor interaction or even via charge interactions [16, 34, 92, 93]. Further, it has been shown that NETs are involved in lytic cell death within the plaque through charge mediated pore formation. Consequently, plaque vulnerability was highly increased [124]. Moreover, epidemiological studies reveal a dramatically increased risk to suffer from myocardial infarction or stroke after a respiratory infection. The risk is at its highest within the very first days [154, 155].

Here we hypothesize that endotoxemia-activated neutrophils cause NET-accumulation which would lead to increased recruitment of immune cells to atherosclerotic lesions and result in accelerated atherosclerosis. Therefore, we studied atherosclerosis development under endotoxemia conditions in a well-established *Apoe*$^{-/-}$ mouse model in early atherosclerosis to observe the effect on NETs in recruitment. Mice enrolled in this study received a high fat diet for 4 weeks to develop early atherosclerotic lesions. In addition to the high fat diet, the acute infection was mimicked by a single LPS challenge.

3.1. Neutrophil extracellular traps accelerate atherosclerosis during endotoxemia

In initial experiments, we tested if endotoxemia causes accelerated lesion formation and if neutrophil extracellular traps impact on this phenomenon.

3.1.1. Endotoxemia NET-formation accelerates atherosclerotic lesion development

Endotoxins are bacteria-derived lipopolysaccharides (LPS) originating from gram-negative bacteria. Commensal gram-negative bacteria colonize the gut and account for 70% of the gut microbiome [182]. However, gram-negative bacteria, commensal or pathogen, have LPS in the outer membrane, which is released to the environment upon cell growth, division, or death [183]. Circulating pyrogens activates leukocytes such as neutrophils and causes NET-release. Neutrophil extracellular trap-formation is at one hand a potent immune defense strategy but on the other hand, it has been associated with fueled inflammation [54, 164]. Neutrophils originate from the bone marrow and extramedullary tissue, like spleen [184]. They are fast mobilized into the bloodstream to rapidly reach the site of infection. Further, under hypercholesterolemia conditions circulating neutrophil numbers are elevated which have been shown to be crucial for lesion development [98]. Epidemiological studies indicating infection as a potent risk factor to suffer from cardiovascular disease, especially within the first days after acute respiratory infection [154].

We studied atherosclerosis in an early atherosclerosis model with mice lacking the *Apoe* gene and feeding them a high fat diet for four weeks (Figure 19 A). Endotoxemia was mimicked by intraperitoneal LPS injection (1mg/Kg BW) four hours before the end of the experiment. To define the role of neutrophil extracellular traps, one group received pharmacological NET-inhibition treatment with BB Cl-

amidine (BB Cl-A), an inhibitor of the peptidylarginine deiminases (PAD) [185]. It has been shown that PAD4 plays a critical role during NET-formation which in turn is involved in atherosclerosis development [135]. BB Cl-A was administered intraperitoneal 24 hours before mice were challenged with LPS and a second BB Cl-A injection followed four hours before the end of the experiment with the LPS challenge. Mice receiving a four h LPS challenge showed a dramatically increased atherosclerotic lesion formation within the aortic roots compared to the control group (PBS). Interestingly, this effect was limited if NET-formation was pharmacologically blocked with BB Cl-A (Figure 19 B). Vessel size of the aortic roots was not affected by the induced endotoxemia as analyzed in H&E staining (Figure 19 C-D).

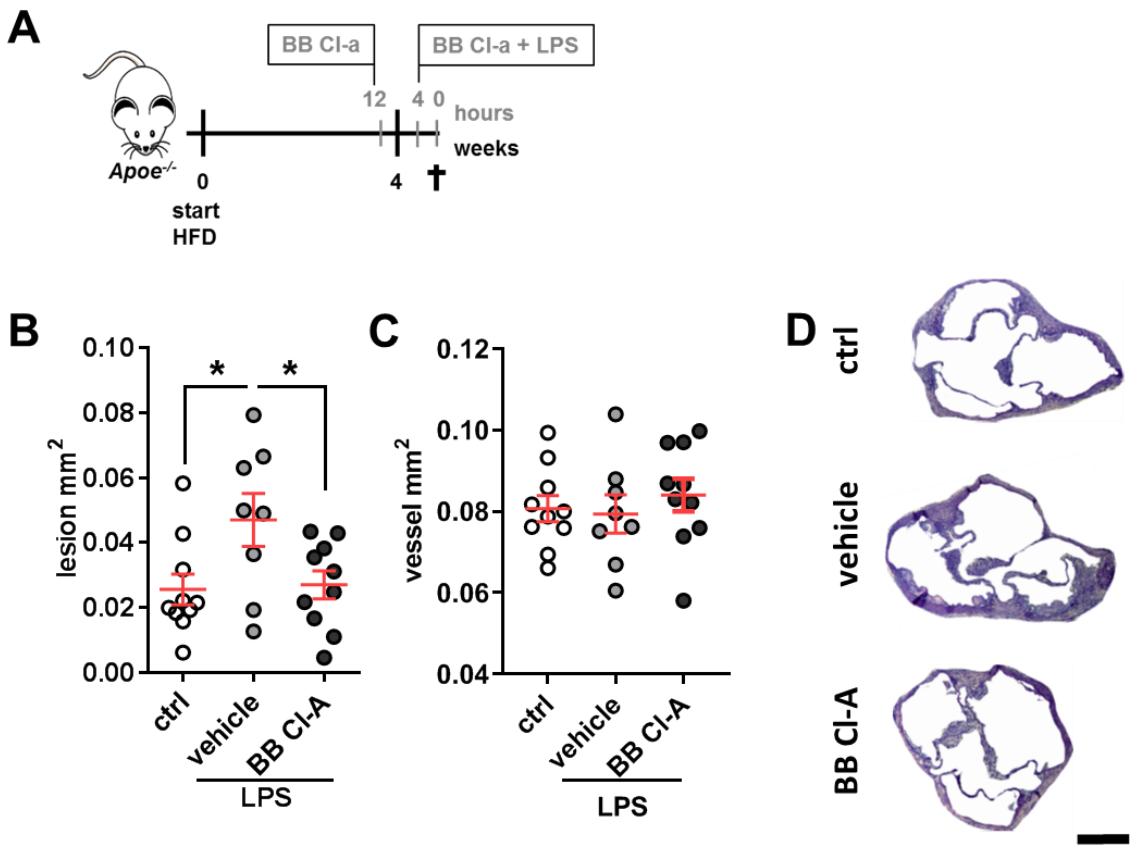

Figure 19: Endotoxemia induced NET-formation heightened atherosclerotic lesion formation.

A) Experimental scheme; *Apoe* –deficient mice fed an HFD for 4 weeks. One mouse group was injected intraperitoneal either with PBS (ctrl) or with LPS (1mg/Kg BW) for four hours (vehicle). A third group was treated with a pharmacological NET- formation inhibitor (BB Cl-amidine, BB Cl-A, (1mg/Kg BW)) 12 h before and with LPS i.p. injection. **B)** The atherosclerotic lesion size was assessed in the aortic root and shown as mm^2. **C)** Additionally, to the lesion size, the size of the aortic root was analyzed and expressed in mm^2. **D)** Representative H&E images of the aortic root, scale bar 300 µm. Data are analyzed by one-way ANOVA with Dunnett's multiple comparisons tests; *p≤0.05, **p≤0.01, ***p≤0.0001. All data are presented as mean ±SEM.

Endotoxemia induced by LPS reduced the number of circulating leukocytes (Figure 20 A, D), as well as bone marrow associated leukocytes (Figure 20 B, E) and splenic leukocytes (Figure 20 C, F). However, LPS is a potent activator of leukocytes, therefore the activation status of these leukocytes, we assessed by measuring the expression level of CD11b on neutrophils and monocytes from the circulation, bone marrow, and spleen. After four hours of LPS treatment, circulating neutrophils and monocytes show a significantly increased CD11b expression (Figure 20 A, D). Interestingly, neutrophil and monocytes from the bone marrow did not show a similar increase in CD11b expression as observed in circulating cells

(Figure 20 B, E). Further, the CD11b level of splenic neutrophils under endotoxemia conditions was not altered compared to splenic monocytes (Figure 20 C, F).

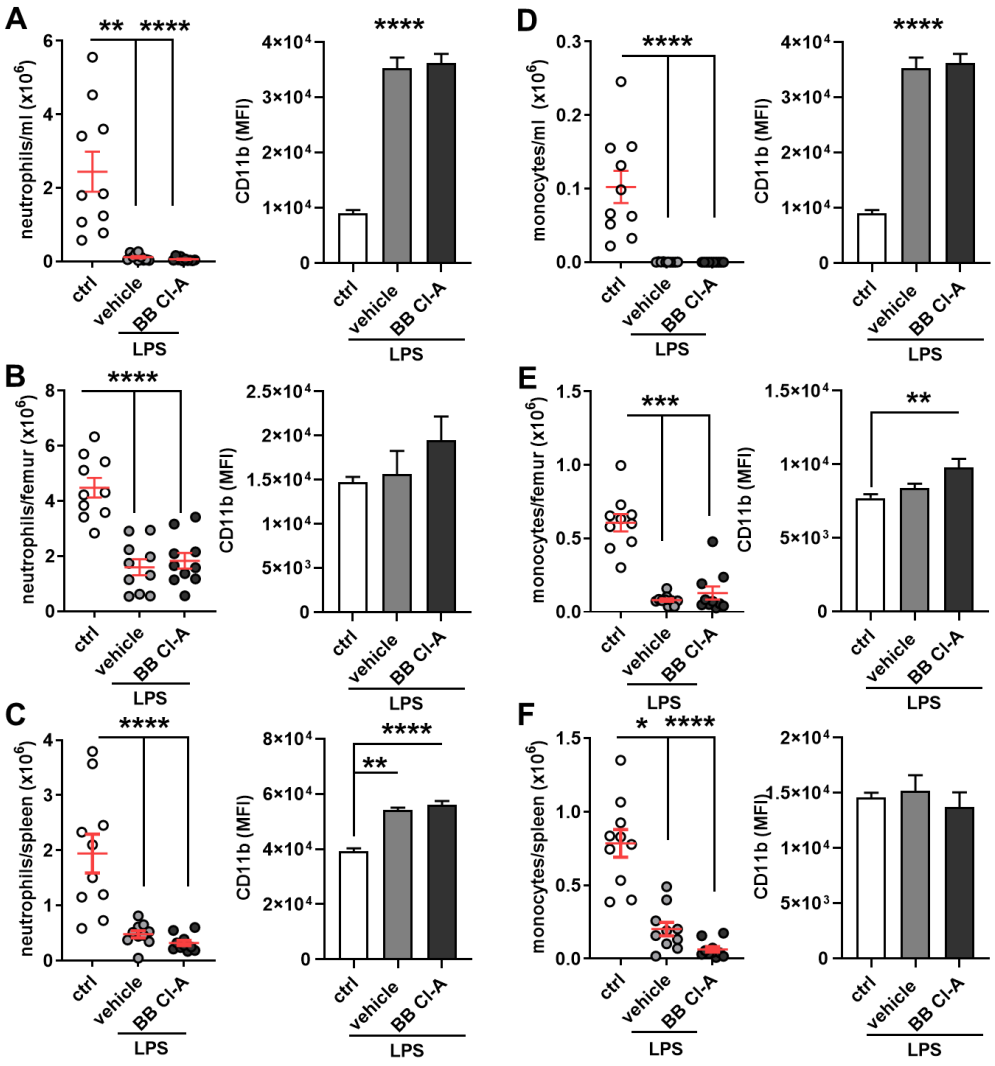

Figure 20: Flow cytometry analysis of hematopoietic tissue and blood.

Four hours after LPS injection blood neutrophil **(A)** and monocyte **(D)** counts are reduced compared to the control group. Whereas the CD11b expression is highly increased. Bone marrow leukocytes **(B, E)** and splenic leukocytes **(C, F)** are also reduced after LPS treatment compared to the control group. Splenic neutrophils show an increased CD11b expression after LPS treatment **(C)** but not bone marrow associated neutrophils **(B)**. Monocyte CD11b expression levels are not altered in bone marrow or spleen in comparison to the control group **(E-F)**. Treatment of endotoxemia mice with BB Cl-A did not reverse the cell count reduction either the CD11b expression level. **A, E, F)** Data are analyzed by Kruskal-Wallis test with Dunn's post-test, and data are shown in **B, C, D)** are analyzed by one-way ANOVA with Dunnett's multiple comparisons test *p≤0.05, **p≤0.01, ***p≤0.0001. All data are presented as mean ±SEM.

3.1.2. Plaque associated cells are elevated during endotoxemia

The first results indicate that NETs seem to play a critical role during accelerating atherosclerotic lesion formation because NET-formation inhibition with BB Cl-A abolished heightened atherosclerotic lesion formation. Dramatically lesion growth can be caused by various means. To determine the lesion composition, histological sections of the aortic roots have been stained with DAPI, to counterstain nuclei. We observed increased cell numbers within the lesion of endotoxemia mice compared to control mice. However, pharmacological treatment with BB Cl-A limited the cell numbers within the lesion of endotoxemia mice (Figure 21 A). Furthermore, mice suffering from endotoxemia showed an increased lesional neutrophil count (Figure 21 B) and elevated numbers of lesion-associated mononuclear cells positively stained for Mac2 (Figure 21 C) within the aortic root. In contrast to that, endotoxemia mice treated with the pharmacological compound BB Cl-A did not show such an increase in lesion associated cells. Taken together, mice suffering from endotoxemia showed a larger atherosclerotic lesion with increased cellularity compared to control mice or pharmacological treaded animals (Figure 21 D).

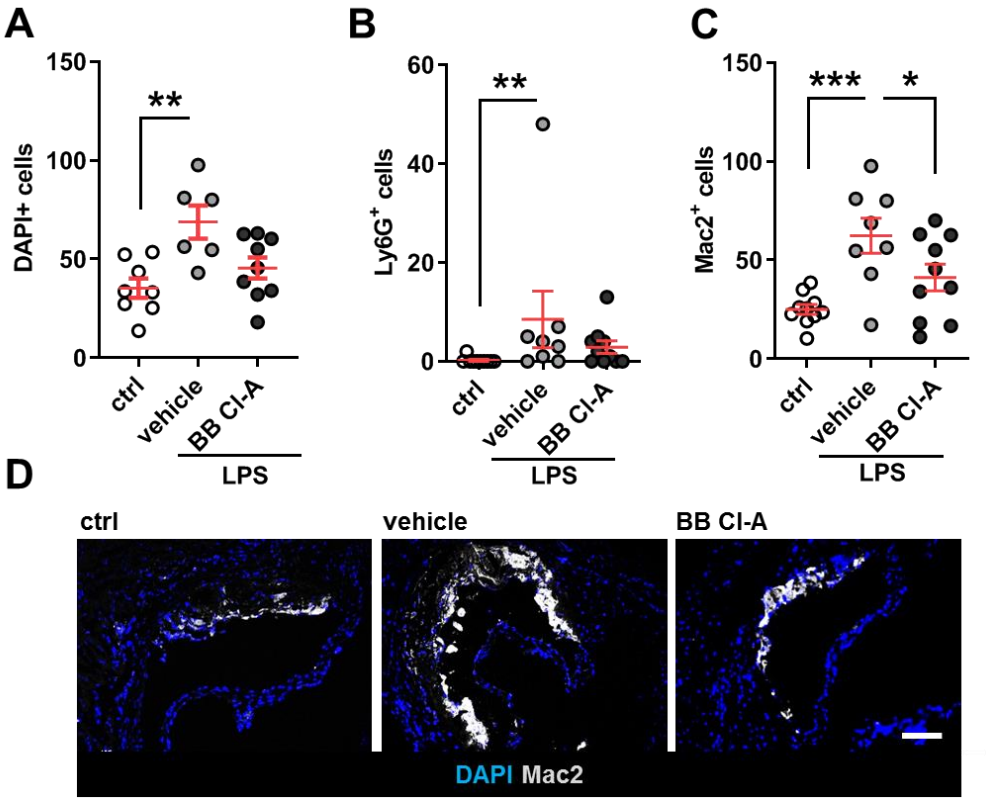

Figure 21: Lesion associated cell increase under endotoxemia conditions.

A-C) The lesion cellularity was overall analyzed by DAPI staining **(A)** and in more detail by co-staining cells with antibodies to Ly6G **(B)** and Mac2 **(C)**. Results were expressed as mean cell numbers per aortic root. **D)** Representative immunohistochemistry image of Mac2 positive staining (grey) (DAPI, blue), scale bar 50 µm. Data are analyzed by Kruskal-Wallis test with Dunn's post-test **(A-B)** and one-way ANOVA with Dunnett's post-test **(C)**; *p≤0.05, **p≤0.01, ***p≤0.0001. All data are presented as mean ±SEM.

3.1.3. Neutrophil extracellular trap formation under endotoxemia conditions

It has already been suggested that NETs play a crucial role during atherogenesis [135, 140]. Therefore, we tested the mice plasma samples for their DNA amount. By measuring the plasma samples with a PicoGreen assay, we observed an increased dsDNA plasma level in mice that suffered from endotoxemia compared to the control group or endotoxemia mice treated with NET-inhibitor BB Cl-A (Figure 22 A). Although the plasma endotoxemia levels (EU/ml) were equally increased in

both groups receiving LPS with or without NET-inhibitor treatment in comparison to the control group (Figure 22 B). Consistent with these results, we observed a correlation between endotoxemia levels and NETs plasma level measured in MPO-DNA ELISA (Figure 22 C).

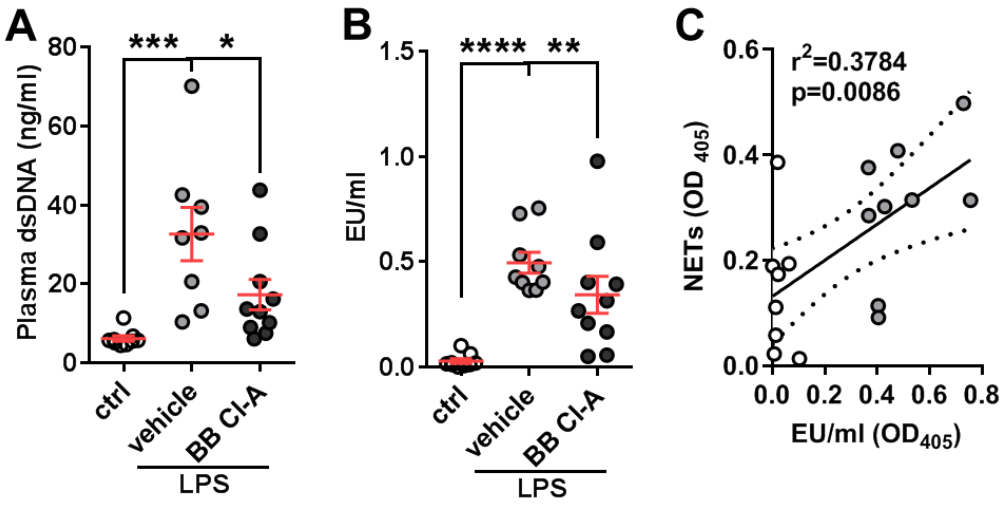

Figure 22: Endotoxemia induces NET-formation.

A) PicoGreen analysis of cell-free dsDNA in plasma samples shown as ng/ml and **(B)** Plasma endotoxin concentration measured with amebocyte lysate assay. **C)** Plasma levels of neutrophil extracellular traps (MPO-DNA ELISA) correlating with plasma endotoxin level (pearson correlation). Data are analyzed by Kruskal-Wallis test with Dunn's post-test; *p≤0.05, **p≤0.01, ***p≤0.0001. All data are presented as mean ±SEM.

3.1.4. Neutrophil extracellular traps trigger myeloid cell adhesion under endotoxemia conditions

The previous findings indicate that NETs might accelerate atherosclerosis. If neutrophils were able to form NETs, atherosclerotic lesions were significantly enlarged and show elevated cellularity in the group of mice suffering from endotoxemia compared to the second endotoxemia group receiving the NET-

inhibitor or to the control group, receiving PBS. Further, endotoxemia mice show high plasma extracellular DNA levels which are lowered if NET-formation is inhibited. Thus, we assume NETs play a critical role in atherosclerotic lesion formation during infection. To test whether neutrophil extracellular traps are present in the arterial lumen and if it has any effect on leukocyte recruitment, we performed intravital microscopy (IVM) of the left common carotid artery.

For this experimental setting, we used mice expressing a green fluorescent protein under the control of the Cx_3cr1, a g-protein coupled receptor which is expressed on monocytes. In addition, these mice lack the *Apoe* gene and received HFD for four weeks. To mimic acute infection, mice were challenged four hours before IVM with LPS (1 mg/Kg BW). A second group received additionally to LPS the NET-formation inhibitor BB Cl-A (Figure 23 A). We exposed the left common carotid artery of $Cx_3cr1^{gfp/WT}$ $Apoe^{-/-}$ mice to examine it with IVM. Mice were injected with a Ly6G-PE antibody and DAPI to counterstain neutrophils and extracellular DNA. Under endotoxemia conditions we observed extracellular DNA in fiber-shape, assuming this would be NET-like structures (Figure 23 B). In contrast, these NET-like structures were strongly reduced in the control group and mice treated with NET-inhibitor (Figure 23 C). Interestingly, under endotoxemia conditions we observed an increased number of luminal adherent neutrophils by Ly6G-PE staining (Figure 23 D) and monocytes (Figure 23 E) if NET-structures were detectable compared to control mice. However, neutrophil adhesion was diminished in endotoxemia mice if NET-formation was inhibited. In agreement with the increased adhesion observed by IVM, we detected also increased neutrophil and monocyte numbers of the descending aorta by flow cytometry, when mice were treated with LPS compared to the control group (Figure 23 F-H). The cell numbers were reduced when endotoxemia mice received BB Cl-A treatment. This data reveals, that endotoxemia might cause NET-formation, which facilitates an increased luminal adhesion of neutrophils and monocytes.

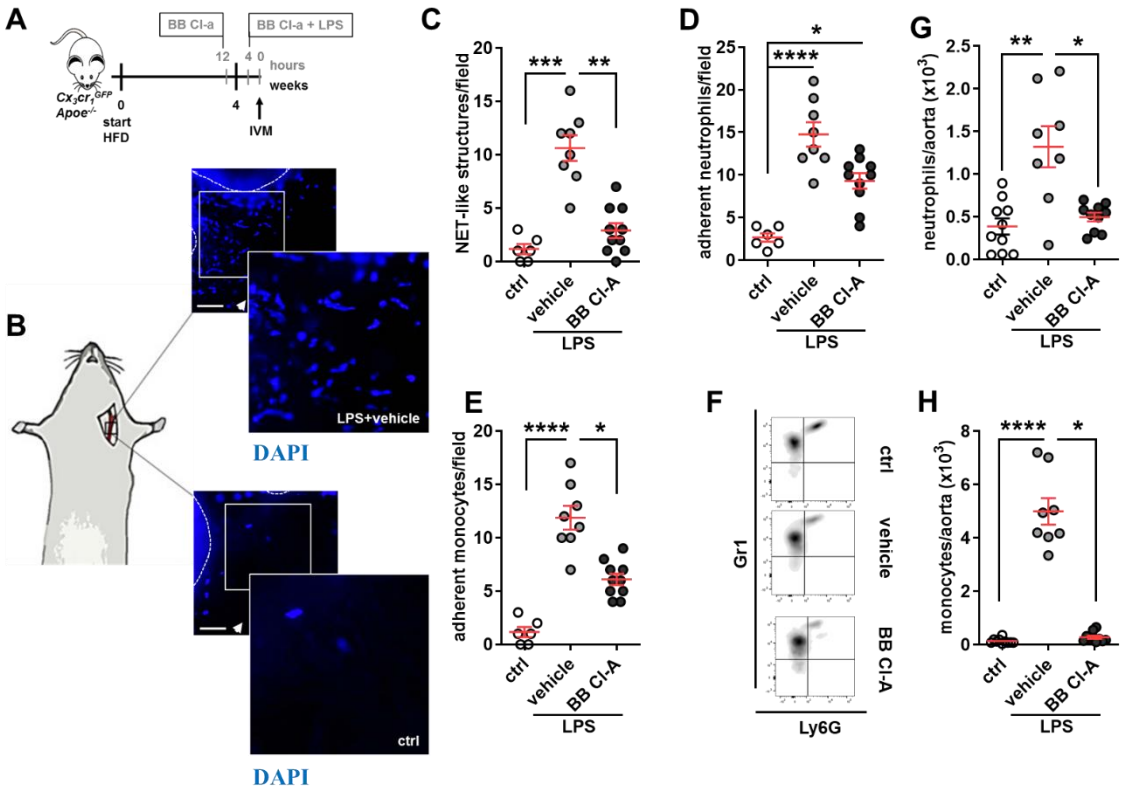

Figure 23: Endotoxemia caused NET-formation fosters luminal leukocyte adhesion.

A) Apoe$^{-/-}$ Cx3cr1^{GFP} mice were fed an HFD for 4 weeks. One experimental group was injected i.p. with PBS (ctrl), a second group with LPS (1mg/Kg BW) four hours (vehicle) before the end of the experiment. A third group received a protein arginine deiminases inhibitor (BB Cl-amidine, BB Cl-A, (1mg/Kg BW, i.p.)) 12 h before and with intraperitoneal LPS injection. **B)** Representative intravital microscopy images of Apoe$^{-/-}$ Cx3cr1^{GFP} mice left common carotid artery, extracellular DNA is shown in blue (DAPI). Scale bar 50 µm. **C-E)** Quantification of intravital microscopy of the carotid artery. **C)** Analysis of luminal NET-like structures (extracellular DNA in fiber shape, stained in blue (DAPI)), **(D)** luminal adherent neutrophils, and **(E)** adherent monocytes. Data are analyzed by Kruskal-Wallis test with Dunn's post-test; *p≤0.05, **p≤0.01, ***p≤0.0001. All data are presented as mean ±SEM.

3.2. Monocyte adhesion to NETs in vitro

The classical recruitment cascade is initiated by selectin-interaction slowing down circulating leukocyte followed by integrin-mediated cell arrest [186]. Beside classical adhesion molecules expressed on activated endothelium, also granule proteins released from neutrophils facilitate monocyte adhesion. It has been shown show

that α defensin, LL-37, and cathepsin G support monocyte adhesion [34, 92]. These proteins are also located in neutrophil extracellular traps [39].

3.2.1. Monocyte adhesion to neutrophil extracellular traps in vitro

The previous results have shown that neutrophil extracellular trap benefits leukocyte adhesion at the bifurcation site *in vivo* where blood flow is disturbed and caused an accelerated lesion formation under endotoxemia conditions in the aortic roots. Next, we asked how neutrophil extracellular traps facilitate luminal leukocyte adhesion. Therefore, we studied monocyte adhesion to NETs *in vitro*. First, we wanted to evaluate if neutrophils per se or simply neutrophil extracellular traps caused monocyte adhesion. Using a static adhesion and a flow adhesion assay we figured out a NET-dependent monocyte adhesion (Figure 24 A-B). Furthermore, the digestion of the NET-backbone DNA before monocyte adhesion did not lead to monocyte adhesion (Figure 24 A, D). However, monocyte adhesion to NETs was not altered by incubating monocytes with paraformaldehyde (PFA), which crosslinks surface proteins to prevent monocyte receptors or adhesion molecules to interact with neutrophils extracellular traps, neither pre-incubating monocytes with pertussis toxin, a pan g-protein coupled receptor antagonist, reduced monocyte adhesion (Figure 24 C, F). Since chemokines and cytokines guide leukocyte trafficking in inflammation, we additionally treated monocytes with different chemokine and cytokine receptor antagonists and with antagonists to formyl peptide receptor (Figure 24 G). Interestingly, the different treatments did not alter the adhesion ability of monocytes to NETs. In addition, we also blocked TLRs to test whether, if danger associated molecules, released during NETosis would activate monocytes for adhesion. However, blocking TLRs with small molecule inhibitors had no influence on monocyte adhesion to NETs (Figure 24 H). Moreover, we also blocked integrins on monocytes with antibodies to VLA4, LFA1, and MAC1 in case netting neutrophils or NETs themselves would cause monocyte adhesion via adhesion molecules (Figure 24 I). However, blocking integrins on the monocyte surface did not alter monocyte adhesion to NETs. Taken together, monocyte adherence to neutrophil extracellular traps seems to be independent on surface molecule interaction *in vitro*.

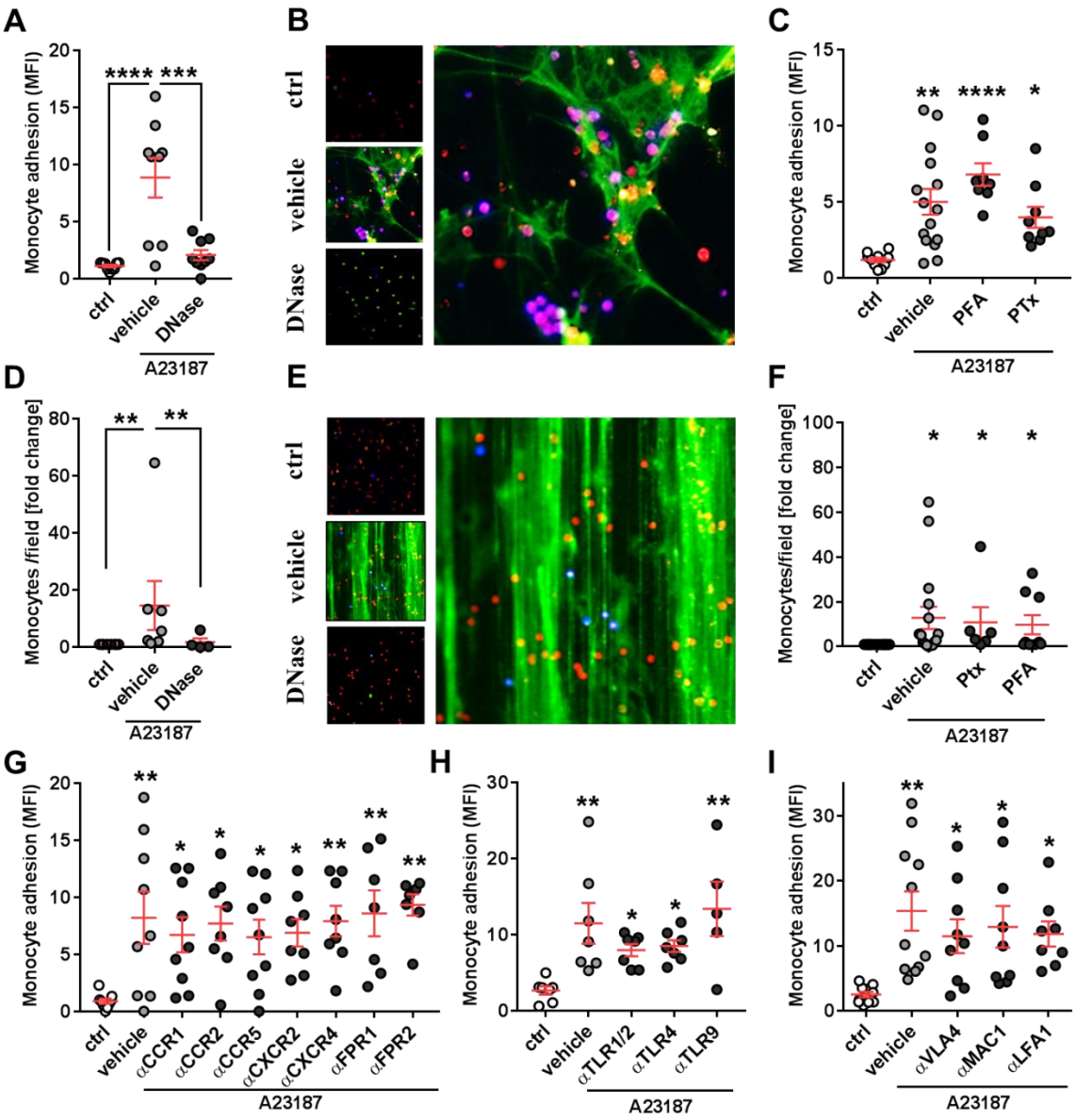

Figure 24: Neutrophil extracellular traps serve as an adhesion scaffold for monocytes in vitro.

A-I) *In vitro* monocyte adhesion to released NETs under static or flow conditions (0.5 dynes/cm^2). **A, D)** Monocytes were left for adherence to unstimulated neutrophils (ctrl), to NETs (vehicle), or digested NETs (DNAse). **C, D, G-I)**. In the second experimental setting, monocytes were pretreated with antagonists to g-protein coupled receptor or pattern-recognition-receptors. Further, monocytes have been incubated with antibodies to integrins and with pan protein g-coupled receptor antagonist or fixative. **B, E)** Representative fluorescence microscopic image of monocyte (violet) adherent to NETs (green; neutrophils red) under static conditions (**(B)** scale bar 50 µM) or under flow conditions (**(E)** scale bar 100 µM). Monocyte adhesion was quantified by mean fluorescence intensity **(A, C, G-I)** or by cells per field **(D, F)**. Data are analyzed by one-way ANOVA; *p≤0.05, **p≤0.01, ***p≤0.0001. All data are presented as mean ±SEM.

3.2.2. NET-resident histone H2A cause monocyte adhesion

The previous results indicate that monocyte adhesion to NETs is independent of cell surface molecule interactions. Therefore, we tested if neutrophil extracellular traps associated proteins were able to cause monocyte adhesion. To this end, we blocked a variety of granule proteins, which have been detected in NETs previously [39]. NETs were either incubated with antibodies to α-defensin (HNP1-3), cathelicidin (LL-37), myeloperoxidase (MPO), proteinase 3 (PR3), neutrophil elastase (NE) or cathepsin G (catG). After incubating NETs with these antibodies, monocytes were added for adhesion. Blocking granular proteins associated with neutrophil extracellular trap structures did not alter monocyte adhesion (Figure 25 A). However, besides granule proteins, also histones are associated with NETs and they account for more than 70% of all proteins within the NET. Therefore, NETs were incubated with antibodies to core histone H2A, H3, citrullinated H3, and H4 before adding monocytes to NETs for adhesion. Finally, monocyte adhesion was reduced compared to vehicle control (Figure 25 B). As visualized in confocal microscopy, H2A covered the NET, and monocytes binding-site is co-localized with histone H2A (Figure 25 C). Since we could not detect any receptor interaction we tested if charge interaction could cause adhesion, because histones are highly cationic charge. Interestingly, incubating monocytes with compounds altering the cell membrane surface charge caused a change in H2A binding to the cell membrane. Meaning, if monocytes were incubated with cholesterol sulfate, which adds negative charges to the cell membrane, more H2A binds to the monocytes, according to its high cationic character. In contrast, incubating monocytes with oleylamine, shifting the membrane charge of monocytes to a less negative charged one, caused less binding of H2A to the membrane (Figure 25 D).

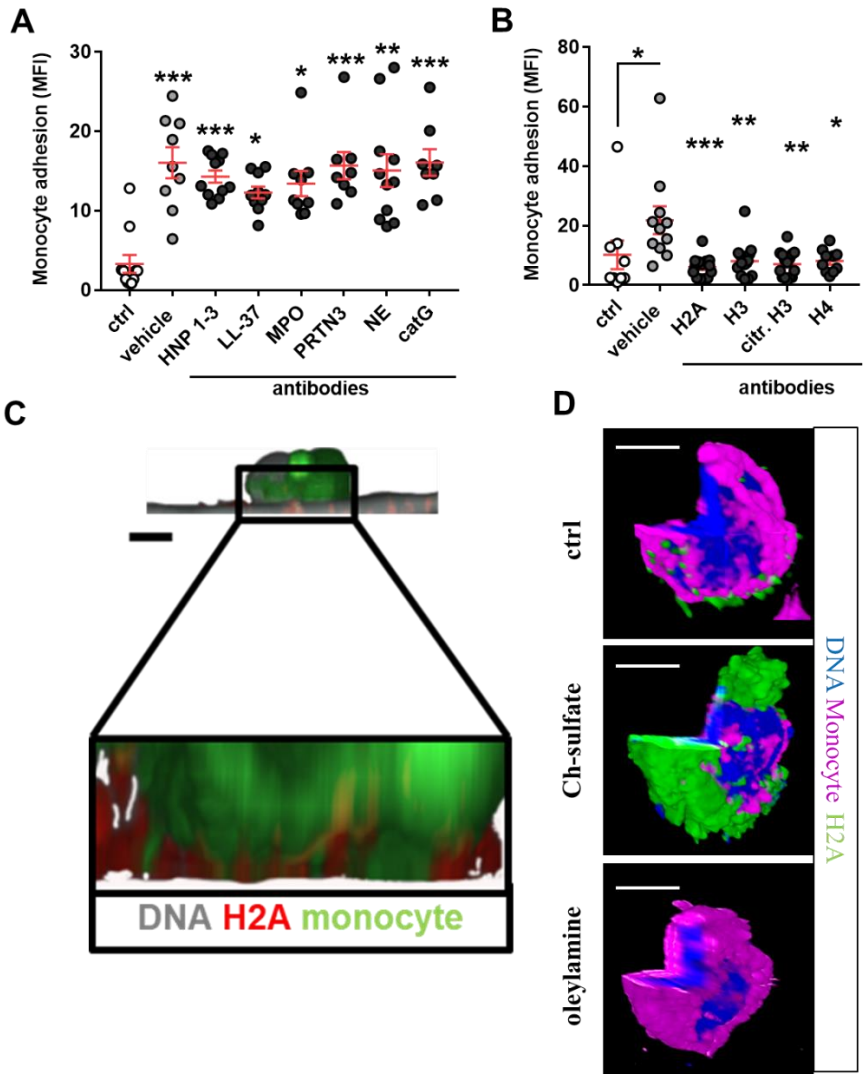

Figure 25: Monocyte adheres to NET-associated histone H2A.

A) Monocyte adhesion to NETs pre-incubated with antibodies to NET-associated antimicrobial peptides and Histones **(B)** analyzed by Kurskal-Wallis test with Dunn's post-test. **C)** Representative immunofluorescence confocal microscopy image (DNA white, monocyte green, H2A red), scale bar 10 µm. **D)** Representative confocal microscopy image of H2A binding monocyte in a charge dependent-manner, DNA blue, monocyte purple, H2A green, scale bar 5 µm. Data are analyzed by unpaired t-test unless otherwise stated; *p≤0.05, **p≤0.01, ***p≤0.0001. All data are presented as mean ±SEM.

3.3. Monocyte adhesion to NETs in charge-dependent fashion *in vitro*

Adhesion is a crucial process for cell communication as well as regulation. Classical adhesion cascade involves integrin, cadherin, and selectin-interactions with its ligands. The protein-protein interactions facilitated cell adhesion underlies van der Waals, hydrophobic- or electrostatic interactions. Most particles show a certain charge in aqueous solution. Leucocytes have on the cell membrane surface a carbohydrate-rich glycocalyx with an overall negative charge. Many charge interactions have been described in nature, *e.g.* bacteria are trapped by neutrophils extracellular traps according to charge interactions or neutrophil-derived MPO facilitate monocyte adhesion in a charge-dependent manner [93, 181, 187].

3.3.1. Neutrophil extracellular traps attract monocytes electrostatically

In agreement with our previous findings *in vitro*, the ζ-potential of monocytes incubated with Ch-sulfate was more negative compared to untreated cells. Further, monocytes incubated with oleylamine showed a less negative ζ-potential (Figure 26 A-B). Monocytes with altered cell surface charges were added for adhesion to NETs under static conditions. The number of adherent monocytes was increased, if monocytes had an increased negative cell surface charge (Figure 26 D-E). This finding correlates with the binding ability of monocytes (Figure 26 C). Our data indicate a charge dependent monocyte adhesion to NETs. To test whether the charge is the crucial mediator, negative beads were incubated with NETs, demonstrating that charge has an impact on cell adhesion *in vitro* (Figure 26 F).

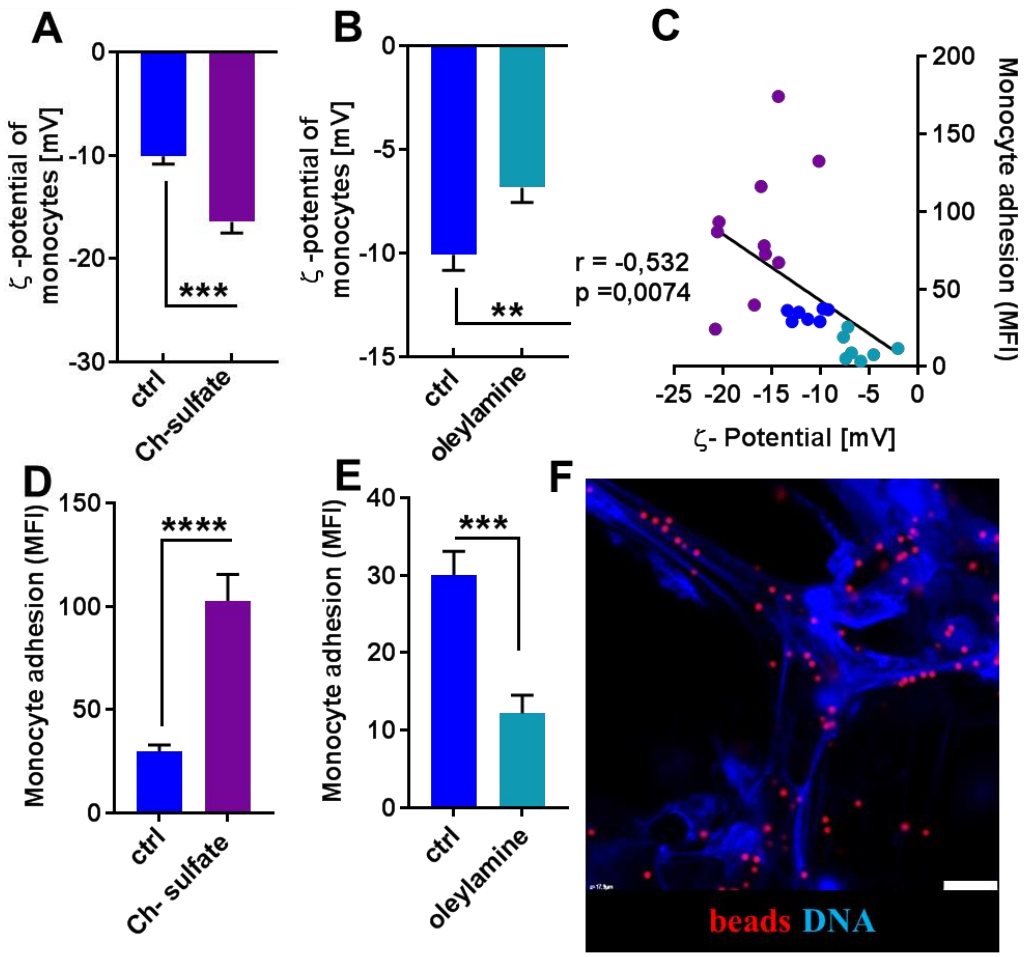

Figure 26: NETs as an electrostatic adhesion scaffold.

A-B) Zeta Potential analysis of isolated monocytes treated with Ch-sulfate **(A)** or oleylamine **(B)**. **C)** Pearson correlation of adhesion ability and zeta-potential of monocytes pre-incubated with Ch-sulfate or oleylamine. **D-E)** Mean fluorescence intensity of adherent monocytes either treated with Ch-sulfate **(D)**, oleylamine **(E),** or left untreated. **F)** Representative fluorescence image of NETs (DAPI, blue) with nonspecific adherent negative charged FluoSpheres® (red), scale bar 10 µm. Data are analyzed by unpaired t-test unless otherwise stated; *p≤0.05, **p≤0.01, ***p≤0.0001. All data are presented as mean ±SEM.

3.3.2. Monocyte adhesion-strength in a charge-dependent manner

In addition to the previous experiments, further examination of monocyte adhesion to NETs with atomic force microscopy was performed to verify the role of charge interaction in monocyte-adhesion to NETs. Monocytes showing a highly negative membrane charge had a strengthened adhesion compared to control cells. Whereas, monocytes incubated with oleylamine showed a decreased adhesion strength measured as the area under the curve (Figure 27 A-B, D, F-H). Furthermore, the adhesion frequency of the differently treated monocytes was altered compared to control monocytes. Highly negative charged monocytes adhesion was 2-fold stronger compared to oleylamine treated monocytes (Figure 27 C, E).

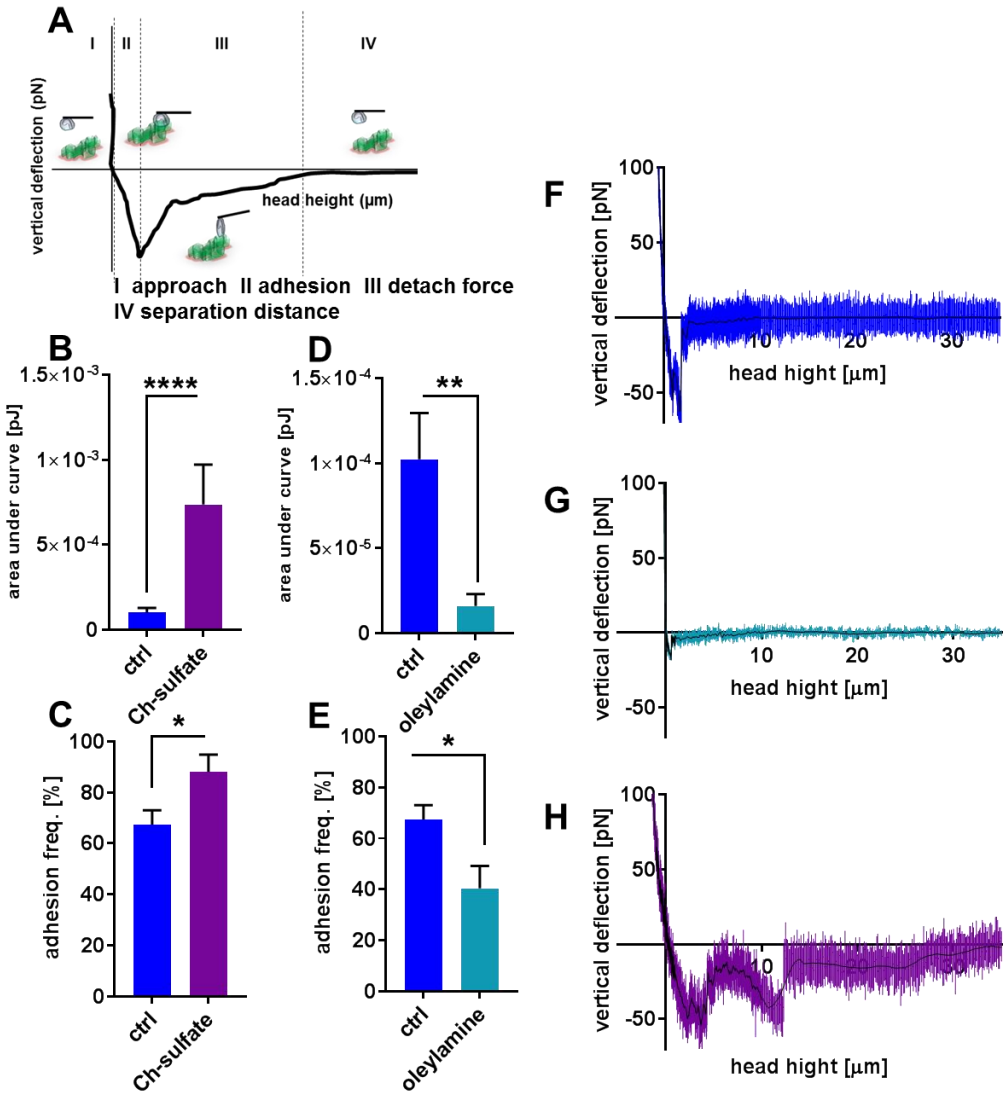

Figure 27: Monocyte-NET adhesion in a charge-dependent manner.

A) Scheme of atomic force microscopy experiment probing monocytes on expelled NETs with 200 pN. **B, D)** Area under the curve showing adhesion strength of monocytes on NETs under different conditions and **(C, E)** adhesion frequency of monocytes. **F, G, H)** Representative atomic force microscopy curves of monocytes probed on NETs treated with either Ch-sulfate or oleylamine. Data are analyzed by unpaired t-test unless otherwise stated; *p≤0.05, **p≤0.01, ***p≤0.0001. All data are presented as mean ±SEM.

3.4. Therapeutical neutralization of H2A prevents accelerated lesion development

Therapeutical strategies aim to modulate neutrophil response to limit neutrophil caused damage [135, 188, 189]. Therefore, studies that focus on diseases caused by hyperactivation of neutrophils aim to inhibit neutrophil function. Nevertheless, insufficient neutrophil activation can also lead to poor innate immune host defense [190]. Consequently, therapeutical strategies modulating neutrophil response are challenging and might be highly depending on the timing when to modulate the immune response and to which extent.

3.4.1. NET-associated H2A cause myeloid cell adhesion *in vivo*

Our experiments revealed a dramatic increase in atherosclerotic lesion development upon the formation of NETs under endotoxemia conditions. We observed an increased luminal leukocyte adhesion if neutrophils form NETs. Therefore, we aimed to interrupt the heightened leukocyte adhesion *in vivo*. *In vitro* experiments have shown that NET-resident histone H2A mediates monocytes adhesion, thus we synthesized a cyclical histone 2A interference peptide (CHIP) to block the leukocyte interaction (Figure 28 B). Mice fed a high fat diet for 4 weeks received the CHIP or antibodies to H2A intravenously upon challenged with LPS (Figure 28 A). First, we observed no altered NET-formation *in vivo* in intravital microscopy (Figure 28 C, F) after CHIP or anti-H2a injection, but luminal adhesion of neutrophils and monocytes were both reduced in mice receiving CHIP and as well in mice receiving antibodies to H2A equality (Figure 28 D-E, G-H).

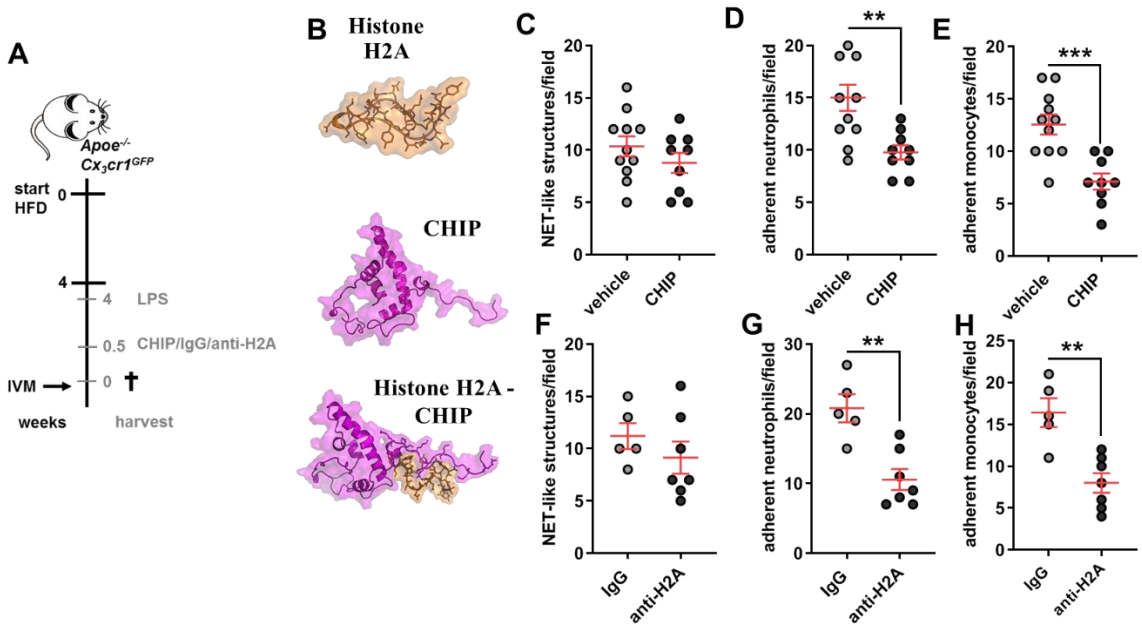

Figure 28: Blocking NET-resident Histone H2A limits luminal leukocyte adhesion.

A) Experimental scheme. **B)** Molecular dynamic simulation of cyclical histone 2A interference peptide (CHIP (purple)), Histone H2A (brown), and the interaction of both. **C, F)** Luminal NET-like structures analyzed in the left common carotid artery of endotoxemia mice left either untreated or treated with CHIP to H2A **(C)** or antibodies to H2A **(F)**. **D, E, G, H)** Counts of luminal adhesive neutrophils **(D, G)** and monocyte **(E, H)** after blocking Histone H2A under acute inflammatory conditions, analyzed by Mann-Whitney test. Data are analyzed by unpaired t-test unless otherwise stated; *p≤0.05, **p≤0.01, ***p≤0.0001. All data are presented as mean ±SEM.

3.4.2. Pharmacological intervention

CHIP limited luminal leukocyte adhesion under endotoxemia conditions. Further, we studied monocyte adhesion properties if NETs were incubated with CHIP. In static adhesion assay, fewer monocytes adhere to NETs if NETs have been pre-incubated with CHIP (Figure 29 A) and as well the adhesion strength was significantly reduced in the atomic force microscopy (Figure 29 B-D). Interestingly, mice treated with CHIP neutralized the effect of accelerated atherosclerosis under endotoxemia conditions (Figure 29 E). Additionally, lesion associated neutrophils and Mac2 positive mononuclear cells were reduced (Figure 29 F-H).

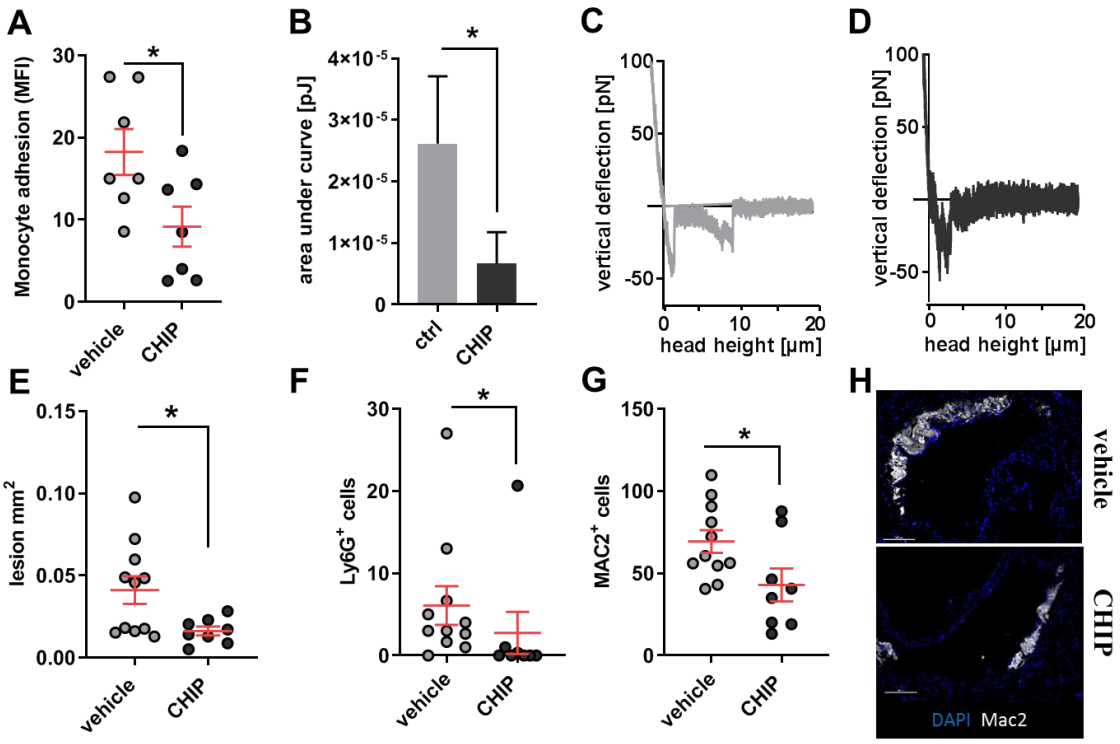

Figure 29: Therapeutically intervention of NET-resident Histone H2A attracted monocytes.

A-D) Showing experiments performed *in vitro* and **E-H)** were ran *in vivo.* **A)** Pharmacological interruption of NET-resident H2A monocyte binding *in vitro* measured as mean fluorescence intensity. **B)** Binding strength analyzed in atomic force microscopy after NETs treated with CHIP. **C-D)** representative atomic force microscopy curves representing adhesion strength. **E)** Atherosclerotic lesion size in aortic roots measured in mm^2. **F-G)** Plaque associated neutrophils ($Ly6G^+$ cells) **(F)** and Mac2 positive cells ($Mac2^+$ cells) **(G)** per aortic root. **H)** Representative immunofluorescence images showing plaque-associated Mac2 positive cells (grey) and nuclei (DAPI, blue), scale bar 50 µm. Data are analyzed by Mann-Whitney test **(A)** or by unpaired t-test **(B, E-G)**; *p≤0.05, **p≤0.01, ***p≤0.0001. All data are resented as mean ±SEM.

4. Summary

The results presented here provide evidence that endotoxemia- activated neutrophils cause accumulation of NETs and favor leukocyte adhesion, which in turn causes accelerated atherosclerosis. During infections, bacteria release LPS, which is a potent activator of circulating immune cells including neutrophils. Activated neutrophils foster inflammation through expelled chromatin (NETs). Neutrophil extracellular traps contain cationic granule proteins which have been shown to support monocyte recruitment to endothelial cells either in a receptor-dependent manner or even charge mediated [16, 34, 92, 93]. But the most abundant protein within NET-structure is histones. They account for 70% of NET-associated proteins [39]. Recently it has been shown that these NET-borne histones cause in a charge dependent fashion plaque vulnerability [124]. Additionally, NETs have been associated with endothelial dysfunction and enhanced atheroprogression [140, 185]. Furthermore, epidemiological studies show a highly increased risk to suffer from CVD after infection within the first three days [154].

The present study shows the first-time enhanced NET-mediated leukocyte adhesion in acute infection and demonstrates the link between endotoxemia-induced NET-release and accelerated lesion formation. Based on *in vivo* experiments we detect luminal NET-like structure, which increases leukocyte adhesion at branch points, and we observe heightened lesion formation within four hours, which could be diminished by inhibiting NET-formation. Neutrophil extracellular traps are decorated with cationic proteins as granule proteins and histones. Surprisingly, monocyte adhesion to NETs was receptor-independent and further independent on the granule proteins, which have been described to facilitate leukocyte adhesion. Even so, if histones were blocked the monocyte adhesion was significantly decreased. Further experiments showed that monocyte adheres to NETs in a charge-dependent manner. Strikingly, therapeutically blocking H2A neutralized accelerated NET-formation under endotoxemia conditions. Nonetheless, limiting overall leukocyte adhesion or NET-formation during infection might lead to insufficient immune response. Therapeutic strategies aiming for a specific intervention could be a promising preventive strategy to reduce cardiovascular events.

5. Discussion

5.1. Endotoxemia accelerates atherosclerosis

Atherosclerosis is a chronic inflammatory disease, which develops over decades. It's characteristic lipid deposition and modification in the intima fosters inflammation [104]. Multiple risk factors for atherosclerosis have already been described, they include smoking as a source of LPS, hypercholesterolemia, or hyperglycemia [143, 191, 192]. The Burneck study showed the impact of endotoxemia on the pathogenesis of atherosclerosis. The authors demonstrated elevated circulating endotoxin levels in patients with chronic infection and suggest gram-negative derived endotoxin levels as a predictor of increased atherosclerosis risk [193]. Additionally, epidemiological studies indicate an increased risk to suffer from CVD within the first three days after a respiratory infection [154, 155]. During infection, neutrophils are classically viewed as the first cells to be recruited and to build the first line of defense. Upon activation, neutrophils adhere to endothelial cells and transmigrate to the site of infection [13]. Additionally, pathogen-associated molecular pattern molecules (PAMPs) as LPS cause neutrophil extracellular trap formation, which in turn leads to endothelial dysfunction [135, 194]. LPS and NETs are known factors to favor atherosclerosis. The underlying mechanism of accelerates pathogenies of atherosclerosis is unknown. Therefore, the present study describes for the first time, a mechanism causing heightened lesion formation under endotoxemia conditions.

First, we observed highly increased atherosclerotic lesion formation under endotoxemia conditions, which was neutralized when neutrophil extracellular trap formation was limited. Knight *et al*. ascribe NETs a critical role during atherosclerosis. They described limited atherosclerotic lesion formation when the enzyme peptidylarginine deiminase (PAD) in Apoe$^{-/-}$ mice was pharmacologically inhibited with Cl-amidine [135]. The study showed besides smaller lesion size, also fewer macrophages within the lesion as well as reduced lesion-associated neutrophils when mice were treated with Cl-amidine. Under endotoxemia conditions, we observe an increased atherosclerotic lesion size with increased

neutrophils and monocytes in the intima. Acute infections caused a decrease of circulating myeloid cells, bone marrow, and splenic myeloid cells while the CD11b expression of circulating neutrophils and monocytes was highly increased, indicating myeloid cells were activated for adhesion, which is independent on pharmacological inhibition with BB Cl-amidine. Since we observed a massive reduction of splenic, bone marrow, and circulating leukocytes under endotoxemia condition independent on Cl-amidine treatment one can speculate that NET-effect could be rather local and might not play an important role in global leukocyte adhesion, which needs to be further investigated. Nevertheless, this observation point to a crucial role for neutrophil extracellular traps during atheroprogression in acute infection. Additionally, we detected increased plasma NET-level with a PicoGreen assay as well as with NET-ELISA, which was diminished after treating mice with BB Cl-amidine. Further, we observed luminal NET-like structures within the murine carotid artery, which fostered neutrophil and monocyte adhesion.

5.2. Neutrophil extracellular traps launch monocyte adhesion

A crucial step during atherogenesis is myeloid cell recruitment which is regulated by adhesion molecules expression on endothelial cells. Leukocyte adhesion is tightly regulated by chemokines and integrins expression [11]. Elevated neutrophil counts benefit atherogenesis while neutropenia reduces atherosclerosis [98]. Interestingly, the importance of neutrophils during atherogenesis was long neglected due to their abundance within the atherosclerotic lesion [118]. Nevertheless, footprints of neutrophils have been detected as a reliable biomarker of atherosclerosis outcome [195, 196]. Further, neutrophils pave the way for monocyte recruitment through released granule protein, which is chemotactic for monocytes and facilitates adhesion [16]. Besides granular protein also NETs can be released by neutrophils. NETs are decorated with a variety of cationic granule proteins and histones [32, 39]. Interestingly, neutropenia leads to insufficient monocyte recruitment [197]. Patients suffering from neutrophil-specific granule deficiency show defects in monocyte

extravasation and chemotaxis *in vitro* [88]. The degranulated proteins, such as α defensin or LL-37 are cationic charged and bind on endothelium, which in turn activates the endothelial cells for elevated expression of adhesion molecules VCAM1 and ICAM1 [16, 198, 199]. Further, secreted α defensin can form complex with platelet-derived CCL5 causing monocyte adhesion through monocyte expressed CCR5 [92]. Cathelicidin activates FPR2 on monocytes leading to upregulated integrin expression, which favors adhesion [35]. However, most of the studies describing neutrophil facilitated monocyte adhesion focus on microcirculation, while atherosclerosis occurs in large vessels. The physiological differences between micro- and macrocirculation are highly important as demonstrated in experiments highlighting a cathepsin G dependent monocyte recruitment in macrocirculation but not in the microcirculation [34, 186]. Taken together, granule proteins LL-37, α defensin, and cathepsin G facilitate monocyte recruitment and adhesion involving g-protein coupled receptors and formyl-peptide receptors. Here, we studied monocyte adhesion to NETs, which was independent of granular proteins within the NETs. Further, we demonstrated that neither g-protein coupled receptor nor integrins or TLRs were involved in monocyte adhesion. Interestingly, the most abundant proteins in the NETs are the highly cationic histones, which we identified in our studies to mediate monocyte adhesion. It has been shown that histones cause in a charge dependent manner pore formation within the plaque, which led to plaque vulnerability [124]. Histones foster inflammation through TLR2 and 4 signaling while chromatin, the NET scaffold and an important danger associated molecule pattern signals through TLR9 [200, 201]. Histones within the nucleosome complex are not supposed to be cytotoxic compared to histones released from NETs after DNA digestion [124, 202, 203].

5.3. NETs facilitate adhesion in a charge-dependent manner

Charge interaction can be found during the innate immune response to support cell-cell interplay, but charge can also prevent uncontrolled cell recruitment. Endothelial

cells are covered with glycocalyx whose main components are glycosaminoglycon, heparan sulfate, and chondroitin sulfate giving cells a typical negative membrane charge. The 500 nm thick endothelial glycocalyx prevents under steady-state uncontrolled leukocyte adhesion [204]. During infection or inflammation, the glycocalyx is shed showing adhesion molecules, allowing leukocyte to adhere and transmigrate [205, 206]. Among the adherent leukocyte to endothelial cells during inflammation, neutrophils are the first cells to be recruited. They release granule proteins, which have antimicrobial activity and have been shown to favor myeloid cell adhesion [16]. Interestingly, myeloperoxidase is one of the released proteins by neutrophils upon activation, which causes myeloid cell adhesion in a charge-dependent manner [93]. Granule proteins show high cationic charges resulting from the arginine-rich composition [198, 199]. Electrostatically cell adhesion has also been shown for elastase and proteinase 3, which are also part of neutrophil extracellular traps [198, 199].

Besides granule proteins, also histone H2A, H2B, H3, and H4 decorate neutrophil extracellular traps. Histones form a core that is wrapped with 147 base pairs of DNA in the nucleosome. The linker histones H1 und H5 connect the nucleosomes and regulate chromatin compactness. Histones are rich amino acid lysin and arginine, both highly cationic giving histones the highly positive charged character [207]. However, leukocytes show a negative membrane charge due to their glycocalyx [179]. In our experiments, we measured the monocyte surface charge with zetaziser and manipulated the monocytes' charge. Our experiments highlighted a charge dependent monocyte adhesion to neutrophil extracellular traps. Further, cell-cell interaction can be measured with atomic force microscopy. So far, cell charge interaction has been studied with cells adhering to well defined charged surfaces or cells [208, 209]. We measure here the first time the force interaction between neutrophil extracellular traps and viable monocytes indicating that monocyte adhesion to neutrophil extracellular traps is charge dependent. Interestingly, charge interaction is an unspecific mechanism make it challenging to study charge interaction *in vivo*. Nevertheless, the group of Nicolaes treated septic mice, where cell free histones cause cytotoxicity, with heparin a highly anionic

charge molecule, neutralized cationic charge pointing to charge interaction *in vivo* [210].

5.4. Therapeutic implication

Atherosclerosis develops over decades and is diagnosed at a clinical stage. The chronic inflammatory disease leads to CVD causing approximately one-third of the death worldwide [211]. Therefore, the prevention of atherosclerosis is an important research field with growing interest. Limitation of the inflammatory processes during atherogenesis can be driven by cholesterol efflux, neutralizing cytokines, promoting leukocyte egress, or inhibiting leukocyte recruitment [111, 212-215]. Nowadays, the treatment of atherogenesis targets well-known atherosclerotic risk factors as hypertension and hypercholesterolemia. Nevertheless, statins treatment or high blood pressure regulating drugs (beta-blocker) do not aim to limit chronic inflammation. But atherosclerosis is nowadays well described as a chronic inflammatory disease, were uncontrolled leukocyte recruitment fuel inflammation [97]. Targeting the imbalanced inflammatory response in combination with the golden standard of cardiovascular disease therapy can be an improvement in the treatment of atherosclerosis. Studies that focused on anti-inflammatory strategies showed a beneficial immune-modulating effect using cytokine-inhibitors [111]. Therefore, disruption of leukocyte recruitment into lesions is believed to be a potent therapeutic target [171, 172]. Thus, blockage of CCL5, which controlled adhesion of monocytes among others shows a reduced atherosclerotic progression in mice, consequently showing reduced macrophage numbers in atherosclerotic plaque and smaller lesion size [172]. Further, inhibition of chemokine CCL2, CCL5, and CX3CL1 reduced leukocyte recruitment and improve lesion stability [171]. Nevertheless, the impairment of overall leukocyte recruitment might lead to weakened immune defense, as observed in the CANTOS-study. The specific neutralization of pro-inflammatory cytokine IL-1ß leads to a higher incidence to suffer from infection and sepsis [216].

However, monocytes have been acknowledged to contribute to atherosclerotic lesion formation, progression, and destabilization [217]. Additionally, insights from human atherosclerotic lesions and mouse studies highlighting neutrophils to accelerate atherosclerotic lesion development [218-220]. Neutrophils assist monocyte adhesion by releasing granule proteins like LL-37 or cathepsin G [16]. Additionally, neutrophil-derived myeloperoxidase has been shown to favor leukocyte adherence to endothelial cells in a charge dependent fashion [93]. Nevertheless, LL-37, cathepsin G, and MPO are also neutrophil extracellular trap associated proteins [39]. NETs are released to limit infection but have also been shown to fuel chronic inflammation as atherosclerosis. Studies using mice deficient in serine protease, neutrophil elastase or PAD4, show a critical role of NETs during atherosclerosis [55, 140]. These data indicating a potential role of neutrophil extracellular traps during atherogenesis. The most abundant proteins within the NETs are histones, which have been shown to trigger plaque vulnerability. Nevertheless, blocking histone was shown to limit plaque vulnerability. Strikingly, in sepsis study, the neutralization of histones during sepsis reduces organ damage [124, 210]. We found NET-resident histone H2A facilitates monocyte adhesion leading to heightened lesion formation during endotoxemia, which was limited after H2A blocking *in vivo*. These results highlight an anti-histone therapy as a potential treatment strategy. Nevertheless, the total blockage of neutrophil extracellular traps might have side effects as insufficient immune response due to its antimicrobial activity in tissue as well as in circulation, which has to be further investigated. Additionally, the time of treatment might also be an important question to answer, since leukocyte recruitment shows time-dependent rhythmicity [91]. Therapies that specifically reduce leukocyte recruitment in synergy with nowadays-used cholesterol-lowering therapies could be a useful strategy to improve the disease outcome in advanced atherosclerosis.

6. Outlook

6.1. Outlook

Many studies highlight the pro-inflammatory role of NETs during the onset of diseases as atherosclerosis. Epidemiological studies highlight a causal link between infection and CVD. But the underlying mechanism remains so far unclear. To find new therapeutic strategies it is important to understand the molecular and cellular mechanisms of atherosclerosis. We describe here the mechanism of endotoxemia accelerated atherosclerosis. We observe that monocyte adheres electrostatically to NET-resident histone H2A, which was reversed by our synthesized histone H2A blocking peptide. Nonetheless, our study reveals further questions for future research.

Here we observe a 50% increased atherosclerotic lesion size after 4 hours of LPS challenge. We show, during acute infection that neutrophil extracellular traps play a critical role to cause a heightened increased lesion formation. So, the question arises if this observed effect remains after a long period or the effect can be reversed. Further, the crosstalk of NETs with other cells like the endothelial cells or monocytes has to be studied in more detail. It has been shown that neutrophil harbor miRNA, which might be also expelled to the environment within the NETs [221]. This miRNA could alter the phenotype of monocytes and activate them for chemokine release which fuels inflammation. These open questions might give a hint of why we observe a quite fast doubling of the atherosclerotic lesion size. Additionally, the effect of NET-mediated leukocyte adhesion during acute infection on advanced atherosclerotic lesion has to be studied in more detail, since the consequences of atherosclerosis as myocardial infarction or stroke occur in the late stage of atherosclerosis [104].

Our study explores accelerated atherosclerosis with a single LPS challenge in young mice. We observed luminal NET-release within four hours. To translate our findings into human more detailed studies are necessary. So far it has been

described that neutrophils of old individuals show impaired phagocytosis and decreased respiratory burst [222, 223]. The ability of neutrophils of elderly individuals to form neutrophil extracellular traps has not so far studied in detail, but due to the decreased bactericidal activity of these neutrophils, it has been suggested that NET-formation is limited [224, 225]. The proof of principle with neutrophils from elderly individuals is necessary to better understand pathomechanism in humans.

During our investigation we designed a histone-based therapeutic treatment strategy, which was applied after the LPS challenge, mimicking an acute infection. It has been shown that insufficient function neutrophils impair pathogen clearance causing a worse outcome for patients. Here we block histone H2A to prevent leukocyte adhesion, which might have an impact on pathogen clearance but also limited pathogen entrapment can be a consequence of blocking cationic proteins within the NET. Further, it has to be considered that different NET-formation stimulus leads to different NET-formation pathway and might also result in different NET-protein composition. Besides NET-composition, also the site of NET-formation may play a major role. Here we observe a massive increase in leukocyte adhesion to arterial vessels, which was reduced after H2A blocking. However, this effect could differ in venous circulation as described for cathepsin G, which favors leukocyte recruitment in the artery but not in veins [34].

Taken together, future investigations focusing on pro-inflammatory processes during atherogenesis will mild atherosclerosis outcome by uncovering pro-inflammatory mechanisms improving treatment for CVD.

Reference

1. Cooper, M.D. and B.R. Herrin, *How did our complex immune system evolve?* Nat Rev Immunol, 2010. **10**(1): p. 2-3.
2. Parkin, J. and B. Cohen, *An overview of the immune system.* Lancet, 2001. **357**(9270): p. 1777-89.
3. Medzhitov, R. and C. Janeway, Jr., *Innate immunity.* N Engl J Med, 2000. **343**(5): p. 338-44.
4. Dranoff, G., *Cytokines in cancer pathogenesis and cancer therapy.* Nat Rev Cancer, 2004. **4**(1): p. 11-22.
5. Beutler, B., *Innate immunity: an overview.* Mol Immunol, 2004. **40**(12): p. 845-59.
6. Medzhitov, R. and C. Janeway, Jr., *Innate immune recognition: mechanisms and pathways.* Immunol Rev, 2000. **173**: p. 89-97.
7. Rousseau, M.C., et al., *Lipopolysaccharide-induced toll-like receptor 4 signaling enhances the migratory ability of human esophageal cancer cells in a selectin-dependent manner.* Surgery, 2013. **154**(1): p. 69-77.
8. Kobayashi, S.D., N. Malachowa, and F.R. DeLeo, *Neutrophils and Bacterial Immune Evasion.* J Innate Immun, 2018. **10**(5-6): p. 432-441.
9. Sokol, C.L. and A.D. Luster, *The chemokine system in innate immunity.* Cold Spring Harb Perspect Biol, 2015. **7**(5).
10. Netea, M.G., et al., *A guiding map for inflammation.* Nat Immunol, 2017. **18**(8): p. 826-831.
11. Ley, K., et al., *Getting to the site of inflammation: the leukocyte adhesion cascade updated.* Nat Rev Immunol, 2007. **7**(9): p. 678-89.
12. Nathan, C., *Neutrophils and immunity: challenges and opportunities.* Nat Rev Immunol, 2006. **6**(3): p. 173-82.
13. Kolaczkowska, E. and P. Kubes, *Neutrophil recruitment and function in health and inflammation.* Nat Rev Immunol, 2013. **13**(3): p. 159-75.
14. Pittman, K. and P. Kubes, *Damage-associated molecular patterns control neutrophil recruitment.* J Innate Immun, 2013. **5**(4): p. 315-23.
15. Soehnlein, O., L. Lindbom, and C. Weber, *Mechanisms underlying neutrophil-mediated monocyte recruitment.* Blood, 2009. **114**(21): p. 4613-23.
16. Soehnlein, O., et al., *Neutrophil secretion products pave the way for inflammatory monocytes.* Blood, 2008. **112**(4): p. 1461-71.
17. Ortega-Gomez, A., M. Perretti, and O. Soehnlein, *Resolution of inflammation: an integrated view.* EMBO Mol Med, 2013. **5**(5): p. 661-74.
18. Viola, J. and O. Soehnlein, *Atherosclerosis - A matter of unresolved inflammation.* Semin Immunol, 2015. **27**(3): p. 184-93.
19. Gorgens, A., et al., *Revision of the human hematopoietic tree: granulocyte subtypes derive from distinct hematopoietic lineages.* Cell Rep, 2013. **3**(5): p. 1539-52.
20. Lawrence, S.M., R. Corriden, and V. Nizet, *The Ontogeny of a Neutrophil: Mechanisms of Granulopoiesis and Homeostasis.* Microbiol Mol Biol Rev, 2018. **82**(1).
21. Casanova-Acebes, M., et al., *Rhythmic modulation of the hematopoietic niche through neutrophil clearance.* Cell, 2013. **153**(5): p. 1025-35.

22. He, W., et al., *Circadian Expression of Migratory Factors Establishes Lineage-Specific Signatures that Guide the Homing of Leukocyte Subsets to Tissues.* Immunity, 2018. **49**(6): p. 1175-1190 e7.
23. Pick, R., et al., *Time-of-Day-Dependent Trafficking and Function of Leukocyte Subsets.* Trends Immunol, 2019. **40**(6): p. 524-537.
24. Lazaro-Diez, M., et al., *Human neutrophils phagocytose and kill Acinetobacter baumannii and A. pittii.* Sci Rep, 2017. **7**(1): p. 4571.
25. Hidalgo, A., et al., *The Neutrophil Life Cycle.* Trends Immunol, 2019. **40**(7): p. 584-597.
26. Mayadas, T.N., X. Cullere, and C.A. Lowell, *The multifaceted functions of neutrophils.* Annu Rev Pathol, 2014. **9**: p. 181-218.
27. Segal, A.W., *How neutrophils kill microbes.* Annu Rev Immunol, 2005. **23**: p. 197-223.
28. Cowland, J.B. and N. Borregaard, *Granulopoiesis and granules of human neutrophils.* Immunol Rev, 2016. **273**(1): p. 11-28.
29. Borregaard, N. and J.B. Cowland, *Granules of the human neutrophilic polymorphonuclear leukocyte.* Blood, 1997. **89**(10): p. 3503-21.
30. Cassatella, M.A., et al., *Biological Roles of Neutrophil-Derived Granule Proteins and Cytokines.* Trends Immunol, 2019. **40**(7): p. 648-664.
31. Scheenstra, M.R., et al., *Cathelicidins PMAP-36, LL-37 and CATH-2 are similar peptides with different modes of action.* Sci Rep, 2019. **9**(1): p. 4780.
32. Brinkmann, V., et al., *Neutrophil extracellular traps kill bacteria.* Science, 2004. **303**(5663): p. 1532-5.
33. Fuchs, T.A., et al., *Novel cell death program leads to neutrophil extracellular traps.* J Cell Biol, 2007. **176**(2): p. 231-41.
34. Ortega-Gomez, A., et al., *Cathepsin G Controls Arterial But Not Venular Myeloid Cell Recruitment.* Circulation, 2016. **134**(16): p. 1176-1188.
35. Wantha, S., et al., *Neutrophil-derived cathelicidin promotes adhesion of classical monocytes.* Circ Res, 2013. **112**(5): p. 792-801.
36. Hemshekhar, M., K.G. Choi, and N. Mookherjee, *Host Defense Peptide LL-37-Mediated Chemoattractant Properties, but Not Anti-Inflammatory Cytokine IL-1RA Production, Is Selectively Controlled by Cdc42 Rho GTPase via G Protein-Coupled Receptors and JNK Mitogen-Activated Protein Kinase.* Front Immunol, 2018. **9**: p. 1871.
37. Branzk, N., et al., *Neutrophils sense microbe size and selectively release neutrophil extracellular traps in response to large pathogens.* Nat Immunol, 2014. **15**(11): p. 1017-25.
38. Ermert, D., et al., *Mouse neutrophil extracellular traps in microbial infections.* J Innate Immun, 2009. **1**(3): p. 181-93.
39. Urban, C.F., et al., *Neutrophil extracellular traps contain calprotectin, a cytosolic protein complex involved in host defense against Candida albicans.* PLoS Pathog, 2009. **5**(10): p. e1000639.
40. Bianchi, M., et al., *Restoration of anti-Aspergillus defense by neutrophil extracellular traps in human chronic granulomatous disease after gene therapy is calprotectin-dependent.* J Allergy Clin Immunol, 2011. **127**(5): p. 1243-52 e7.
41. Saitoh, T., et al., *Neutrophil extracellular traps mediate a host defense response to human immunodeficiency virus-1.* Cell Host Microbe, 2012. **12**(1): p. 109-16.

42. Funchal, G.A., et al., *Respiratory syncytial virus fusion protein promotes TLR-4-dependent neutrophil extracellular trap formation by human neutrophils.* PLoS One, 2015. **10**(4): p. e0124082.
43. Khandpur, R., et al., *NETs are a source of citrullinated autoantigens and stimulate inflammatory responses in rheumatoid arthritis.* Sci Transl Med, 2013. **5**(178): p. 178ra40.
44. Rada, B., *Neutrophil Extracellular Traps and Microcrystals.* J Immunol Res, 2017. **2017**: p. 2896380.
45. Caudrillier, A., et al., *Platelets induce neutrophil extracellular traps in transfusion-related acute lung injury.* J Clin Invest, 2012. **122**(7): p. 2661-71.
46. Manfredi, A.A., et al., *The Neutrophil's Choice: Phagocytose vs Make Neutrophil Extracellular Traps.* Front Immunol, 2018. **9**: p. 288.
47. Hwang, C.S., et al., *Eosinophil extracellular trap formation is closely associated with disease severity in chronic rhinosinusitis regardless of nasal polyp status.* Sci Rep, 2019. **9**(1): p. 8061.
48. von Kockritz-Blickwede, M., et al., *Phagocytosis-independent antimicrobial activity of mast cells by means of extracellular trap formation.* Blood, 2008. **111**(6): p. 3070-80.
49. Yousefi, S., et al., *Catapult-like release of mitochondrial DNA by eosinophils contributes to antibacterial defense.* Nat Med, 2008. **14**(9): p. 949-53.
50. Sollberger, G., D.O. Tilley, and A. Zychlinsky, *Neutrophil Extracellular Traps: The Biology of Chromatin Externalization.* Dev Cell, 2018. **44**(5): p. 542-553.
51. Steinberg, B.E. and S. Grinstein, *Unconventional roles of the NADPH oxidase: signaling, ion homeostasis, and cell death.* Sci STKE, 2007. **2007**(379): p. pe11.
52. Yousefi, S., et al., *Viable neutrophils release mitochondrial DNA to form neutrophil extracellular traps.* Cell Death Differ, 2009. **16**(11): p. 1438-44.
53. Yipp, B.G., et al., *Infection-induced NETosis is a dynamic process involving neutrophil multitasking in vivo.* Nat Med, 2012. **18**(9): p. 1386-93.
54. Hakkim, A., et al., *Impairment of neutrophil extracellular trap degradation is associated with lupus nephritis.* Proc Natl Acad Sci U S A, 2010. **107**(21): p. 9813-8.
55. Warnatsch, A., et al., *Inflammation. Neutrophil extracellular traps license macrophages for cytokine production in atherosclerosis.* Science, 2015. **349**(6245): p. 316-20.
56. Amulic, B., et al., *Cell-Cycle Proteins Control Production of Neutrophil Extracellular Traps.* Dev Cell, 2017. **43**(4): p. 449-462 e5.
57. Albrengues, J., et al., *Re-cyclin' Cell-Cycle Components to Make NETs.* Dev Cell, 2017. **43**(4): p. 379-380.
58. Papayannopoulos, V., et al., *Neutrophil elastase and myeloperoxidase regulate the formation of neutrophil extracellular traps.* J Cell Biol, 2010. **191**(3): p. 677-91.
59. Chen, K.W., et al., *Noncanonical inflammasome signaling elicits gasdermin D-dependent neutrophil extracellular traps.* Sci Immunol, 2018. **3**(26).
60. Sollberger, G., et al., *Gasdermin D plays a vital role in the generation of neutrophil extracellular traps.* Sci Immunol, 2018. **3**(26).

61. Douda, D.N., et al., *SK3 channel and mitochondrial ROS mediate NADPH oxidase-independent NETosis induced by calcium influx.* Proc Natl Acad Sci U S A, 2015. **112**(9): p. 2817-22.
62. Wang, Y., et al., *Histone hypercitrullination mediates chromatin decondensation and neutrophil extracellular trap formation.* J Cell Biol, 2009. **184**(2): p. 205-13.
63. Li, P., et al., *PAD4 is essential for antibacterial innate immunity mediated by neutrophil extracellular traps.* J Exp Med, 2010. **207**(9): p. 1853-62.
64. Buchanan, J.T., et al., *DNase expression allows the pathogen group A Streptococcus to escape killing in neutrophil extracellular traps.* Curr Biol, 2006. **16**(4): p. 396-400.
65. Lauth, X., et al., *M1 protein allows Group A streptococcal survival in phagocyte extracellular traps through cathelicidin inhibition.* J Innate Immun, 2009. **1**(3): p. 202-14.
66. Wartha, F., et al., *Capsule and D-alanylated lipoteichoic acids protect Streptococcus pneumoniae against neutrophil extracellular traps.* Cell Microbiol, 2007. **9**(5): p. 1162-71.
67. Carmona-Rivera, C., et al., *Neutrophil extracellular traps induce endothelial dysfunction in systemic lupus erythematosus through the activation of matrix metalloproteinase-2.* Ann Rheum Dis, 2015. **74**(7): p. 1417-24.
68. Sur Chowdhury, C., et al., *Enhanced neutrophil extracellular trap generation in rheumatoid arthritis: analysis of underlying signal transduction pathways and potential diagnostic utility.* Arthritis Res Ther, 2014. **16**(3): p. R122.
69. Yasutomo, K., et al., *Mutation of DNASE1 in people with systemic lupus erythematosus.* Nat Genet, 2001. **28**(4): p. 313-4.
70. Jimenez-Alcazar, M., et al., *Host DNases prevent vascular occlusion by neutrophil extracellular traps.* Science, 2017. **358**(6367): p. 1202-1206.
71. Yanez, A., et al., *Granulocyte-Monocyte Progenitors and Monocyte-Dendritic Cell Progenitors Independently Produce Functionally Distinct Monocytes.* Immunity, 2017. **47**(5): p. 890-902 e4.
72. Swirski, F.K., et al., *Identification of splenic reservoir monocytes and their deployment to inflammatory sites.* Science, 2009. **325**(5940): p. 612-6.
73. Jakubzick, C., et al., *Minimal differentiation of classical monocytes as they survey steady-state tissues and transport antigen to lymph nodes.* Immunity, 2013. **39**(3): p. 599-610.
74. Auffray, C., M.H. Sieweke, and F. Geissmann, *Blood monocytes: development, heterogeneity, and relationship with dendritic cells.* Annu Rev Immunol, 2009. **27**: p. 669-92.
75. Geissmann, F., S. Jung, and D.R. Littman, *Blood monocytes consist of two principal subsets with distinct migratory properties.* Immunity, 2003. **19**(1): p. 71-82.
76. Cros, J., et al., *Human CD14dim monocytes patrol and sense nucleic acids and viruses via TLR7 and TLR8 receptors.* Immunity, 2010. **33**(3): p. 375-86.
77. Yona, S., et al., *Fate mapping reveals origins and dynamics of monocytes and tissue macrophages under homeostasis.* Immunity, 2013. **38**(1): p. 79-91.
78. Dutta, P., et al., *Myocardial infarction accelerates atherosclerosis.* Nature, 2012. **487**(7407): p. 325-9.

79. Puchner, A., et al., *Non-classical monocytes as mediators of tissue destruction in arthritis.* Ann Rheum Dis, 2018. **77**(10): p. 1490-1497.
80. Sun, W., et al., *Targeting Notch-Activated M1 Macrophages Attenuates Joint Tissue Damage in a Mouse Model of Inflammatory Arthritis.* J Bone Miner Res, 2017. **32**(7): p. 1469-1480.
81. Vestweber, D., *How leukocytes cross the vascular endothelium.* Nat Rev Immunol, 2015. **15**(11): p. 692-704.
82. McEver, R.P., *Selectins: lectins that initiate cell adhesion under flow.* Curr Opin Cell Biol, 2002. **14**(5): p. 581-6.
83. Alon, R., et al., *The integrin VLA-4 supports tethering and rolling in flow on VCAM-1.* J Cell Biol, 1995. **128**(6): p. 1243-53.
84. Zarbock, A., et al., *Leukocyte ligands for endothelial selectins: specialized glycoconjugates that mediate rolling and signaling under flow.* Blood, 2011. **118**(26): p. 6743-51.
85. Kuwano, Y., et al., *Rolling on E- or P-selectin induces the extended but not high-affinity conformation of LFA-1 in neutrophils.* Blood, 2010. **116**(4): p. 617-24.
86. Nymo, S., et al., *Human Endothelial Cell Activation by Escherichia coli and Staphylococcus aureus Is Mediated by TNF and IL-1beta Secondarily to Activation of C5 and CD14 in Whole Blood.* J Immunol, 2016. **196**(5): p. 2293-9.
87. Janardhan, K.S., S.K. Sandhu, and B. Singh, *Neutrophil depletion inhibits early and late monocyte/macrophage increase in lung inflammation.* Front Biosci, 2006. **11**: p. 1569-76.
88. Gallin, J.I., et al., *Human neutrophil-specific granule deficiency: a model to assess the role of neutrophil-specific granules in the evolution of the inflammatory response.* Blood, 1982. **59**(6): p. 1317-29.
89. Borregaard, N., *Neutrophils, from marrow to microbes.* Immunity, 2010. **33**(5): p. 657-70.
90. Ward, P.A., *Chemotoxis of mononuclear cells.* J Exp Med, 1968. **128**(5): p. 1201-21.
91. Winter, C., et al., *Chrono-pharmacological Targeting of the CCL2-CCR2 Axis Ameliorates Atherosclerosis.* Cell Metab, 2018. **28**(1): p. 175-182 e5.
92. Alard, J.E., et al., *Recruitment of classical monocytes can be inhibited by disturbing heteromers of neutrophil HNP1 and platelet CCL5.* Sci Transl Med, 2015. **7**(317): p. 317ra196.
93. Klinke, A., et al., *Myeloperoxidase attracts neutrophils by physical forces.* Blood, 2011. **117**(4): p. 1350-8.
94. Reitsma, S., et al., *The endothelial glycocalyx: composition, functions, and visualization.* Pflugers Arch, 2007. **454**(3): p. 345-59.
95. Prame Kumar, K., A.J. Nicholls, and C.H.Y. Wong, *Partners in crime: neutrophils and monocytes/macrophages in inflammation and disease.* Cell Tissue Res, 2018. **371**(3): p. 551-565.
96. Medzhitov, R., *Origin and physiological roles of inflammation.* Nature, 2008. **454**(7203): p. 428-35.
97. Geovanini, G.R. and P. Libby, *Atherosclerosis and inflammation: overview and updates.* Clin Sci (Lond), 2018. **132**(12): p. 1243-1252.
98. Drechsler, M., et al., *Hyperlipidemia-triggered neutrophilia promotes early atherosclerosis.* Circulation, 2010. **122**(18): p. 1837-45.

99. Mayer, F.J., et al., *Prognostic value of neutrophils in patients with asymptomatic carotid artery disease.* Atherosclerosis, 2013. **231**(2): p. 274-80.
100. Benjamin, E.J., et al., *Heart Disease and Stroke Statistics-2017 Update: A Report From the American Heart Association.* Circulation, 2017. **135**(10): p. e146-e603.
101. Libby, P., *Inflammation in atherosclerosis.* Nature, 2002. **420**(6917): p. 868-74.
102. Hadi, H.A., C.S. Carr, and J. Al Suwaidi, *Endothelial dysfunction: cardiovascular risk factors, therapy, and outcome.* Vasc Health Risk Manag, 2005. **1**(3): p. 183-98.
103. Libby, P., P.M. Ridker, and G.K. Hansson, *Progress and challenges in translating the biology of atherosclerosis.* Nature, 2011. **473**(7347): p. 317-25.
104. Lusis, A.J., *Atherosclerosis.* Nature, 2000. **407**(6801): p. 233-41.
105. Gimbrone, M.A., Jr., *Vascular endothelium, hemodynamic forces, and atherogenesis.* Am J Pathol, 1999. **155**(1): p. 1-5.
106. Kwon, G.P., et al., *Contribution of macromolecular structure to the retention of low-density lipoprotein at arterial branch points.* Circulation, 2008. **117**(22): p. 2919-27.
107. Jeurissen, M.L.J., et al., *Prevention of oxLDL uptake leads to decreased atherosclerosis in hematopoietic NPC1-deficient Ldlr(-/-) mice.* Atherosclerosis, 2016. **255**: p. 59-65.
108. Zhou, Z., et al., *Lipoprotein-derived lysophosphatidic acid promotes atherosclerosis by releasing CXCL1 from the endothelium.* Cell Metab, 2011. **13**(5): p. 592-600.
109. Takei, A., Y. Huang, and M.F. Lopes-Virella, *Expression of adhesion molecules by human endothelial cells exposed to oxidized low density lipoprotein. Influences of degree of oxidation and location of oxidized LDL.* Atherosclerosis, 2001. **154**(1): p. 79-86.
110. Fatkhullina, A.R., I.O. Peshkova, and E.K. Koltsova, *The Role of Cytokines in the Development of Atherosclerosis.* Biochemistry (Mosc), 2016. **81**(11): p. 1358-1370.
111. Combadiere, C., et al., *Combined inhibition of CCL2, CX3CR1, and CCR5 abrogates Ly6C(hi) and Ly6C(lo) monocytosis and almost abolishes atherosclerosis in hypercholesterolemic mice.* Circulation, 2008. **117**(13): p. 1649-57.
112. Marx, S.O., H. Totary-Jain, and A.R. Marks, *Vascular smooth muscle cell proliferation in restenosis.* Circ Cardiovasc Interv, 2011. **4**(1): p. 104-11.
113. Bennett, M.R., S. Sinha, and G.K. Owens, *Vascular Smooth Muscle Cells in Atherosclerosis.* Circ Res, 2016. **118**(4): p. 692-702.
114. Lemaitre, V., et al., *ApoE knockout mice expressing human matrix metalloproteinase-1 in macrophages have less advanced atherosclerosis.* J Clin Invest, 2001. **107**(10): p. 1227-34.
115. Liang, J., et al., *Macrophage metalloelastase accelerates the progression of atherosclerosis in transgenic rabbits.* Circulation, 2006. **113**(16): p. 1993-2001.
116. Mazo, I.B., S. Massberg, and U.H. von Andrian, *Hematopoietic stem and progenitor cell trafficking.* Trends Immunol, 2011. **32**(10): p. 493-503.

117. Soehnlein, O., et al., *Distinct functions of chemokine receptor axes in the atherogenic mobilization and recruitment of classical monocytes.* EMBO Mol Med, 2013. **5**(3): p. 471-81.
118. Soehnlein, O., *Multiple roles for neutrophils in atherosclerosis.* Circ Res, 2012. **110**(6): p. 875-88.
119. Kuckleburg, C.J. and P.J. Newman, *Neutrophil proteinase 3 acts on protease-activated receptor-2 to enhance vascular endothelial cell barrier function.* Arterioscler Thromb Vasc Biol, 2013. **33**(2): p. 275-84.
120. Soehnlein, O. and L. Lindbom, *Phagocyte partnership during the onset and resolution of inflammation.* Nat Rev Immunol, 2010. **10**(6): p. 427-39.
121. Rotzius, P., et al., *Distinct infiltration of neutrophils in lesion shoulders in ApoE-/- mice.* Am J Pathol, 2010. **177**(1): p. 493-500.
122. Williams, H., et al., *MMP-7 mediates cleavage of N-cadherin and promotes smooth muscle cell apoptosis.* Cardiovasc Res, 2010. **87**(1): p. 137-46.
123. Laxton, R.C., et al., *A role of matrix metalloproteinase-8 in atherosclerosis.* Circ Res, 2009. **105**(9): p. 921-9.
124. Silvestre-Roig, C., et al., *Externalized histone H4 orchestrates chronic inflammation by inducing lytic cell death.* Nature, 2019. **569**(7755): p. 236-240.
125. Ammollo, C.T., et al., *Extracellular histones increase plasma thrombin generation by impairing thrombomodulin-dependent protein C activation.* J Thromb Haemost, 2011. **9**(9): p. 1795-803.
126. Garcia-Romo, G.S., et al., *Netting neutrophils are major inducers of type I IFN production in pediatric systemic lupus erythematosus.* Sci Transl Med, 2011. **3**(73): p. 73ra20.
127. Farrera, C. and B. Fadeel, *Macrophage clearance of neutrophil extracellular traps is a silent process.* J Immunol, 2013. **191**(5): p. 2647-56.
128. Nakazawa, D., et al., *The responses of macrophages in interaction with neutrophils that undergo NETosis.* J Autoimmun, 2016. **67**: p. 19-28.
129. Nakazawa, D., et al., *Abnormal conformation and impaired degradation of propylthiouracil-induced neutrophil extracellular traps: implications of disordered neutrophil extracellular traps in a rat model of myeloperoxidase antineutrophil cytoplasmic antibody-associated vasculitis.* Arthritis Rheum, 2012. **64**(11): p. 3779-87.
130. Fuchs, T.A., A. Brill, and D.D. Wagner, *Neutrophil extracellular trap (NET) impact on deep vein thrombosis.* Arterioscler Thromb Vasc Biol, 2012. **32**(8): p. 1777-83.
131. Kolaczkowska, E., et al., *Molecular mechanisms of NET formation and degradation revealed by intravital imaging in the liver vasculature.* Nat Commun, 2015. **6**: p. 6673.
132. Knight, J.S., C. Carmona-Rivera, and M.J. Kaplan, *Proteins derived from neutrophil extracellular traps may serve as self-antigens and mediate organ damage in autoimmune diseases.* Front Immunol, 2012. **3**: p. 380.
133. Xu, J., et al., *Extracellular histones are major mediators of death in sepsis.* Nat Med, 2009. **15**(11): p. 1318-21.
134. Papayannopoulos, V., D. Staab, and A. Zychlinsky, *Neutrophil elastase enhances sputum solubilization in cystic fibrosis patients receiving DNase therapy.* PLoS One, 2011. **6**(12): p. e28526.

135. Knight, J.S., et al., *Peptidylarginine deiminase inhibition reduces vascular damage and modulates innate immune responses in murine models of atherosclerosis.* Circ Res, 2014. **114**(6): p. 947-56.
136. Soehnlein, O., et al., *Neutrophils as protagonists and targets in chronic inflammation.* Nat Rev Immunol, 2017. **17**(4): p. 248-261.
137. Bruscia, E.M. and T.L. Bonfield, *Cystic Fibrosis Lung Immunity: The Role of the Macrophage.* J Innate Immun, 2016. **8**(6): p. 550-563.
138. Grayson, P.C., et al., *Neutrophil-Related Gene Expression and Low-Density Granulocytes Associated With Disease Activity and Response to Treatment in Antineutrophil Cytoplasmic Antibody-Associated Vasculitis.* Arthritis Rheumatol, 2015. **67**(7): p. 1922-32.
139. Denny, M.F., et al., *A distinct subset of proinflammatory neutrophils isolated from patients with systemic lupus erythematosus induces vascular damage and synthesizes type I IFNs.* J Immunol, 2010. **184**(6): p. 3284-97.
140. Liu, Y., et al., *Myeloid-Specific Deletion of Peptidylarginine Deiminase 4 Mitigates Atherosclerosis.* Front Immunol, 2018. **9**: p. 1680.
141. Wang, H., et al., *Obesity-induced Endothelial Dysfunction is Prevented by Neutrophil Extracellular Trap Inhibition.* Sci Rep, 2018. **8**(1): p. 4881.
142. Zeng, L., et al., *Myeloperoxidase-derived oxidants damage artery wall proteins in an animal model of chronic kidney disease-accelerated atherosclerosis.* J Biol Chem, 2018. **293**(19): p. 7238-7249.
143. Albrengues, J., et al., *Neutrophil extracellular traps produced during inflammation awaken dormant cancer cells in mice.* Science, 2018. **361**(6409).
144. Okuda, S., et al., *Lipopolysaccharide transport and assembly at the outer membrane: the PEZ model.* Nat Rev Microbiol, 2016. **14**(6): p. 337-45.
145. Zhang, H., et al., *Lipoprotein release by bacteria: potential factor in bacterial pathogenesis.* Infect Immun, 1998. **66**(11): p. 5196-201.
146. Bishop, R.E., *Fundamentals of endotoxin structure and function.* Contrib Microbiol, 2005. **12**: p. 1-27.
147. Raetz, C.R. and C. Whitfield, *Lipopolysaccharide endotoxins.* Annu Rev Biochem, 2002. **71**: p. 635-700.
148. Pussinen, P.J., et al., *Endotoxemia is associated with an increased risk of incident diabetes.* Diabetes Care, 2011. **34**(2): p. 392-7.
149. Epstein, S.E., Y.F. Zhou, and J. Zhu, *Infection and atherosclerosis: emerging mechanistic paradigms.* Circulation, 1999. **100**(4): p. e20-8.
150. Minick, C.R., et al., *Atheroarteriosclerosis induced by infection with a herpesvirus.* Am J Pathol, 1979. **96**(3): p. 673-706.
151. Hajjar, D.P., et al., *Virus-induced atherosclerosis. Herpesvirus infection alters aortic cholesterol metabolism and accumulation.* Am J Pathol, 1986. **122**(1): p. 62-70.
152. Cohen, J., *The immunopathogenesis of sepsis.* Nature, 2002. **420**(6917): p. 885-91.
153. Nagarajan, V., et al., *Seasonal and circadian variations of acute myocardial infarction: Findings from the Get With The Guidelines-Coronary Artery Disease (GWTG-CAD) program.* Am Heart J, 2017. **189**: p. 85-93.
154. Smeeth, L., et al., *Risk of myocardial infarction and stroke after acute infection or vaccination.* N Engl J Med, 2004. **351**(25): p. 2611-8.

155. Clayton, T.C., M. Thompson, and T.W. Meade, *Recent respiratory infection and risk of cardiovascular disease: case-control study through a general practice database.* Eur Heart J, 2008. **29**(1): p. 96-103.
156. Moazed, T.C., et al., *Murine models of Chlamydia pneumoniae infection and atherosclerosis.* J Infect Dis, 1997. **175**(4): p. 883-90.
157. Campbell, L.A., et al., *Preclinical models for Chlamydia pneumoniae and cardiovascular disease: hypercholesterolemic mice.* Clin Microbiol Infect, 1998. **4 Suppl 4**: p. S23-S32.
158. Campbell, L.A. and C.C. Kuo, *Chlamydia pneumoniae--an infectious risk factor for atherosclerosis?* Nat Rev Microbiol, 2004. **2**(1): p. 23-32.
159. Burnett, M.S., et al., *Atherosclerosis in apoE knockout mice infected with multiple pathogens.* J Infect Dis, 2001. **183**(2): p. 226-231.
160. Stoll, L.L., G.M. Denning, and N.L. Weintraub, *Potential role of endotoxin as a proinflammatory mediator of atherosclerosis.* Arterioscler Thromb Vasc Biol, 2004. **24**(12): p. 2227-36.
161. Wiesner, P., et al., *Low doses of lipopolysaccharide and minimally oxidized low-density lipoprotein cooperatively activate macrophages via nuclear factor kappa B and activator protein-1: possible mechanism for acceleration of atherosclerosis by subclinical endotoxemia.* Circ Res, 2010. **107**(1): p. 56-65.
162. Geng, S., et al., *The persistence of low-grade inflammatory monocytes contributes to aggravated atherosclerosis.* Nat Commun, 2016. **7**: p. 13436.
163. Vajen, T., et al., *Blocking CCL5-CXCL4 heteromerization preserves heart function after myocardial infarction by attenuating leukocyte recruitment and NETosis.* Sci Rep, 2018. **8**(1): p. 10647.
164. Clark, S.R., et al., *Platelet TLR4 activates neutrophil extracellular traps to ensnare bacteria in septic blood.* Nat Med, 2007. **13**(4): p. 463-9.
165. Newby, A.C., et al., *Vulnerable atherosclerotic plaque metalloproteinases and foam cell phenotypes.* Thromb Haemost, 2009. **101**(6): p. 1006-11.
166. Strong, J.P., et al., *Prevalence and extent of atherosclerosis in adolescents and young adults: implications for prevention from the Pathobiological Determinants of Atherosclerosis in Youth Study.* JAMA, 1999. **281**(8): p. 727-35.
167. Boekholdt, S.M., et al., *Very low levels of atherogenic lipoproteins and the risk for cardiovascular events: a meta-analysis of statin trials.* J Am Coll Cardiol, 2014. **64**(5): p. 485-94.
168. Ridker, P.M., et al., *Cardiovascular benefits and diabetes risks of statin therapy in primary prevention: an analysis from the JUPITER trial.* Lancet, 2012. **380**(9841): p. 565-71.
169. Khan, S.U., et al., *Association of Lowering Low-Density Lipoprotein Cholesterol With Contemporary Lipid-Lowering Therapies and Risk of Diabetes Mellitus: A Systematic Review and Meta-Analysis.* J Am Heart Assoc, 2019. **8**(7): p. e011581.
170. Preiss, D., et al., *Risk of incident diabetes with intensive-dose compared with moderate-dose statin therapy: a meta-analysis.* JAMA, 2011. **305**(24): p. 2556-64.
171. Ravindran, D., et al., *Chemokine binding protein 'M3' limits atherosclerosis in apolipoprotein E-/- mice.* PLoS One, 2017. **12**(3): p. e0173224.

172. Braunersreuther, V., et al., *A novel RANTES antagonist prevents progression of established atherosclerotic lesions in mice.* Arterioscler Thromb Vasc Biol, 2008. **28**(6): p. 1090-6.
173. Alves-Filho, J.C., F. Spiller, and F.Q. Cunha, *Neutrophil paralysis in sepsis.* Shock, 2010. **34 Suppl 1**: p. 15-21.
174. MacIntyre, C.R., et al., *Influenza vaccine as a coronary intervention for prevention of myocardial infarction.* Heart, 2016. **102**(24): p. 1953-1956.
175. Song, Z., P. Brassard, and J.M. Brophy, *A meta-analysis of antibiotic use for the secondary prevention of cardiovascular diseases.* Can J Cardiol, 2008. **24**(5): p. 391-5.
176. Boyum, A., *Isolation of mononuclear cells and granulocytes from human blood. Isolation of monuclear cells by one centrifugation, and of granulocytes by combining centrifugation and sedimentation at 1 g.* Scand J Clin Lab Invest Suppl, 1968. **97**: p. 77-89.
177. Wichapong, K., et al., *Rational modulator design by exploitation of protein-protein complex structures.* Future Med Chem, 2019. **11**(9): p. 1015-1033.
178. Wichapong, K., et al., *Structure-Based Design of Peptidic Inhibitors of the Interaction between CC Chemokine Ligand 5 (CCL5) and Human Neutrophil Peptides 1 (HNP1).* J Med Chem, 2016. **59**(9): p. 4289-301.
179. Hoover, R.L., R.T. Briggs, and M.J. Karnovsky, *The adhesive interaction between polymorphonuclear leukocytes and endothelial cells in vitro.* Cell, 1978. **14**(2): p. 423-8.
180. Clogston, J.D. and A.K. Patri, *Zeta potential measurement.* Methods Mol Biol, 2011. **697**: p. 63-70.
181. Benoit, M. and H.E. Gaub, *Measuring cell adhesion forces with the atomic force microscope at the molecular level.* Cells Tissues Organs, 2002. **172**(3): p. 174-89.
182. Boutagy, N.E., et al., *Metabolic endotoxemia with obesity: Is it real and is it relevant?* Biochimie, 2016. **124**: p. 11-20.
183. Hauser, A.B., et al., *A gut feeling on endotoxemia: causes and consequences in chronic kidney disease.* Nephron Clin Pract, 2011. **118**(2): p. c165-72; discussion c172.
184. Soehnlein, O., *Neutrophil Research, Quo Vadis?* Trends Immunol, 2019. **40**(7): p. 561-564.
185. Knight, J.S., et al., *Peptidylarginine deiminase inhibition disrupts NET formation and protects against kidney, skin and vascular disease in lupus-prone MRL/lpr mice.* Ann Rheum Dis, 2015. **74**(12): p. 2199-206.
186. Eriksson, E.E., et al., *Importance of primary capture and L-selectin-dependent secondary capture in leukocyte accumulation in inflammation and atherosclerosis in vivo.* J Exp Med, 2001. **194**(2): p. 205-18.
187. Peschel, A. and H.G. Sahl, *The co-evolution of host cationic antimicrobial peptides and microbial resistance.* Nat Rev Microbiol, 2006. **4**(7): p. 529-36.
188. Van Avondt, K., L. Maegdefessel, and O. Soehnlein, *Therapeutic Targeting of Neutrophil Extracellular Traps in Atherogenic Inflammation.* Thromb Haemost, 2019. **119**(4): p. 542-552.
189. Ham, A., et al., *Peptidyl arginine deiminase-4 activation exacerbates kidney ischemia-reperfusion injury.* Am J Physiol Renal Physiol, 2014. **307**(9): p. F1052-62.
190. Bouma, G., et al., *Recent advances in the understanding of genetic defects of neutrophil number and function.* Br J Haematol, 2010. **151**(4): p. 312-26.

191. Nissen, S.E., et al., *Statin therapy, LDL cholesterol, C-reactive protein, and coronary artery disease.* N Engl J Med, 2005. **352**(1): p. 29-38.
192. Madjid, M., et al., *Systemic infections cause exaggerated local inflammation in atherosclerotic coronary arteries: clues to the triggering effect of acute infections on acute coronary syndromes.* Tex Heart Inst J, 2007. **34**(1): p. 11-8.
193. Kiechl, S., et al., *Chronic infections and the risk of carotid atherosclerosis: prospective results from a large population study.* Circulation, 2001. **103**(8): p. 1064-70.
194. Liu, S., et al., *Neutrophil extracellular traps are indirectly triggered by lipopolysaccharide and contribute to acute lung injury.* Sci Rep, 2016. **6**: p. 37252.
195. Zhang, R., et al., *Association between myeloperoxidase levels and risk of coronary artery disease.* JAMA, 2001. **286**(17): p. 2136-42.
196. Kai, H., et al., *Peripheral blood levels of matrix metalloproteases-2 and -9 are elevated in patients with acute coronary syndromes.* J Am Coll Cardiol, 1998. **32**(2): p. 368-72.
197. Mokart, D., et al., *Monocyte deactivation in neutropenic acute respiratory distress syndrome patients treated with granulocyte colony-stimulating factor.* Crit Care, 2008. **12**(1): p. R17.
198. Cai, T.Q. and S.D. Wright, *Human leukocyte elastase is an endogenous ligand for the integrin CR3 (CD11b/CD18, Mac-1, alpha M beta 2) and modulates polymorphonuclear leukocyte adhesion.* J Exp Med, 1996. **184**(4): p. 1213-23.
199. David, A., et al., *Interaction of proteinase 3 with CD11b/CD18 (beta2 integrin) on the cell membrane of human neutrophils.* J Leukoc Biol, 2003. **74**(4): p. 551-7.
200. Allam, R., et al., *Histones from dying renal cells aggravate kidney injury via TLR2 and TLR4.* J Am Soc Nephrol, 2012. **23**(8): p. 1375-88.
201. Shintani, Y., et al., *TLR9 mediates cellular protection by modulating energy metabolism in cardiomyocytes and neurons.* Proc Natl Acad Sci U S A, 2013. **110**(13): p. 5109-14.
202. Gauthier, V.J., L.N. Tyler, and M. Mannik, *Blood clearance kinetics and liver uptake of mononucleosomes in mice.* J Immunol, 1996. **156**(3): p. 1151-6.
203. Silk, E., et al., *The role of extracellular histone in organ injury.* Cell Death Dis, 2017. **8**(5): p. e2812.
204. Constantinescu, A.A., H. Vink, and J.A. Spaan, *Endothelial cell glycocalyx modulates immobilization of leukocytes at the endothelial surface.* Arterioscler Thromb Vasc Biol, 2003. **23**(9): p. 1541-7.
205. Hofmann-Kiefer, K.F., et al., *Serum heparan sulfate levels are elevated in endotoxemia.* Eur J Med Res, 2009. **14**: p. 526-31.
206. Henry, C.B. and B.R. Duling, *TNF-alpha increases entry of macromolecules into luminal endothelial cell glycocalyx.* Am J Physiol Heart Circ Physiol, 2000. **279**(6): p. H2815-23.
207. Muller, M.M. and T.W. Muir, *Histones: at the crossroads of peptide and protein chemistry.* Chem Rev, 2015. **115**(6): p. 2296-349.
208. Friedrichs, J., et al., *A practical guide to quantify cell adhesion using single-cell force spectroscopy.* Methods, 2013. **60**(2): p. 169-78.

209. Moreno-Cencerrado, A., et al., *Investigating cell-substrate and cell-cell interactions by means of single-cell-probe force spectroscopy.* Microsc Res Tech, 2017. **80**(1): p. 124-130.
210. Wildhagen, K.C., et al., *Nonanticoagulant heparin prevents histone-mediated cytotoxicity in vitro and improves survival in sepsis.* Blood, 2014. **123**(7): p. 1098-101.
211. Roth, G.A., et al., *Global, Regional, and National Burden of Cardiovascular Diseases for 10 Causes, 1990 to 2015.* J Am Coll Cardiol, 2017. **70**(1): p. 1-25.
212. Westerterp, M., et al., *Cholesterol Efflux Pathways Suppress Inflammasome Activation, NETosis, and Atherogenesis.* Circulation, 2018. **138**(9): p. 898-912.
213. Ridker, P.M., et al., *Interleukin-1beta inhibition and the prevention of recurrent cardiovascular events: rationale and design of the Canakinumab Anti-inflammatory Thrombosis Outcomes Study (CANTOS).* Am Heart J, 2011. **162**(4): p. 597-605.
214. Potteaux, S., et al., *Suppressed monocyte recruitment drives macrophage removal from atherosclerotic plaques of Apoe-/- mice during disease regression.* J Clin Invest, 2011. **121**(5): p. 2025-36.
215. Feig, J.E., et al., *LXR promotes the maximal egress of monocyte-derived cells from mouse aortic plaques during atherosclerosis regression.* J Clin Invest, 2010. **120**(12): p. 4415-24.
216. Ridker, P.M., et al., *Antiinflammatory Therapy with Canakinumab for Atherosclerotic Disease.* N Engl J Med, 2017. **377**(12): p. 1119-1131.
217. Ley, K., Y.I. Miller, and C.C. Hedrick, *Monocyte and macrophage dynamics during atherogenesis.* Arterioscler Thromb Vasc Biol, 2011. **31**(7): p. 1506-16.
218. van Leeuwen, M., et al., *Accumulation of myeloperoxidase-positive neutrophils in atherosclerotic lesions in LDLR-/- mice.* Arterioscler Thromb Vasc Biol, 2008. **28**(1): p. 84-9.
219. Ionita, M.G., et al., *High neutrophil numbers in human carotid atherosclerotic plaques are associated with characteristics of rupture-prone lesions.* Arterioscler Thromb Vasc Biol, 2010. **30**(9): p. 1842-8.
220. Megens, R.T., et al., *Presence of luminal neutrophil extracellular traps in atherosclerosis.* Thromb Haemost, 2012. **107**(3): p. 597-8.
221. Juzenas, S., et al., *A comprehensive, cell specific microRNA catalogue of human peripheral blood.* Nucleic Acids Res, 2017. **45**(16): p. 9290-9301.
222. Butcher, S.K., et al., *Senescence in innate immune responses: reduced neutrophil phagocytic capacity and CD16 expression in elderly humans.* J Leukoc Biol, 2001. **70**(6): p. 881-6.
223. Simell, B., et al., *Aging reduces the functionality of anti-pneumococcal antibodies and the killing of Streptococcus pneumoniae by neutrophil phagocytosis.* Vaccine, 2011. **29**(10): p. 1929-34.
224. Wenisch, C., et al., *Effect of age on human neutrophil function.* J Leukoc Biol, 2000. **67**(1): p. 40-5.
225. Ortmann, W. and E. Kolaczkowska, *Age is the work of art? Impact of neutrophil and organism age on neutrophil extracellular trap formation.* Cell Tissue Res, 2018. **371**(3): p. 473-488.

Acknowledgement

I would like to express my gratitude to everyone who supported me during the last almost 5 years to encourage me in my PhD project. Especially, I would like to thank:

My supervisor Univ.-Prof. Dr. Dr. med. Oliver Soehnlein for his support and critical discussions in the past years. He gave me the chance to work on a fascinating project, which I was able to present on meetings and conferences. Furthermore, my thesis advisory committee members Dr. Barbara Schraml, Dr. Christoph Reichel and Dr. rer. nat. Yvonne Döring who supported me to comply my PhD project.

Pati and Janine, for always helping me with cryo sections and staining protocols.

Carla, for helping me in the lab during my first year, when everything was new. You helped to find my way around.

Sanne and Quinte for the Dutch spirit and they never hesitating to help me.

Carlos and Almu for being helpful with their excellent advices and scientific suggestions.

Laura and PC for keeping the team spirit.

Past and present colleagues at the basement, for good company.

My family and husband for always believing in me.

Appendix

LMU LUDWIG-MAXIMILIANS-UNIVERSITÄT MÜNCHEN

Dean's Office
Medical Faculty

MMRS

Affidavit

Helfrich, Ariane

Surname, first name

Pettenkoferstr. 9

Street

80336, München

Zip code, town

Germany

Country

I hereby declare, that the submitted thesis entitled

NET-attraction: The role of neutrophil extracellular traps in monocyte adhesion and its impact on atherosclerosis during endotoxemia.

is my own work. I have only used the sources indicated and have not made unauthorised use of services of a third party. Where the work of others has been quoted or reproduced, the source is always given.

I further declare that the submitted thesis or parts thereof have not been presented as part of an examination degree to any other university.

München, 06.07.2020

Place, date

Ariane Helfrich

Signature doctoral candidate

LMU LUDWIG-MAXIMILIANS-UNIVERSITÄT MÜNCHEN

Dean's Office
Medical Faculty

MMRS

Confirmation of congruency between printed and electronic version of the doctoral thesis

Helfrich, Ariane

Surname, first name

Pettenkoferstr. 9

Street

80336, München

Zip code, town

Germany

Country

I hereby declare that the electronic version of the submitted thesis, entitled

NET-attraction: The role of neutrophil extracellular traps in monocyte adhesion and its impact on atherosclerosis during endotoxemia.

is congruent with the printed version both in content and format.

München,06.07.2020

Place, date

Ariane Helfrich

Signature doctoral candidate